Wind Flow Studies for Drifting Snow on Roads

Skúli Þórðarson

International spelling of the author's
name is Skuli Thordarson

Thesis submitted to the Faculty of Engineering Science and
Technology, Norwegian University of Science and Technology,
in partial fulfilment of the requirements for the degree Doctor of
Engineering

Department of Road and Railway Engineering
Norwegian University of Science and Technology
NTNU

May, 2002

ABSTRACT

During strong winds, drifting snow causes problems on roads in many harsh winter climate countries. Increased snow-removal costs, reduced access and safety problems are typical results of excessive snowdrift sedimentation and bad visibility along many roads in the exposed regions.

The objective of the study is to enhance knowledge on drifting snow behaviour on roads and to develop design criteria for better road construction in mountainous areas and other areas where frequent snowfall and strong winds occur. The study is focused on road cuts, because road sections with terrain cuts are the most vulnerable both concerning visibility and snow depositing on the road. The study is mainly based on CFD (Computational Fluid Dynamics) and field measurements. Field studies were carried out in both Norway and Iceland, and include snow surveys, wind measurements and a visibility registration. A wind tunnel study on snow drifting around a model avalanche dam is also a part of the thesis.

Wind flow in road cuts was simulated and the resulting wind speed distribution and flow pattern were compared to snow surveys. On basis of this comparison and by considering experimental relationships between wind flow and snow drifting, new design principles were proposed.

An important result of the study is the distinction between wind flow and snow drifting in gently sloping road cuts and in steep road cuts, respectively. Wind and snow drifting in gently sloping cuts and on leeward facing hillsides can usually be described as a two-dimensional flow. On the other hand, steep road cuts generally create a vortex moving parallel the road, and the resulting flow pattern must be described in three dimensions.

Results for gently sloping road cuts suggest that in order to achieve a drift free road, it must be placed downwind of the equilibrium snowdrift surface. This implies that a considerable speed up in the wind has to occur over the road embankment to facilitate snow erosion from the road surface. A statistical method to predict equilibrium snowdrift surfaces by using terrain information only is proposed. The model is based on weighing terrain slopes, and creates a streamlined surface to imitate the shape of the equilibrium snowdrift surface.

For steep cuts, a design that features an expanded cut width at both ends of the cut was tested. The design increases the speed of the transverse vortex under the cut edge, and generates less turbulence than a straight cut, which is believed to have a positive effect on the visibility. The proposed design also moves the critical low speed areas away from the road, and should therefore result in less snow accumulation on the road.

It is concluded that plain wind flow simulations are a helpful tool to learn about snow drifting on roads, and can be used to test the quality of a proposed design. The suggested design principles for road cuts are promising for full scale testing.

PREFACE

In this thesis, I applied the tools and theories of fluid mechanics to learn about snow drifting on roads. Working on an interdisciplinary study between road engineering and fluid mechanics, it has been a challenge for me to find the balance between the two extremes; either to become to fascinated about the fast developing world of Computational Fluid Dynamics (CFD) and not delivering answers for road engineering, or on the extreme opposite to focus too much on results for roads and endanger the physics of fluid mechanics. In any case, I hope that this thesis will be an inspiration to road engineers and others working with infrastructure in snow drifting areas.

TABLE OF CONTENTS

1. INTRODUCTION

1.1 Background

Snow drifting is here defined as the transport of snow particles by the wind. In many regions around the world, snow drifting on roads is a serious problem. The hazard due to snow drifting is twofold: (1) High concentration of snow particles in the air leads to hazardous driving conditions due to reduced visibility, and (2) drifting snow depositing on the road surface can form large snowdrifts that introduce traffic hazard and even leave the road impassable. The main consequences of snow drifting on roads is higher accident risk, increased maintenance costs and poor accessibility.

The appearance of snow drifting problems on roads is depending on the road design, the topography on the site and the climate. Steep and mountainous terrain usually makes roads more vulnerable to snow drifting than a flat or a moderately sloping terrain, since steep hillsides frequently require terrain cuts along the road. The amount of snowfall during the winter and the frequency of strong winds is very important, and particularly the frequency of snowfall events with simultaneous strong winds. Concerning the road design itself, the location of the road with respect to topographic features and the prevailing snow drifting wind direction, and the design of the road cross section is essential.

1.2 Objective and scope of the study

The main objective of the thesis is to enhance the knowledge on road engineering in snow drifting areas. It is focused on road cuts, because they introduce the most frequent and severe snow drifting problems. By the application of Computational Fluid Dynamics (CFD), the goal is to analyse wind and snow drifting conditions in road cuts, and to propose and test alternative design principles for road cuts.

CFD is the main tool of the study, which also considers results from field investigations. Only pure wind flow simulations were utilized, and their results were compared to snow surveys, to learn about the interactions of wind flow pattern in the terrain and snow drifting. Although great advances have been achieved in the numerical simulation of snow drifting together with the air flow, the state of the art snow drifting models are not likely to give more reliable results than the pure wind flow simulations applied in the study. The complex physics of snow drifting are still to date not fully understood. Meanwhile, the snow drifting models rely heavily on experimental calibration and their accuracy is still questionable. They are therefore of limited use in engineering applications. Results from pure wind flow simulations give information about snow drifting and sedimentation through experimental knowledge on the connection between wind speed and snow drifting. They enable qualitative comparison of snow drifting conditions without questioning the validity of calculated drift formations as in snow drifting models. Also, to the road engineer, understanding the interactions of terrain, wind, snow drifting and road design is crucial for good results in the planning process.

Results from two field programs are presented in the thesis. Field studies to support the numerical wind flow simulations were done on National Road no. 1 at Bolstadarhlidarbrekka in Iceland. Another field program was conducted on County Road no. 232, Kaperdalen road, on the island Senja in Troms county in Norway. The field program in Norway was not connected to the numerical wind flow studies, but was an important opportunity for the author to learn about snow drifting on roads in situ.

A wind tunnel research on snow drifting around a scale model avalanche dam is also included in the study. Although not directly related to road engineering, the topic is of high relevance to the objective of the current thesis.

1.3 Report structure

The thesis is divided into nine chapters and six papers. The main research work and contribution of the thesis to road engineering in snow drifting areas is found in the included papers. The papers also review state of the art in the relevant fields of work. Three of the papers were presented at international conferences, one has been accepted for publication in a scientific journal and two are submitted to a scientific journal.

Although each paper is relying on the topics of several or even all of the introducing chapters, they are linked to the chapters according to their primary subjects in Table 1.1. The contents of the individual chapters are in brief as follows:

Chapter 2	*Wind flow over terrain*: Basic definition of the wind and its interactions with the earth surface. Gradient and thermal driven winds, wind in complex terrain.
Chapter 3	*Snow topics*: Properties of the snow cover, the physics of snow drifting, transport rate of snow and wind speed, snow concentration in the air and visibility.
Chapter 4	*Modeling techniques*: Basic equations, turbulence, numerical modeling of wind and snow drifting, physical modeling.
Chapter 5	*Road engineering in snow drifting areas:* Winter service and maintenance on roads, benefits of snow control design, snow control performance of the different road elements, road aesthetics and snow drifting.
Chapter 6	*Field observations*: The use of meteorologic data in road planning, results from field observations and recommended countermeasures on the study sites.
Chapter 7	*Papers context*: A short summary on the included papers and their interactions.

Chapter 8   *Conclusions*: Results summary, conclusions and recommendations for future works.

Table 1.1: Primary concepts of the submitted papers linked to the introducing chapters.

Paper no.	Chapter 2 Wind flow over terrain	Chapter 3 Snow topics	Chapter 4 Modeling techniques	Chapter 5 Road engineering	Chapter 6 Field observations
I[a]	X		X		
II[b]		X	X		X
III[c]	X	X		X	X
IV[d]	X	X		X	X
V[e]		X		X	
VI[f]	X	X	X		

a. Paper I: Simulation of two-dimensional wind flow and snow drifting application for roads: Part I. In Hjorth-Hansen et al. (ed.), Snow Engineering: Recent Advances and Development. Proceedings of the 4th International Conference on Snow Engineering. A.A Balkema, Rotterdam.
b. Paper II: Simulation of two-dimensional wind flow and snow drifting application for roads: Part II. In Hjorth-Hansen et al. (ed.), Snow Engineering: Recent Advances and Development. Proceedings of the 4th International Conference on Snow Engineering. A.A Balkema, Rotterdam.
c. Paper III: Snow sedimentation in gently sloping road cuts. (Submitted to Cold Regions Science and Technology).
d. Paper IV: Snow drifting on roads under steep sidehill cuts. (Submitted to Cold Regions Science and Technolgy).
e. Paper V: Design criteria for roads in snow-drifting areas. Proceedings of the XIth International Winter Road Congress, 28-31 January 2002. PIARC, Sapporo.
f. Paper VI: Wind tunnel experiments and numerical simulations of snow drifting around an avalanche protecting dam. (Accepted for publication in Environmental Fluid Mechanics).

2. WIND FLOW OVER TERRAIN

2.1 Geostrophic winds

Describing the surface wind, let us start high up in the troposphere where geostrophic winds are blowing, see Figure 2.1. The motion of air is frictionless and the only force that balances the pressure gradient in the flow is the Coriolis force, which results from the earths rotation. Viscosity effects are neglible and ideally no turbulence is present. All fluid parcels in the same vertical column move in harmony, i.e. there is no vertical displacement of air.

As a first approximation to describe the flow motion, the geostrophic equations in the horizontal plane apply, together with hydrostatic approximation in the vertical direction and mass continuity. The geostrophic equations are (Cushman-Roisin, 1994):

$$-fv = -\frac{1}{\rho_0}\frac{\partial p}{\partial x} \tag{2.1}$$

$$fu = -\frac{1}{\rho_0}\frac{\partial p}{\partial y} \tag{2.2}$$

where
f = Coriolis parameter, varying with longitude, $f \approx 10^{-4}\,[1/s]$
u, v = velocity components in the horizontal x-y plane
ρ_0 = air density
p = pressure

Isolating u and v in these equations reveals that the velocity vector $\langle u, v \rangle$ is perpendicular to the pressure gradient, $\langle \partial p/\partial x, \partial p/\partial y \rangle$. As a result, the wind is not
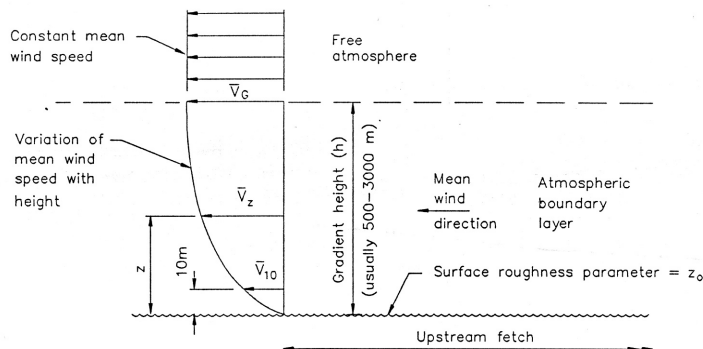
Figure 2.1 The troposphere. The geostrophic wind, $\overline{V}_G$, and the boundary layer wind, $\overline{V}_Z$ (from Barltrop, 1991).

flowing across the lines of constant pressure (isobars), but along them. This is the most important feature of geostrophic flows. On the northern hemisphere, the currents flow with the high pressures on their right, explaining why wind blows clockwise around high pressure zones and counter clockwise around low pressure zones.

Below the free atmosphere, the earth excerts friction on the wind, causing the speed to gradually reduce to zero at the ground surface. As a result, a layer where viscous effects in the flow are important develops in the lowest 400-1000 m of the atmosphere. This is the surface boundary layer or the Ekman layer. The flow must now be described by also including the inertia terms, time dependency and viscosity terms due to the vertical velocity gradient (Cushman-Roisin, 1994):

$$\frac{\partial u}{\partial t} + u\frac{\partial u}{\partial x} + v\frac{\partial u}{\partial y} + w\frac{\partial u}{\partial z} - fv = -\frac{1}{\rho_0}\frac{\partial p}{\partial x} + \nu\frac{\partial^2 u}{\partial z^2} \tag{2.3}$$

$$\frac{\partial v}{\partial t} + u\frac{\partial v}{\partial x} + v\frac{\partial v}{\partial y} + w\frac{\partial v}{\partial z} - fu = -\frac{1}{\rho_0}\frac{\partial p}{\partial y} + \nu\frac{\partial^2 v}{\partial z^2} \tag{2.4}$$

Previously undefined parameters here are the kinematic viscosity of air, ν and velocity in the vertical (z) direction, w. The effect of wind speed gradients and viscosity on the flow is flow motion fluctuating in time and space, called turbulence. Close to the ground, the shear stress due to turbulence is much higher than the molecular shear stress. It is therefore usual to replace the molecular kinematic viscosity by a turbulent viscosity, ν_T, according to the Boussinesq approximation. Turbulence is discussed in more detail in chapter 4.1.

The wind flow in the lowest levels of the atmosphere is further influenced by the presence of the ground. This influence is not only from the large scale landscape and smaller terrain formations but also due to the surface structure of the ground, e.g. the vegetation or surface texture. On the length scales of interest to the current study $(L \approx 10^2 m)$ it is reasonable to neglect the Coriolis terms from the calculations. This is possible because the flow structure in the lowest 10 % of the boundary layer is not significantly affected by Coriolis force (Arya, 1982). On the other hand, the set of equations must be expanded to include also the viscous terms for horizontal wind speed gradients, since these can have a magnitude comparable to the vertical gradients in complex landscape. Another simplification used here is the assumption of small density variations in the vertical direction due to thermal stratification of the air. The equation for conservation of mass in a constant density flow thus actually describes conservation of volume:

$$\frac{\partial u}{\partial x} + \frac{\partial v}{\partial y} + \frac{\partial w}{\partial z} = 0 \tag{2.5}$$

2.2 The logarithmic wind profile

At the ground surface the wind velocity actually becomes zero. This is the so called no-slip condition. The no-slip condition results in shear stress in the flow, and a high vertical velocity gradient. For the further work, the friction velocity is defined. The friction velocity is an indicator on the magnitude of turbulent and molecular shear stress caused by the wind on the ground surface:

$$u_* = \sqrt{\frac{\tau_0}{\rho}} \tag{2.6}$$

Here, ρ is the density of air and τ_0 is the sum of turbulent and molecular shear stresses on the ground. Looking at two-dimensional flow in the x-direction only, it is obvious that the vertical wind speed gradient (du/dz) plays an important role. Now suppose that the gradient only depends on u_*, the height above ground and an experimental constant. Dimensional analysis then suggests that the gradient increases with increased friction velocity and increases towards the ground, which can be written as:

$$\frac{du}{dz} = a\frac{u_*}{z} \tag{2.7}$$

Integration yields:

$$\int du = au_*\int \frac{1}{z}\, dz \tag{2.8}$$

$$\Rightarrow u = au_*(\ln z + b)$$

In practice, $1/a$ is known as the von Karman's constant, κ, experimentally determined equal to 0.4 and the constant of integration is $b = $ -ln z_0. The resulting equation is known as the logarithmic wind profile (Stull, 1988):

$$u(z) = \frac{u_*}{\kappa} \ln\left(\frac{z}{z_0}\right) \tag{2.9}$$

The equation describes the vertical wind speed development over a flat surface in a neutrally stable atmosphere, i.e. when the potential temperature is constant with height (Liljequist, 1957). The parameter z_0 is called the roughness height. It determines the lowest height at which the logarithmic wind profile is algebraically valid, and is also a measure of the physical roughness of the ground surface. It should be mentioned that similarity arguments show that eq. (2.9) may not be valid below z of order 20 to 50 z_0 as stated by Wieringa (1993) citing Tennekes (1973, 1982). By wind speed measurements at different heights, eq. (2.9) is commonly used to estimate the friction velocity and the roughness height.

A fairly rough or vegetated surface is represented by a high roughness parameter, z_0, and opposite for a smoother surface. Mobile surfaces, such as an erodible snow cover or the sea water present a roughness height varying with the friction velocity:

$$z_0 = c \frac{u_*^2}{g} \tag{2.10}$$

According to Wieringa (1993), Charnock (1955) proposed $c = 0.0185$ for sea waves, Vugts and Cannemeijer (1981) found $c = 0.04$ for dry sand, and for fresh cold snow the value 0.015 was found by Joffre (1982) and 0.018 by Schmidt (1982). Typical values of the roughness parameters for solid and mobile surfaces were reviewed by Wieringa. Some examples from this review are presented in Table 1.

Table 1: Typical surface roughness values.

Type of surface	z_0 (m)
Flat snow field	0.0001 - 0.0007
Rough ice field	0.001 - 0.012
Short grass and moss	0.008 - 0.03
Continuous bushland	0.35 - 0.45
Mature pine forest	0.8 - 1.6
Dense low buildings	0.4 - 0.7

Over surfaces densely covered with large obstacles, such as forest trees or houses, eq. (2.9) has to be corrected to adjust to the mean height at where the aerodynamic drag acts. This demands introduction of the displacement height, d, which shifts the logarithmic profile upwards (Figure 2.2):

$$u(z) = \frac{u_*}{\kappa} \ln\left(\frac{z-d}{z_0} \right) \tag{2.11}$$

Typical values for d can be around 0.7 times the height of the obstacles on the ground, depending on their shape and spacing (Wieringa, 1993).
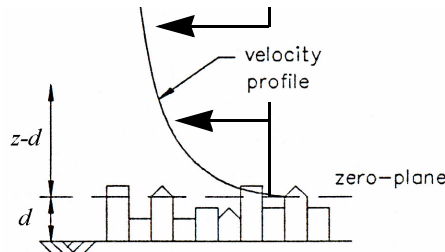
Figure 2.2 The shift in the zero-plane for the logarithmic wind profile (from Barltrop, 1991).

2.3 Internal boundary layer

The previous section emphasised how the surface roughness has impact on the local wind speed. Over a given fetch, changes in surface roughness will therefore reflect in changes in the wind profile. As the surface roughness changes, an internal boundary layer starts to develop and grows deeper along the new fetch.

Stull (1988) presented the following parametrization for the growth of the internal boundary layer depth during neutral conditions. The situation is illustrated in Figure 2.3:

$$\frac{\delta}{z_{01}} = \left[0.75 + 0.03 \ln\left(\frac{z_{02}}{z_{01}}\right) \right] \cdot \left[\frac{x}{z_{01}} \right]^{0.8} \tag{2.12}$$

where

δ = depth of the internal boundary layer

z_{01} = roughness length upwind of the border

z_{02} = roughness length downwind of the border

x = distance from the border along the new surface

The equation is useful for estimating the suitable position and elevation for wind speed gauges.
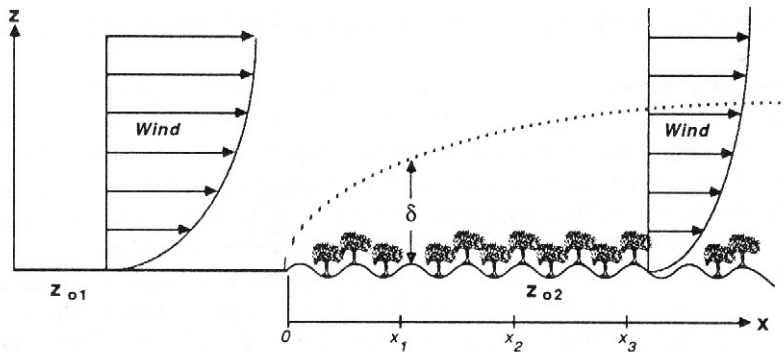
Figure 2.3 Explanation to the parameters of eq. (2.12), by Stull (1988).

2.4 Catabatic winds and see-breeze

Assuming a neutrally stratified warm residual layer over the mountain system, the radiative cooling of a mountain surface at night will cool down the air adjacent to the surface, so it becomes colder than the free air at the same altitude. The following difference in density results in shallow (2 - 20 m) winds down the mountain sides, parallel with the mountain slope gradient. These winds normally have speeds on the order of 1 - 5 m/s (Stull, 1988).

The cold air accumulates at the valley bottom, and may be drained down the valley. The resulting winds, along the valley can have a depth of 10 to 400 meters, and wind velocities of 1 - 8 m/s can be reached. Those winds are called mountain- or drainage winds. The cold air is replaced from above by an opposite directed wind, of about twice the depth of the former and half the velocity. In the daytime, the inverse phenomenon is found, called the valley wind. Such geographically-generated circulations usually result in low wind speeds, and these winds can easily be modified or eliminated by mesoscale winds. However, according to Dannevig (1968) these winds can reach high enough speeds to cause snow drifting and should be accounted for in road planning in some areas. Besides that, catabatic winds can merge with mesoscale gradient winds and increase their speed.

Sea-breeze occurs when the land surface next to the sea warms up and causes warm air to rise and to be replaced by colder air from the sea. At night, when the land surface cools down again, cool air flows out to the sea, called land breeze. Where mountains border the sea, valley-winds and sea-breeze may interact and form stronger winds.

2.5 Flow over complex terrain

The logarithmic wind profile presented by eq. (2.9) is strictly speaking only valid over a relatively flat ground in a neutrally stable atmosphere. Where the wind passes over complex terrain, the vertical wind profile will deviate from the logarithmic one. As an example, on the upwind side of hills, the wind speed close to the surface is higher than the logarithmic profile describes and at the hill summit a substantial speed-up will occur. At the hill foot both upwind and downwind of a hill the wind speed is generally lower than the free flow speed away from the hill.

The stability of the atmosphere can also affect the overall flow behaviour around the hill. Consider a temperature inversion at elevation z_i, higher than an adjacent two-dimensional terrain ridge, Figure 2.4. Depending on the wind speed and the height of the inversion above the ridge summit, the flow may (a) slightly shift the inversion downwards over the top and possibly separate on the leeward side, or (b) with higher wind speed and a lower inversion it may draw the inversion down the leeward slope resulting in a shallow high velocity stream and cause a hydraulic jump at the hill foot. This, together with the discussion on catabatic winds in the previous section, demonstrates that it is hard to generalize flow conditions for any hill- or mountain side. Specially when using simpler models of the wind flow, these effects should be
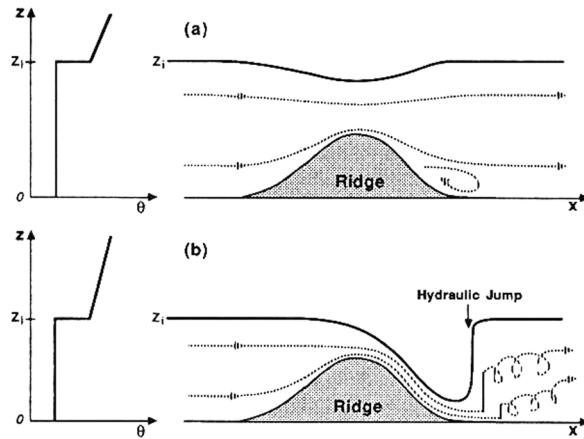
Figure 2.4 Flow over a 2D ridge. The diagrams on the left indicate the vertical virtual temperature profile including the presence of temperature inversions. From Stull (1988).

kept in mind. Additional material on the flow over hills is found in papers I, III and VI.

3. SNOW TOPICS

3.1 The snow cover

The properties of the snow cover affect snow drifting. A brief summary on the most important subjects concerning this should therefore be given here. The following section is mainly based on Male (1980).

As soon as snow crystals are deposited on the ground they are exposed to an altering process, referred to as metamorphism. The snowflakes are reduced in surface area and seek a more stable thermodynamic state. This process results in stronger bonds between the particles, making the snow cover more resistant to the eroding forces of the wind. The snow pack is modified by rain, melting and re-freezing, and relocation of snow by the wind. As a result, the snow cover develops a characteristic layered structure of relatively impermeable fine grained layers and more course structured layers of higher permeability.

The energy exchange between the snow cover and the atmosphere causes changing temperature distribution in the snow cover and is the driving force behind metamorphism. Metamorphism is a result of vapour movement through the snow pack. The thermal history of the snow cover can be idealized as a combination of two conditions; a uniform temperature through the snow pack and a constant temperature gradient.

3.1.1 Equitemperature metamorphism

The first sign of equitemperature metamorphism is the rounding of sharp corners and a decrease in thickness at the base of the individual branches. Furthermore, the slender necks disappear and the snow crystal breaks up into smaller grains. This process is accompanied by the formation of bonds between the particles, known as sintering. As this process proceeds, the grains grow in size and tend to become more equidimensional. The number of grains decreases as well, when smaller grains disappear and the larger ones grow. As the grains grow larger and become more round, the metamorphism is slowed down as a more thermodynamical stable state is reached. The process is shown graphically in Figure 3.1.

The exchange of vapour during equitemperature metamorphism is a result of local variance in vapour pressure in the vicinity of the grains, which depends on the curvature of the grains and surface stress. As an example of the efficiency of the metamorphism, a particle of radius 1 µm can disappear in an hour while a particle of ten times that radius would last four days. A particle of radius 100 µm would accordingly last over a year.
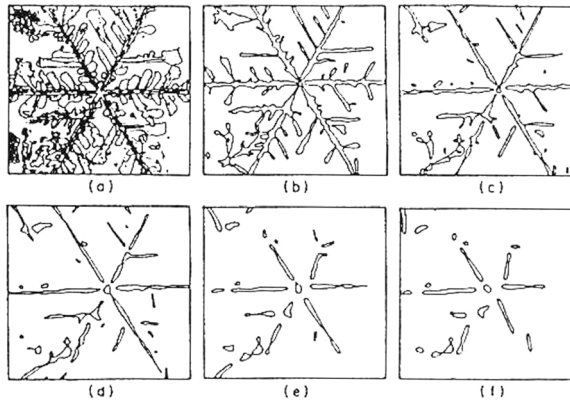
Figure 3.1 Equitemperature metamorphism of a dendritic snow crystal at -7° (a) Original crystal, (b) after 2 days, (c) after 10 days, (d) after 15 days, (e) after 30 days, (f) after 36 days. (Male 1980: drawn from photographs in Yosida et al. 1955).

3.1.2 Temperature gradient metamorphism

Temperature gradients through the snow pack are a result of the temperature difference between the ground and the atmosphere. During winter, the temperature near the ground is usually higher than the temperature near the upper surface. The temperature gradient causes vapour to migrate vertically through the snow pack towards the upper surface.

Crystal types growing in a temperature gradient snow pack are commonly referred to as depth hoar. Their shape depends on the gradient magnitude, grain size and density of the original snow. These crystals are classified into two categories; solid-type depth hoar crystals and skeleton-type depth hoar crystals. The solid-type crystals have the general shape of a plate or a column with sharp edges and corners. A layer of these crystals appears as a relatively hard, fine grained compact snow. The skeleton-type crystals have a larger size and have the form of cups, needles, scrolls and plates. The surface of such layer is characterized as stepped or ribbed, and the layer has very low strength.

3.2 Snow drifting

3.2.1 Transport modes

Snow transport by means of the wind appears mainly in three different modes. This distinction between transport modes was described by Bagnold (1941) for wind driven transport of sand. The three transport modes are surface creep, saltation and turbulent diffusion or suspension.

Surface creep

Particles migrate along the surface as a result from interparticle collisions, without leaving the particle bed. Recent investigators have described the so called reptation of particles, which refers to the motion of particles that are splashed a short distance up from the bed by the impact of saltating particles, but do not enter a typical saltating trajectory. Nishimura and Hunt (2000) state that this definition replaces the original term of surface creep, but Gauer (1999), citing Anderson et al. (1991) defines reptation as a distinguished transport mode, coexistent with surface creep. However, surface creep or reptation provide a relatively small contribution to the total transport flux, and is in most modeling work included in the saltation.

Saltation

Particles in saltation travel along characteristic trajectories. The typical particle path is determined by a nearly vertical ejection from the bed and is then deflected downwind due to drag force by the wind, and falls to the surface under a narrow angle. Particles in saltation can also be affected by the turbulent fluctuations of the wind to follow more irregular trajectories. This motion has been called modified saltation. Saltation of snow is initiated at wind speeds around 5 - 8 m/s, depending on the snow cover properties. Saltating particles bombard the surface bed and contribute to the ejection of new particles. The saltation height is depending on the wind speed and is only a few centimetres above the surface, see Figure 3.2.
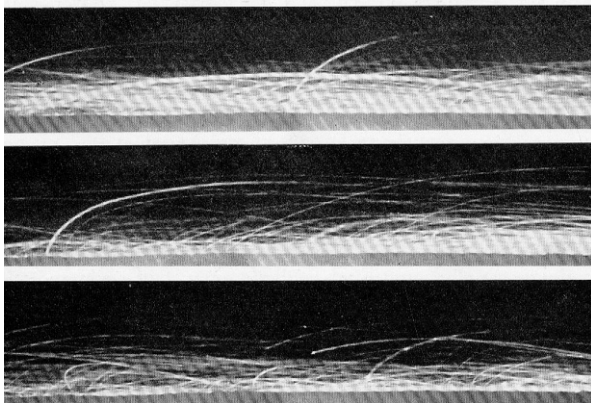
Figure 3.2 Kobayashi's photos of saltating snow particles (1972). Wind speed from top to bottom; 5.0, 4.8 and 3.9 m/s. Each photo frame is 4 cm high.

Turbulent suspension

At wind speeds 7 - 15 m/s, depending on the snow particle size distribution and other properties, particles start to be captured by the turbulent eddies of the wind and become suspended in the air. At high wind speeds, suspension is the dominant transport mode. Particles in suspension can migrate tenths of metres above the surface and only the sublimation rate limits the distance a particle can travel (in other words a particle can be held in suspension until it is completely evaporated).

3.2.2 Snow transport capacity of the wind

When the wind blows along the snow cover, it excerts shear stress on the surface, which in turn causes ejection of snow particles from the surface. This shear stress is usually given in terms of the friction velocity, u_*, defined by eq. (2.6). Assuming the presence of a logarithmic wind profile, eq. (2.9), the friction velocity has a linear relationship with the wind speed at a given reference height. This allows for either working with snow transport rates as a function of the friction velocity or the wind speed at a given height.

Starting with snow transport by saltation, Pomeroy and Gray (1990) found the following experimental relationship:

$$Q_{saltation} = \frac{u_{10}^{1.295}}{2118} - \frac{1}{17.37\, u_{10}^{1.295}} \tag{3.1}$$

where $Q_{saltation}$ [kg m^{-1} s^{-1}] is the transport rate of snow in saltation, and u_{10} is the wind speed at 10 m height.

In the suspension layer, the concentration of suspended snow in the air can be parametrizised by using one dimensional continuity equation for turbulent diffusion (Mellor, 1965) in the vertical direction:

$$w \cdot c - v_T \frac{dc}{dz} = 0 \tag{3.2}$$

where w is the vertical component of the particle velocity (assumed to be the same as the vertical component of the air velocity), c is the particle concentration and v_T is the turbulent viscosity of the air (assuming that the turbulent mass transfer coefficient is equal to the turbulent viscosity). When the turbulent eddy viscosity is expressed as $\kappa u_* z$, (Mellor, 1965) the solution to the equation is expressed as:

$$c(z) = c_{ref} \left(\frac{z}{z_{ref}} \right)^{-w/(\kappa u_*)} \tag{3.3}$$

where c_{ref} is the particle concentration at a reference height z_{ref}, w is the particle fall speed in still air, κ is the von Karman constant, and u_* is the friction velocity. The drift density, or the concentration of snow particles in the air, is highest close to the surface and decreases exponentially with height, as given by eq. (3.3). This relationship is reflected in the measurements by Budd et al. (1965) in Figure 3.3, which also shows how the concentration at the higher levels increases substantially with increased wind speed. For example, according to Figure 3.3, at 2 m height and wind speed 11.7 m/s the concentration is 0.2 g/m^3 but for wind speed 22.1 m/s the value is about 4 g/m^3. The concentration of snow in the air is important for the visibility, which is addressed in the next section.
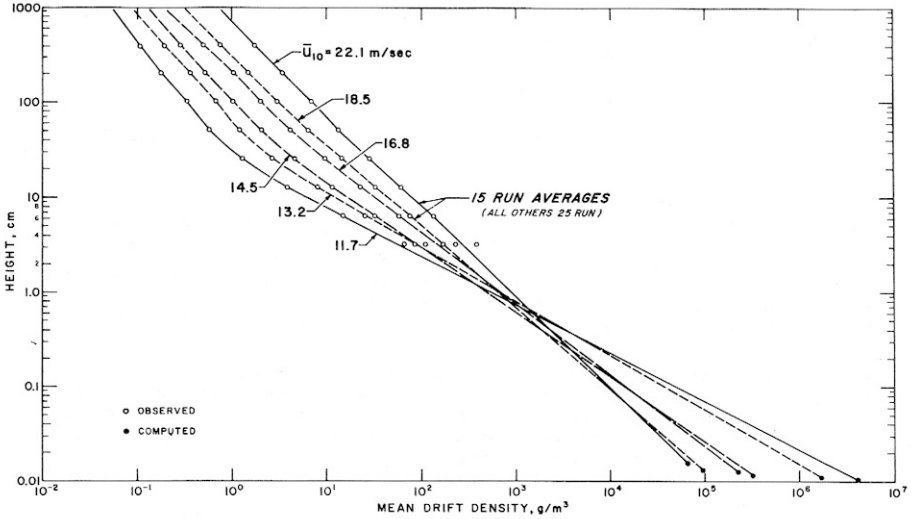
Figure 3.3 Vertical distribution of the snow concentration, including both saltating and suspended particles. From Budd et al. (1965).

An estimate for the snow concentration at a reference height at top of the saltation layer was given by Liston and Sturm (1998):

$$c_{ref} = \frac{Q_{saltation}}{2.8\, u_{*th}\, z_{ref}} \tag{3.4}$$

where u_{*th} is the so called threshold friction velocity, which is the minimum friction velocity needed to maintain saltation. It should be noted that the height of the saltation layer, z_{ref}, is proportional to the roughness height during saltation, eq. (2.10), according to Owen (1964). Now eq. (3.3) is ready for integration through the height of the suspension layer $[z_{ref} - z_{top}]$, together with the vertical wind speed distribution, given by the logarithmic wind profile in eq. (2.9). Applying the lower boundary conditions given by eq. (3.4), the transport rate for the suspended part of the drifting snow is found:

$$Q_{suspension} = \int_{z_{ref}}^{z_{top}} c(z)\, u(z)\, dz \tag{3.5}$$

For the purposes of the current study, the relationship between the wind speed and snow transport is essential. The basic principle is that snow is eroded from the surface where wind speed increases and deposited where the wind speed decreases. Measurements done by a number of investigators have shown that the amount of snow transported by the wind increases approximately by the third power of the wind speed. Empirical models from different studies are compared in Figure 3.4.
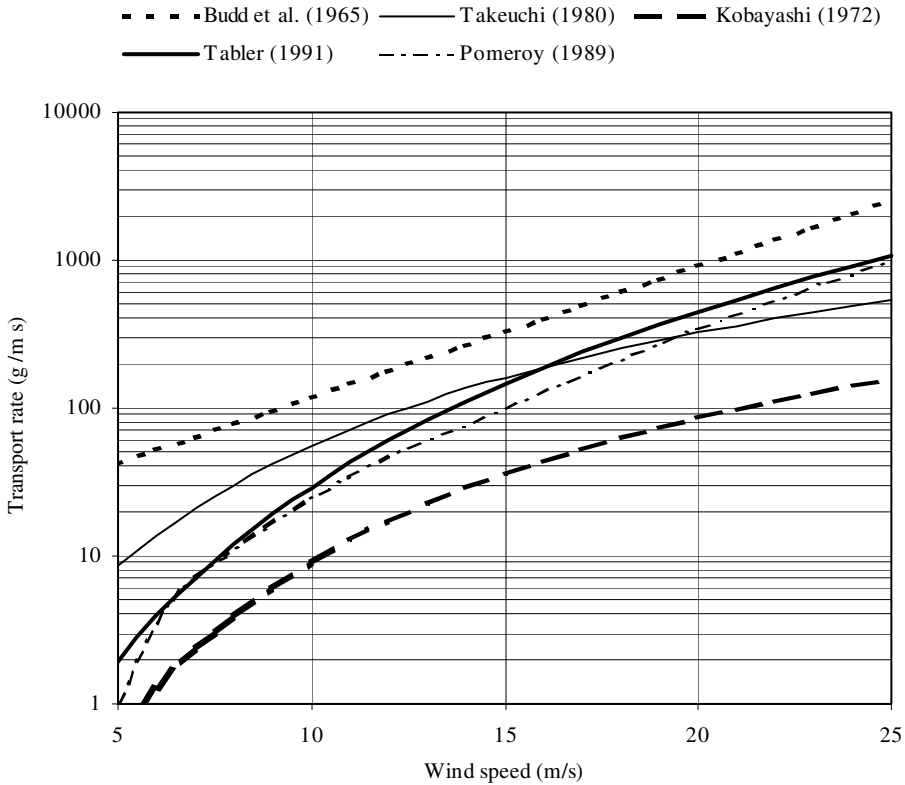
Figure 3.4 Empirical transport rate models for drifting snow by different authors.

The models presented in Figure 3.4 show great variance in the transported amounts. This is inevitable since the conditions for snow drifting are not only depending on the local wind speed, but also on the properties of the snow cover. For a fresh, loose snow cover, and especially during snow fall, the critical wind speed for snow drifting to initiate is lower than for a hardened snow cover, and the maximum amount of blowing snow can be higher.

When snow drifting is initiated, the transport rate increases along the surface until a so called steady state snow drifting is reached, which implies that the wind is saturated with snow particles. The distance or the fetch needed to achieve steady state drifting is depending on the snow cover properties. This distance can be as short as 300 m during snow fall (Takeuchi, 1980) and is longer for harder snow cover. During steady state drifting, if wind speed in an area is lower than on an upwind adjacent area, snow is deposited. It is common to assume steady state conditions in modeling of snow drifting, but less is known about the deposition of snow when the wind is not saturated with snow particles, for example when the fetch is short or when only a few particles can be eroded from the snow cover.

On long fetches, the sublimation of drifting snow is responsible for substantial loss of snow volume, which becomes absorbed as water vapour in the air. Tabler (1994)

estimates the maximum distance over which a single snow particle can be transported until it is fully evaporated to be no more than 3000 m.

3.3 Visibility in snow storm

Snow drifting results in high enough particle concentration in the air to impair visibility. Light in the atmosphere is scattered and absorbed by the gas molecules and other larger particles suspended in the air. Scattering and absorption by particles causes extinction of light, thus affecting the visibility. The number and size of larger non-molecular particles suspended in the air is highly variable, and therefore the extinction varies to. Particles in the atmosphere are of many kinds; smoke, dust, salt particles from the sea, water droplets or ice. In general meteorological context, the most important particles regarding visibility are liquid droplets. The methods established to estimate the extinction of light by spherical particles have been used in the study on visibility in snow storms and during snow fall. The optics theory reviewed here is mainly based on Middleton (1952), with snow drifting applications from Mellor (1966), Budd et al. (1965) and Liljequist (1957).

3.3.1 Extinction of light in the atmosphere

Consider a beam of light, having flux F at a cross section located at a distance r from the source, Figure 3.5. Reduction in flux, dF, caused by a thin slice of air, dr, may be considered proportional to the original flux F:

$$dF = -\sigma F \, dr \qquad (3.6)$$

where σ is the extinction coefficient. Integration of eq. (3.6) yields:

$$F = F_0 \, e^{-\sigma r} \qquad (3.7)$$

where F_0 is the original flux emitted, and F is the reduced flux over distance r.

The extinction coefficient is the sum of the respective coefficients for scattering, b, and absorption, k: $\sigma = b + k$. In the case of water droplets in the air, the proportion
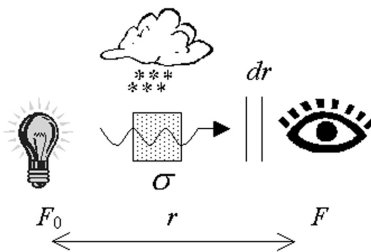
Figure 3.5 Extinction of light in the atmosphere.

of absorbed flux to scattered flux due to a particle, is only about 10^{-5}. Assuming that snow particles are no more absorbing than water droplets, extinction of light in blowing snow may be considered as a result of light scattering only.

3.3.2 Contrast

Before defining contrast, luminance or brightness should be introduced. Luminance is the luminous flux per unit of projected area per unit solid angle leaving a given point in a given direction. It is an inherent property of a ray of light, being the same at any distance in the given direction (in the absence of light extinction). Contrast denotes difference in brightness between two objects, B and B', or between an object and its background. Contrast is defined as:

$$C = \frac{B - B'}{B'}$$ (3.8)

If the object is less luminous than its background the contrast is negative, reaching -1 for an ideal black object of luminance 0. If the object is brighter than its background, C is positive. At night, looking at bright lights, C can have very large values. In the daytime, contrasts greater than 10 seldom occur.

The reduction of contrast

Looking at two objects (or an object and its background) which seen at a short distance have the luminance B_0 and B_0', and B_R and B_R' when seen from a distance R. Duntley's (1948) theory of contrast reduction suggests the relationship:

$$B_R - B'_R = (B_0 - B'_0)\, e^{-\sigma R}$$ (3.9)

The inherent contrast between the objects is

$$C_0 = \frac{B_0 - B'_0}{B'_0}$$ (3.10)

and their apparent contrast seen at distance R is

$$C_R = \frac{B_R - B'_R}{B'_R}$$ (3.11)

Now eq. (3.9) can be written on the form

$$C_R = C_0 \left[\frac{B'_0}{B'_R} \right] e^{-\sigma R}$$ (3.12)

which is the most general expression for the law of contrast reduction in the atmosphere.

In the special case when an object is seen against the horizon sky, the value inside the parentheses in eq. (3.12) becomes 1, since the inherent and apparent brightness of the horizon sky must be the same. This would also be the case concerning a snow filled atmosphere even if the horizon sky is not seen as a reference, according to Mellor (1966).

3.3.3 Mathematical expression of visual range

Visibility, or visual range is commonly used to indicate the maximum distance at which an object of definite area and shape can be seen. More specifically this means the distance at which a difference in contrast between two objects or an object and its background is two percent, which is the standard meteorological definition.

Applying eq. (3.12) with C_R equal the liminal contrast $C_R = +/- \; 0.02$ (the lowest contrast observed by the eye), the definition of visual range for a black object (inherent contrast $C_0 = -1$) can be written as

$$0.02 \; = \; e^{-\sigma V} \tag{3.13}$$

$$\Rightarrow \; V \; = \; \frac{3.9}{\sigma_0}$$

where σ_0 is the extinction coefficient and V is the visual range.

3.3.4 Extinction coefficient as a function of snow density

The relationship between the extinction coefficient and the snow concentration in the air is of fundamental interest to this study. Assuming no absorption, the extinction coefficient can be estimated from the number and size of spherical particles present in an element of air:

$$\sigma \; = \; \sum_{i=1}^{n} N_i \cdot K_i \cdot \pi \cdot r_i^2 \tag{3.14}$$

The summation runs through the entire particle size distribution present and

r_i = radius of the particles of size i
σ = extinction coefficient
N_i = number of particles of size i
K_i = scattering area ratio for particle size i.
A function of the proportion r/λ (Radius to wavelength)

The scattering area ratio K, is according to the electromagnetic theory a function of the ratio of the area of the wave front acted on by the particle, and the particle itself. For large particles, K tends asymptotically towards 2, as particle size increases. For

blowing snow particles, which are large in this context, this means twice the scattering of light as would be expected from geometrical conditions.

3.3.5 Measurements of visibility in snow storm

An inverse relationship between the visibility and number and size of snow particles in the air is suggested by eq. (3.13) and eq. (3.14). For a given particle size distribution, the same should also be true for the snow concentration in the air, that is the mass of snow suspended in the air. Measurements from Mellor (1966) and Budd et al. (1965) have confirmed the inverse relationship between visibility and snow concentration in the air:

$$V = \frac{D}{c} \tag{3.15}$$

where V (m) is the visual range, D is a constant mainly depending on the particle size distribution and c (g/m^3) is the snow concentration. The results from Mellor (1966) and Budd et al.(1965) are shown in Figure 3.6. The data from Budd et al. suggest that D in eq. (3.15) equals 100.

Because increasing wind speed increases the snow concentration in the air, the visibility is connected to the wind speed during snow drifting. The results in Figure 3.7 were obtained by Liljequist (1957).
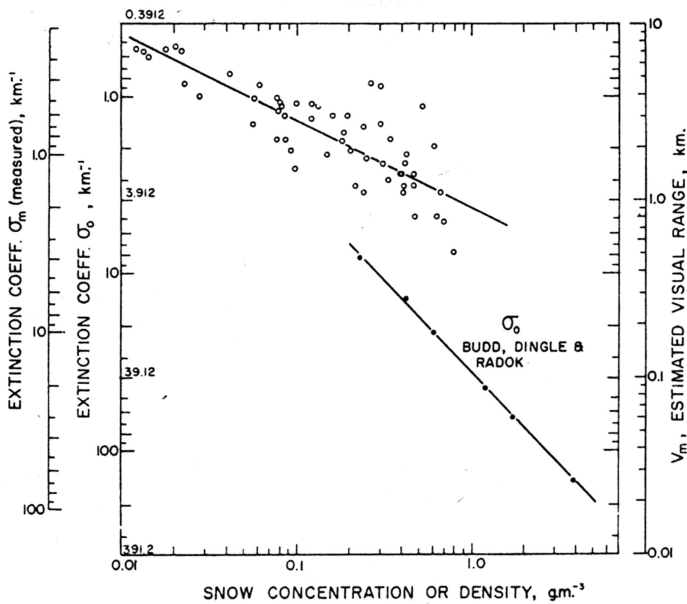
Figure 3.6 Visibility as a function of the snow concentration and the extinction coefficient. Results from Mellor (1966) as open circles and from Budd at al. (1965) as filled circles.
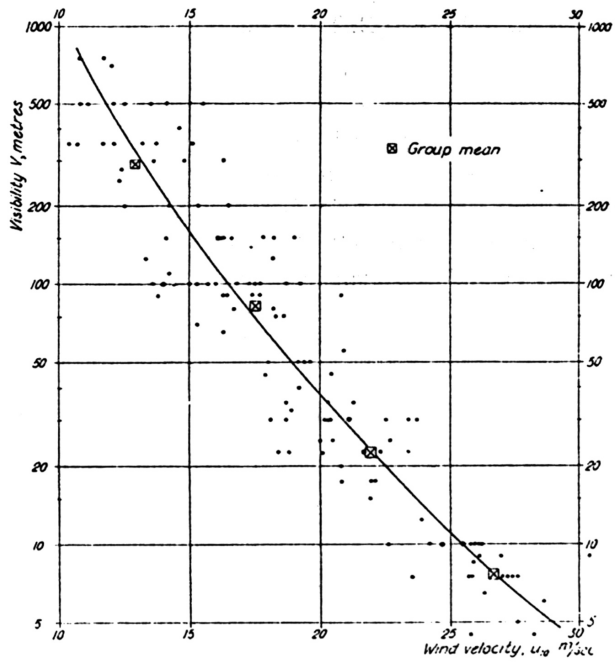
Figure 3.7 Results from Liljequist (1957) show a connection between the visibility and the wind speed measured at 10 m height.

4. MODELING TECHNIQUES

4.1 Computational modeling

4.1.1 Basic equations

The equations for the motion of air in the atmosphere were introduced in chapter 2. The equations actually apply for a diversity of fluid flows and are commonly referred to as the Navier-Stokes equations. For incompressible Newtonian fluid flow, neglecting body forces (e.g. Coriolis and weight) they can be written in compact notation as (White, 1988; Gerhart et al., 1992):

$$\frac{\partial u_i}{\partial t} + u_j \frac{\partial u_i}{\partial x_j} = -\frac{1}{\rho}\frac{\partial p}{\partial x_i} + \frac{\mu}{\rho}\frac{\partial^2 u_i}{\partial x_j \partial x_j} \tag{4.1}$$

where one equation is achieved for each coordinate direction, $(x_1, x_2, x_3) = (x, y, z)$ The flow velocity components are $(u_1, u_2, u_3) = (u, v, w)$, p is the pressure, μ is the molecular viscosity of the fluid and ρ is its density. In constant density flows, it is convenient to use the kinematic viscosity, $\nu = \mu/\rho$. Together with the continuity equation for incompressible flow, eq. (2.5), the four equations give four unknown variables to be solved, and thus provide a complete accurate description of the instantaneous values of the flow parameters.

For turbulent flows, direct solution of the equations is computationally very expensive, and for most practical applications not feasible. In most engineering and meteorological flow modeling, only the time-averaged flow qualities are of interest and not all the details of the turbulence. We therefore seek a set of equations that describes the mean flow variables and the effect of the turbulence on these.

For this purpose, we perform so called Reynolds-averaging on eq. (4.1): All the flow variables are divided into a mean value and a fluctuating component and the resulting equations are averaged and simplified by applying the continuity equation. The result is the Reynolds-averaged Navier-Stokes equations (RANS), (White, 1988; Gerhart et al., 1992):

$$\rho \left[\frac{\partial U_i}{\partial t} + U_j \frac{\partial U_i}{\partial x_j} \right] = -\frac{\partial P}{\partial x_i} + \mu \frac{\partial^2 U_i}{\partial x_j \partial x_j} - \frac{\partial}{\partial x_j}\rho \overline{u_i u_j} \tag{4.2}$$

where capital letters indicate the mean or averaged quantities of the flow variables and $-\rho u_i u_j$ represents the turbulent stresses or the Reynolds stresses, written with overbar in the equation as a result from the averaging process before. The Reynolds stresses present six new unknown variables in the set of equations, making it non-solvable as such. A way to model the effect of the Reynolds stress on the flow is therefore needed.

4.1.2 Turbulence modeling

In the generalized eddy-viscosity concept, the turbulent stresses are related to the mean flow gradients through a turbulent viscosity (Andersson, 1988):

$$-\rho \overline{u_i u_j} = \rho \nu_T \left(\frac{\partial U_i}{\partial x_j} + \frac{\partial U_j}{\partial x_i} \right) - \frac{2}{3} \rho k \delta_{ij}$$
(4.3)

where ν_T represents the eddy viscosity, δ_{ij} is a unity diagonal matrix and k is the mean kinetic energy of the turbulent motion, defined as

$$k = \frac{1}{2} (\overline{u_i u_i}) = \frac{1}{2} (\overline{u^2} + \overline{v^2} + \overline{w^2})$$
(4.4)

When k is not treated as a dependent variable of the model equations, k is conveniently absorbed in the unknown kinematic pressure, under the first term on the right hand side in eq. (4.2). When using the $k - \varepsilon$ turbulence model as described below, that is not necessary since k then is a dependent variable calculated in its own transport equation.

For the dominating Reynolds stress component in a two-dimensional shear flow, eq. (4.3) becomes a simpler expression:

$$-\rho \overline{uv} = \rho \nu_T \frac{\partial U}{\partial y}$$
(4.5)

Substituting eq. (4.3) into eq. (4.2) leaves us with only one additional unknown variable that needs to be modeled, namely the eddy viscosity. The RANS, when using the eddy viscosity concept then take the form (Andersson, 1988):

$$\frac{\partial U_i}{\partial t} + U_j \frac{\partial U_i}{\partial x_j} = -\frac{\partial}{\partial x_i} \left[\frac{P}{\rho} + \frac{2}{3} k \right] + \frac{\partial}{\partial x_j} \left[(\nu + \nu_T) \left(\frac{\partial U_i}{\partial x_j} + \frac{\partial U_j}{\partial x_i} \right) \right]$$
(4.6)

Several models for estimating ν_T are available. The simplest are algebraic models like constant eddy viscosity models and mixing length models. They can produce good results in simpler shear flows and are easy to use. Some of their limitations are that they can not predict flow in recirculating zones or in separating boundary layers.

Probably the most popular turbulence model in engineering applications, is the standard $k - \varepsilon$ model. In the model, the mean kinetic energy of the turbulent motion, k, and its dissipation rate, ε, are related to the eddy viscosity:

$$\nu_T = c_\mu' \frac{k^2}{\varepsilon}$$
(4.7)

where $c'_\mu = 0.09$ is an experimental constant. The turbulent energy, k, and the dissipation rate, ε, each has its own partial differential equation which will not be described here. The $k - \varepsilon$ turbulence model adds two new partial differential equations to be solved along with the RANS equations, and thus increases the computational costs substantially. Richards and Hoxey (1993) described the application of the $k - \varepsilon$ model in computational wind engineering and proposed alternative boundary conditions.

4.1.3 Modeling of snow drifting

Although modeling of the snow drifting itself is not considered in this thesis, some of the recent work on this should be mentioned. There are mainly three different approaches found in the works of snowdrift investigators: (1) Two-fluid modeling techniques, (2) particle tracking methods and (3) semi-empirical steady state snow drifting models.

1. *Two-fluid models*. The mixture of air and snow is treated as a mixture of two fluids. The two equations, continuity and Navier-Stokes, are solved for each phase, resulting in two sets of equations to be solved. The mass balance of each of the phases is considered in a control volume, referred to as Eulerian mapping. The snow particles are physically coupled with the airflow through a drag interaction term in the equations. Mass concentration and velocity of the snow phase is solved directly by the set of equations associated with the snow phase (Decker 1991). An example of the most recent works here is the physically based numerical model of Gauer (1999). The physical basis for his model is stronger than for the semi-empirical models as mass conservation in the model is accounted for by mutually coupling the suspension and the saltation layer by boundary conditions.

2. *Particle tracking models*. This method treats the airflow as in the former case, on an Eulerian frame, but the snow is treated as a cloud of particles, each particle being tracked as it moves under the drag from the continuous fluid. A Lagrangian equation of motion is solved for each particle, resulting in a huge collection of equations for the entire domain. Velocity and concentration of the snow phase can be solved by averaging the Lagrangian statistics of individual particle behaviour over the entire domain. Although giving a good physical interpretation of the particle transport, this method is less feasible than the two fluid model since it takes much more computational resources (Decker 1991). Sundsboe and Hansen (1997) tried a particle tracking model for simulation of snow drifting around a porous snow fence.

3. *Semi-empirical snow drifting models*. These models are based on empirical formulation of the snow quantities transported by saltation, and on turbulent diffusion theory for the snow particles in suspension, see eq. (3.1) and eq. (3.5). The models have been applied with some success for snow redistribution in a mesoscale environment for hydrological water budget purposes, for example by Liston and Sturm (1998), Jaedicke (2001) and Bruland (2002). However, due to

its limited physical interpretation, this modeling technique is neither applicable for tasks involving complex flow geometry i.e. separating and recirculating flows nor in microscale situations where small slope variations are important.

4.1.4 Current approach

The simulation work described in the attached papers is all done with the flow solver Flow3D (Flow Science, NM USA). The code solves the RANS on a finite difference scheme. A standard $k - \varepsilon$ turbulence model was chosen for all simulations, with default boundary conditions from the flow solver. The solver has been used in snow and wind engineering before by several other investigators (Thiis, 2000; Sundsboe, 1997; Wiik, 1999).

 The arguments for choosing pure wind flow simulations for this work rather than using a combined wind flow and snow drifting simulation were presented in chapter 1.2. The basis for interpretation of snow drifting using wind flow simulations is the empirical relationships between the wind speed, snow erosion and deposition presented in chapter 3.2. Streamline analysis is also a helpful tool to map the flow structure, especially in the 3D simulations.

 Flow3D applies a rectangular calculation mesh and uses the FAVOR technique to adapt the mesh to the flow geometry. This is done by integrating a volume fraction into the momentum equations to account for partially blocked computational cells at the boundary to geometric objects in the flow field. The FAVOR method makes grid generation a straight forward task and enables complex geometry to be resolved without time-consuming grid generation. Although the FAVOR method is very handy for the integration of terrain in the flow field, the rectangular discretization results in spatially fluctuating values in the flow field very close to the boundary.

 As stated in chapter 3.2.2, the shear stress at ground level or the friction velocity, u_*, is most important for the snow transport rate. In the numerical approach used here, the wind speed at a fixed reference height is used as and indicator of the magnitude of the friction velocity. This choice assumes that the vertical wind speed distribution from the reference point and down to the surface follows the logarithmic profile. Applying eq. (2.9) with a constant z value, we get

$$u(z_{ref}) \; = \; \frac{u_*}{\kappa} \ln\!\left(\frac{z_{ref}}{z_0}\right) \tag{4.8}$$

$$\Rightarrow u(z_{ref}) \; = \; const \cdot u_*$$

The accuracy of this approach is higher the closer to the surface z_{ref} is chosen. In any case, it is the relative variation of u_* along the surface and not its exact value that is of interest in this study and therefore I find this approach satisfactory.

 In the 2D simulations, the wind speed evolution curve along the surface was extracted at reference height equal to the vertical spacing of computational cells at the surface, most often 1 or 2 m. This was found to be the minimum distance from the surface to avoid spatial fluctuations due to the numerical boundary conditions in the
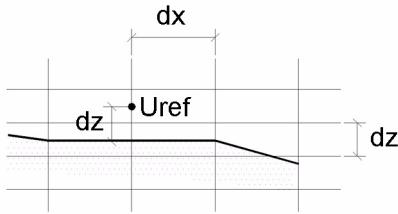
Figure 4.1 Location of the reference speed value, Uref, for estimating u_*. Dimension of computational cells is dz and dx in the vertical and horizontal directions respectively.

flow solver. The principle is illustrated in Figure 4.1. The wind speed distribution from the 3D simulations is presented as grayscale images. In this case, the grayscale rendering in the post-processing system (Field View: Intelligent Light, NJ USA) equalizes the fluctuations at the boundary and the reference wind speed is taken at ground level.

4.2 Wind tunnel and other physical modeling

Many attempts have been done to simulate snow drifting around scale models in wind tunnels or in water flumes, using different particles. Outdoor experiments with scale models have also been tried and in recent years, the use of cold wind tunnels has enabled the use of artificial snow particles as the entrained material.

Common to all scale model experiments with snow drifting is the task of achieving similarity between the model and the prototype. Fulfilling all the similarity criteria in any given experiment is impossible, and the experimental setup has to compromise to focus on the most important parameters at the expense of others. However, investigators have different opinion on which similitude parameters are the most important. A review over parameters used by different workers is found in Iversen (1980) and Naaim-Bouvet (1995).

Physical experiments can serve as good indicators on the relative qualities of different designs. Although not necessarily giving exact results for the prototype, the experiments can give valuable information on which option serves best under full scale snow drifting conditions. A qualitative comparison of scale models, albeit advances in numerical modeling, is still an important tool in snow drifting research.

In this thesis, paper VI, scale model experiments in a cold wind tunnel were carried out (Figure 4.2). Snow drifting around an avalanche dam model was simulated in the Jules Verne Climatic Wind Tunnel. The Jules Verne facility in Nantes was described by Gandemer et al. (1997) while the avalanche dam experiments were described in detail by Haraldsdottir et al. (2002). The experiments compared the effect of different wind directions on the snowdrift accumulation around the dam model. In paper VI, numerical wind flow simulations were used to evaluate the model similarity with respect to the prototype, but the similarity was questionable due to the small geometric scale used, 1:100.

Another example of a qualitative comparison in a cold wind tunnel is the experiments done by Gurer (2002), where different snow fences were tested in a cold

Figure 4.2 Snow depth measurements by surface tracing on a paper sheet in the Jules Verne Climatic Wind Tunnel.

wind tunnel. Norem et al. (2002) used smoke in a wind tunnel to interpret the generation of snow-cloud behind heavy vehicles in an experiment that allowed for the comparison of different countermeasures such as the use of spoilers. Sand suspended in water was also used by Norem (1975) to compare the visibility in different road cuts and the effect of snow fences on the visibility on the road. Tabler (1980) successfully tested snow fences in scale 1:30 outdoors.

Even though a qualitative comparison of options can be informative, some minimum requirements have to be fulfilled regarding the model similitude. As an example of this, Baker and Dutch (1995) compared porous and solid snow fences using sand in a wind tunnel, a study where similitude to snow drifting was not considered. They ran their experiments at wind speeds just above the threshold value for initiation of saltation, and found that solid barriers accumulated more snow deposits than porous fences. For full scale snow drifting, the opposite is true (Tabler, 1988).

5. ROAD ENGINEERING IN SNOW-DRIFTING AREAS

5.1 Snow control, maintenance and service

As emphasised in chapter 1.1, the most important consequences of snow drifting on roads are higher accident risk, increased maintenance costs and poor accessibility. Accessibility and safety are improved mainly by three means; snow control design of the road[1], higher maintenance level and increased service. Higher maintenance level applies for example to more frequent snow removal cycles, use of rotary snow blowers and friction control. Examples of winter road services are organized convoy driving (Norway and Sweden), patrolling and collecting and distributing information on weather and driving conditions.

On roads that are exposed to snow drifting but do not feature any special snow control design, access and safety can be improved with higher maintenance and service. However, if snow control is not considered in the design, high snowbanks on the road shoulder will usually cause reduced visibility already during moderate storms and the increased maintenance effort may not help that much. Access to the road may be highly dependent on controlled convoy driving, which features low traffic speed and delays. The result is higher maintenance and service costs through the whole lifetime of the road, and yet the required access and safety levels may not necessarily be achieved.

Road design that considers snow control can increase the initial investment for the road, but on the other hand it reduces the maintenance and service costs. Accessibility, visibility and safety is also better. Therefore, snow control aimed design in the first place is advantageous for the total costs, considering investment contra accumulated annual costs through the lifetime of the road.

The winter maintenance and road design have to mutually interact for optimal results. As an example, on low traffic volume roads in heavy snow areas, where the maintenance resources are limited, the road design has to facilitate operation of the road without the need for extensive snow removal. On the other hand, major roads which have an important transport function are often equipped with on site machinery, which reduces the demand for storage capacity of drifted snow along the road. In other words, more snow accumulation on the road surface can be accepted due to frequent snow removal and stand-by rotary blowers.

The Roadex project report (2001) contains information on the winter maintenance of low traffic volume roads in Norway, Sweden, Finland, Scotland and Iceland. The main goal of the study was to identify state-of-the-art in maintenance techniques, traffic information systems and snow drifting and friction control measures. The report reveals how different procedures are needed for different topography and climate in the actual regions.

---

1. Snow control design might include the use of snow fences, which are not discussed in the thesis.

5.2 Importance of snow control

The required performance of the road design and the required maintenance and service level should consider the demand for accessibility. For some roads, reduced access and delays can be accepted and for other roads it can not. The acceptable access level on a road is depending mainly on the following factors:

1. Traffic volume in winter
2. Road classification
3. Critical transport functions (medical, fresh merchandise etc.)

Should good access be required throughout the winter, the demand for snow control design and maintenance level is consequently high. To maintain the required accessibility, the demand for snow control also increases with the snow drifting exposure of the road. The snow drifting exposure depends on the following factors:

1. Climate
2. Landscape and local topography
3. Vegetation (forest and bush-land provides shelter and retards drifting)

A simple model of the interactions between the topics that have been addressed is presented in Figure 5.1. The diagram shows how the snow drifting exposure demands higher level of snow control design for the road in order to maintain a certain access level. A proposed definition of the access levels might be:

Normal access: Free traffic flow or minor interruptions. Lowered traffic speed accepted.

Reduced access: Delays and periodic closures. Controlled access by convoy driving.

Poor access: Frequent or prolonged closures.

The model in Figure 5.1 suggests that no special design needs to be applied for a low level of snow drift exposure to maintain normal access. It also suggests that for the highest level of snow drift exposure, poor access is an inevitable result, independent of the road design. This is because during extreme weather, the strong winds result in risk of vehicles being blown off the road, and the road should be closed. It should not be forgotten that road tunnels have been built in some places, only to avoid snow drifting. The line between "normal" and "reduced" access is quite steep, suggesting that snow control design gives good results for moderate to relatively high snow drift exposure. On the other hand, the line between "poor" and "reduced" access is less steep, indicating that for the most severe exposure levels, snow control design is less advantageous, mainly due to visibility problems associated with the highest wind speeds. The use of snow fences, which has not been considered here in the snow control design, might increase the size of the "reduced" access area on the account of
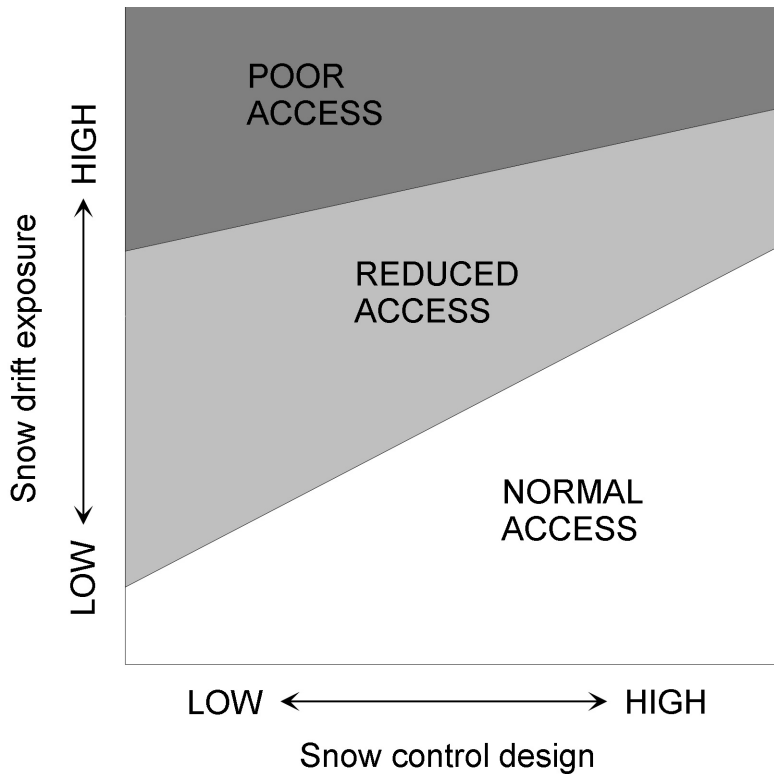
Figure 5.1 The diagram shows how, for a given level of snow drifting exposure (vertical axis), higher access requirements demands higher level of snow control (horizontal axis) in the road design.

the poor access area. In the overall evaluation, the direct and indirect costs of reduced access should be accounted for when the degree of snow drift control and access level is chosen.

5.3 Elements of the road structure

Snow drifting sets requirements to the different elements of the road structure and the interaction of these elements. An element of the road structure is here defined as any surface connected to the road such as the backslope of cuts, ditch, foreslope (embankment slope), road shoulders and the road surface.

However, before discussing the requirements to the road cross section, the most important goal of the road planning should be addressed. For optimal results, it is essential that the route location with respect to the terrain is carefully chosen. A successful route location results in fewer and shorter sections where special measures in the road cross section are needed. For snow control in road design, Norem in Norway and Tabler in USA have published the most extensive recommendations in recent years. Both these investigators have listed up various criteria for route selection, which will not be included here. However, one of the most important

criteria is highly relevant for this thesis: To avoid locating the road inside natural snow deposition areas. To identify these areas, a three-dimensional wind field simulation over the terrain has proved to be a successful method.

The following summary includes the most important elements of the road cross section that are relevant in snow control design.

Road cuts

Road cuts are probably the most important elements and are the main subject of this theses. Previous recommendations for road cuts are reviewed in paper III and paper IV and will not be repeated here.

Embankment height

On fill sections, the embankment height of the road should be increased in heavy snow areas. This reduces the height of the snow-banks on the road shoulder and improves the visibility. According to Tabler (1994), the minimum embankment height over the surrounding terrain should be 0.4 S + 0.6 (m), where S is the mean annual snow depth on the ground. Norem (1994) on the other hand also relates the embankment height to the average number of days with strong winds. His proposal is introduced in Table 5.1.

Table 5.1: Norem's recommendation for embankment height (1994).

Number of days with strong[a] winds per month	Embankment height	Minimum height
> 15	$S + 0.5$ m [b]	2.0
10 - 15	S	1.5
6 - 10	S in exposed areas, 1.0 m in sheltered areas	1.0
< 6	No special requirements	

a. Strong winds defined as higher than 10.8 m/s
b. S is average snow depth on the surrounding terrain

Embankment slope

Steep embankment slope results in a relatively sharp angle between the road surface and the foreslope. As a result, the wind fails to follow the curvature of the surface and has more tendency to create a low-speed snow accumulation zone on the road surface. An embankment slope of 1:4 has proved to give better results than a slope of 1:2. This is documented by both Norem and Tabler. Norem additionally recommends that the transition from the road shoulder to the embankment slope should be rounded with a radius of 2 times the embankment height, G. The principle is illustrated in Figure 5.2.
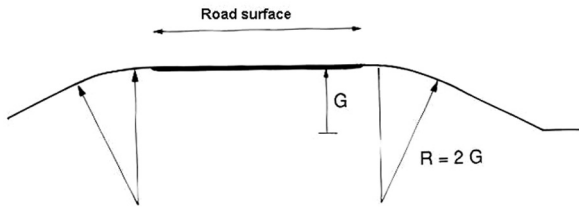
Figure 5.2 Recommended rounding of the road shoulder (Norem, 1975).

Tabler found that the tendency to deposit snow on the road surface increases with increased sideslope and increased embankment height. For embankments higher than 2 m, Tabler therefore suggests a sideslope of stepwise increasing slope segments from the shoulder and down to the foot of the embankment. This creates a more streamlined surface and eliminates the need for a safety guard rail on high fills.

Super-elevation in curves

The transverse slope of the road surface (perpendicular to the road axis) usually applied in curves increases the angle between the road surface and the embankment slope. As a result, the wind has a tendency to deposit snow on the road when the wind direction is from the opposite direction of the turn. Consequently, the upwind embankment slope should be flattened out when the center of curvature is downwind, to maintain the same flow conditions across the road in the curve as on adjacent tangents. Tabler recommends that the angle between the road surface and the embankment windward slope should not exceed 10.2° in curves.

5.4 Road aesthetics

In the Nordic countries, many of the roads that have the highest snow drifting exposure are located in precious landscape. This includes mountain roads and passes which are important for tourism. Road aesthetics is therefore an important topic that should be considered in snow control design.

Countermeasures to snow drifting on roads can involve large earthwork volumes, such as excavation of wide ditches, levelling of adjacent terrain and high fill sections. Negative effects on the landscape can therefore be exaggerated. The ideals of road aesthetics were reviewed by Amundsen in her doctoral thesis (1995). Majority of these ideals coincides with the interests of snow control design. As an example, the rounding of slope transitions is found positive for the visual appearance of the road. Another example is presented in Figure 5.3. The sketches display that the road should follow the direction of the terrain features and avoid crossing them, which also is positive for snow control. Snow control measures that involve high embankments or levelling of the adjacent terrain give a better view from the road, which makes travelling on the road a more pleasant experience.

(a)
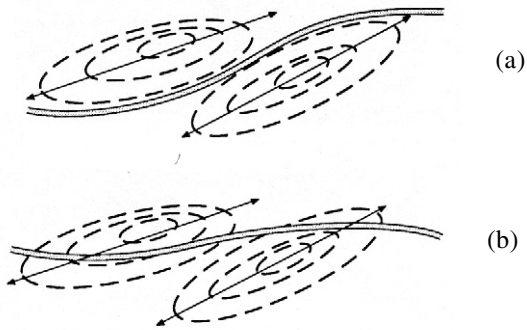
Figure 5.3 For a pleasant visual appearance in the landscape, the road should follow the direction of terrain features (a) and not cross them (b) (Amundsen, 1995). This is positive for snow control.

(b)

6. FIELD OBSERVATIONS

6.1 Use of meteorologic data in road planning

Norem (1994) recommended how to get relevant information from meteorologic data for road planning in snow drifting areas. Wind speeds lower than a certain value do not contribute to snow drifting problems, and therefore these should be filtered out from the data. Furthermore, he pointed out that the wind directions that frequently bring snow fall are the most important for the road, and that lower wind speeds have impact on the snow problems only in the presence of snowfall. To identify the worst wind directions, he developed a procedure that classifies wind directions according to a scoring system, where each direction is weighed with respect to frequency of strong winds and precipitation. When a continuous series of measurements is available for at least one winter season, or preferably an averaged series from several years of observations, the following method was proposed by Norem:

$$P_{dir} = \sum_{i=1}^{n} (V-5) + \sum_{i=1}^{s} (V-9) \qquad (6.1)$$

where

P_{dir} = Sum of points for a particular wind direction
n = Number of observations with simultaneous snowfall and wind speed over 5 m/s
s = Number of observations without snowfall and wind speed over 9 m/s
V = Registered wind speed

A radial diagram (similar to a wind rose) can then be made of the calculated P values to display the impact of each wind direction on snow drifting.

In many cases, measurements from a weather station located up to several kilometres from the actual site can give good enough information on the conditions at the road site. Where landscape is complex and wind directions and precipitation amounts are affected by nearby mountains, a weather station should be installed close to the actual road site as early as possible in the planning process.

6.2 Kaperdalen study site

6.2.1 Introduction

Field investigations on County Road no. 232 Kaperdalsvegen mountain pass in Troms county in Norway were carried out for two winter seasons (1998-99 and 1999-00), see Figure 6.1. The road has an important function, being the only road connection available for the community it serves. The objective for the investigations was to learn about the interactions of climate, driving conditions and the winter maintenance demand for the road. Another important goal was to locate the worst sections along the road and propose measures to reduce the snow problems and to improve the accessibility of the road.

The results from Kaperdalen were reported to the Public Road Administration in Troms in January 2001. This includes results from an automatic weather station, snow surveys and visibility observations on the road during snow storm. Ideas on rebuilding portions of the road and modifying the adjacent terrain were also included. Due to the nature of both the climate and the landscape in Kaperdalen, the data collected there was not found applicable for the fluid dynamical analysis in the present thesis. The reason for this is that the snow problems on the road are mainly due to the high snowfall amounts and high frequency of strong winds, and less due to the microscale landscape around the road.

Kaperdalen mountain pass is located on the west-side of the island Senja, facing the Atlantic Ocean. Even if the elevation of the site is not high, only about 360 m a.s.l., the climate is similar to the climate on higher mountain roads in Norway. The average temperature during the winter is however higher at the coast. Maritime climate governs the weather, with high precipitation amounts and frequent strong winds in the winter. The mean January temperature[1] is about -2 to -6 °C, the average annual number of days[2] with snowfall is about 50 and the mean winter precipitation[3] is about 500 mm. The problems on the road are mainly a result of the extreme snow amounts and the strong winds while the micro-scale landscape around the road plays a minor role. However, the mesoscale landscape plays an important role for the wind speed and direction because the site is located in a narrow valley.

An automatic weather station[4] (AWS) was installed in Kaperdalen in October 1998. It registered wind speed and direction, temperature and air humidity. Visibility observations on the road and notifications if precipitation was present were done manually by the snow plough operators. The registrations were based on a system developed by Norem (1975), where each observation is assigned a numerical value according to the estimated visual range along the road. In addition to that, the maintenance crew also kept a diary over the accessibility of the road, registering days

---

1. Norwegian Meteorological Institute: Nordic temperature maps, report no. 09/00.
2. Statens Kartverk: National Atlas of Norway: Climate.
3. Statens Kartverk: National Atlas of Norway: Water, snow and ice.
4. AWS 2700, Aanderaa Instruments: Bergen, Norway.
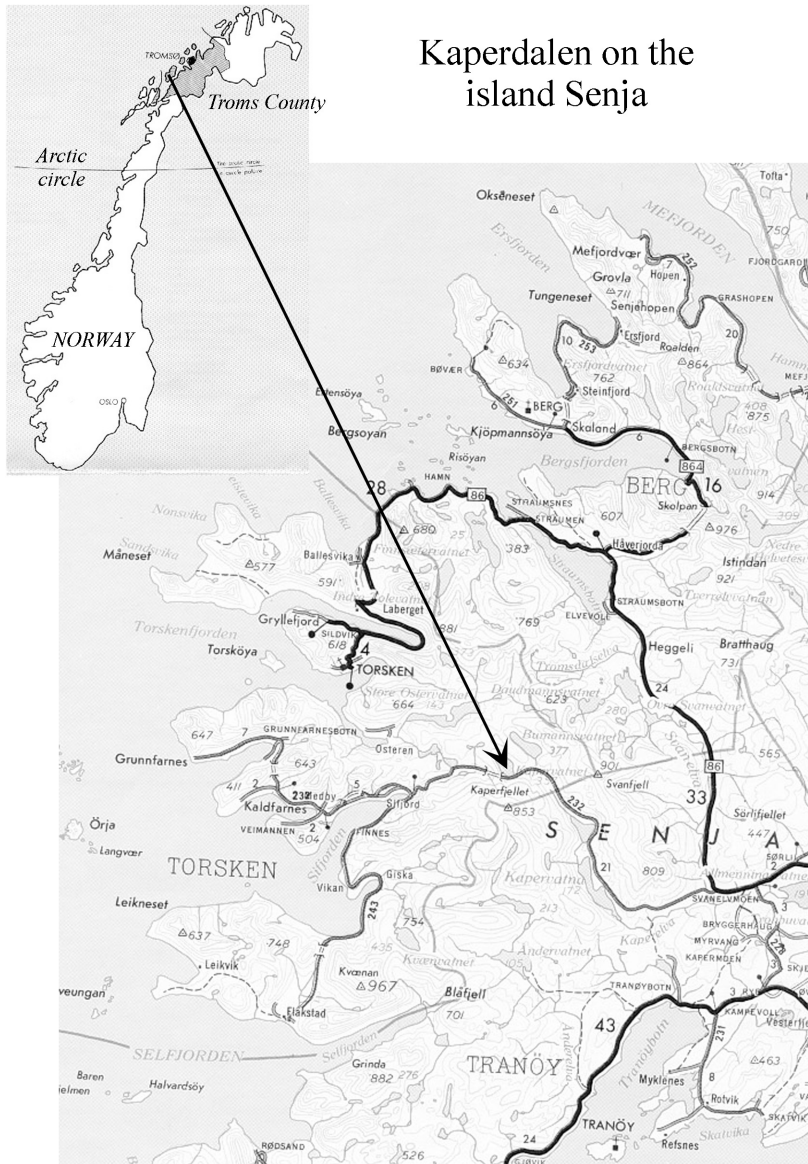
Figure 6.1 The study site at Kaperdalen valley on the island Senja.

with road closure and convoy driving etc. Snow surveys were done with optical surveying equipment (total station).

6.2.2 Results

6.2.3 Wind registrations

The first winter (1998-99) turned out to be unusually calm. Both snowfall amounts and the frequency of strong winds were low. On the other hand, the second winter (1999-00) was on the extreme opposite, with tremendous snow fall amounts and long periods of continuous storm. I found the two completely different winters a good combination for the means of the study.

Neither the occurrence nor the amount of snowfall was registered in the AWS in Kaperdalen and therefore it was not possible to use the method presented by eq. (6.1). Instead, wind roses were made for both all wind speeds and strong winds (>8 m/s) only. For the winter 1999-2000 a wind rose based on precipitation events registered manually by the maintenance crew was also made.

The comparison of results for strong wind speeds shows that easterly winds governed the weather the first winter (Figure 6.2) and westerly winds the second winter (Figure 6.3). The narrow sectors for the prevailing strong winds confirm the nature of the landscape to guide the wind along the valley. The frequency of strong winds was almost the same for the two winters, 24.1 % and 26.3 % respectively, and

Kaperdalen 1998-1999

Windspeeds >8.0 m/s
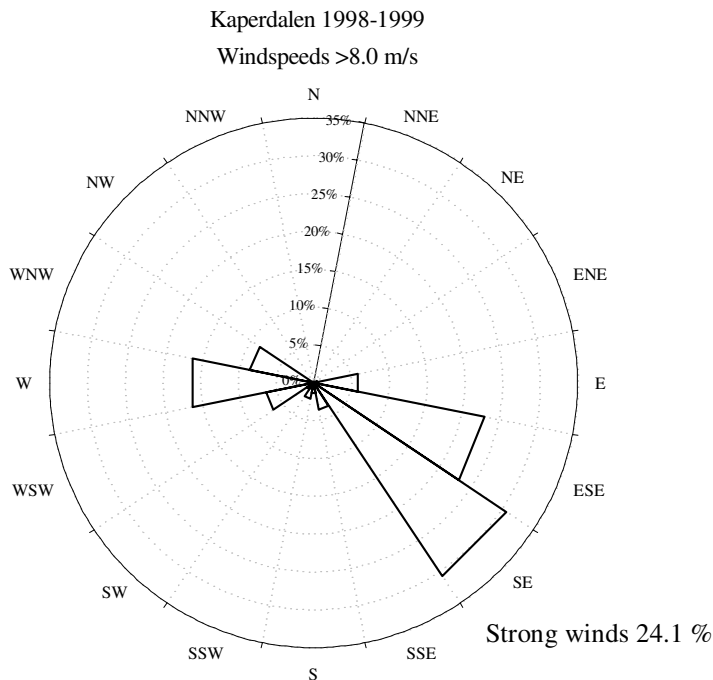
Figure 6.2 Wind rose for strong winds during the winter 1998-1999.

Kaperdalen 1999-2000

Windspeeds >8.0 m/s
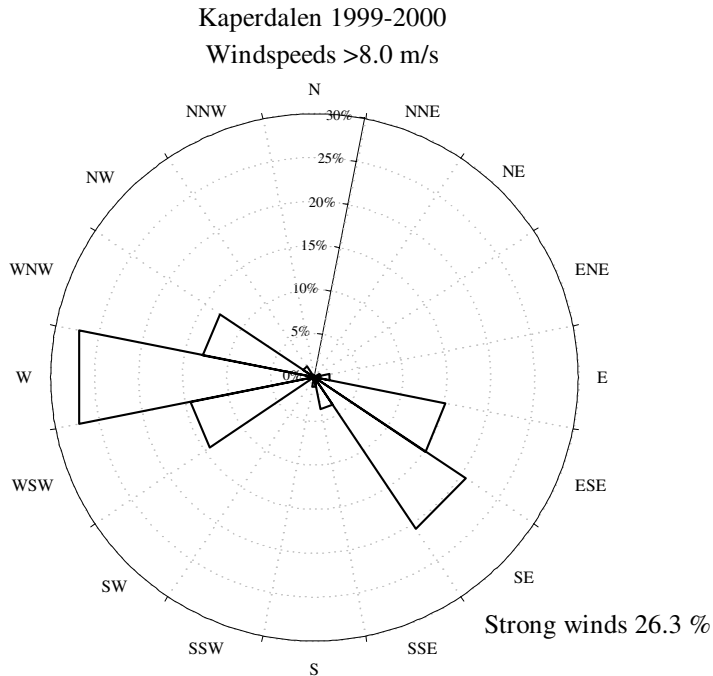
Figure 6.3 Wind rose for strong winds during the winter 1999-2000.

therefore the amount of snow and the wind speed during snowfall explain why the snow drifting problems were worse the second winter.

To demonstrate the importance of accounting for the snowfall events with simultaneous strong winds, Figure 6.4 was prepared by extracting only wind speed and direction when snowfall was registered manually in the road diary by the maintenance crew. The figure shows that winds from W and WNW are dominating for strong winds with simultaneous snowfall and are therefore the most hazardous for the snow drifting problems on the road. To further demonstrate how the wind conditions during snowfall are important, Figure 6.5 shows that precipitation during the first winter fell under calm winds from the south and during strong winds from the west the second winter.

6.2.4 Driving conditions

The road was divided into eight sections and the visibility along each was estimated by the truck driver from his seat. The observation system was described by Norem (1975) and is based on assigning a value for each observation according to the estimated visual range, as in Table 2. The investigated road sections are displayed in Figure 6.6. There are five sections along a 1600 m long portion east of the tunnel and three sections stretching over 800 m west of the tunnel. Table 3 shows an overview of the available diary entries. It should be noted that not all storms that actually occurred during the winter 1999-2000 are necessarily included in the diary for two

Kaperdalen 1999-2000
Precipitation directions
with similtaneuos strong winds
(>8.0 m/s)

Based on 32
manual observations
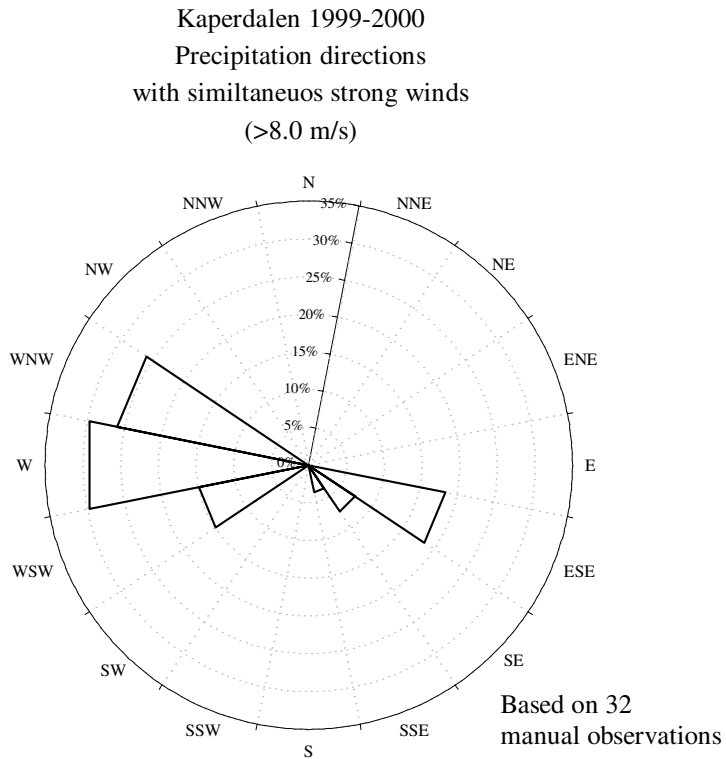
Figure 6.4 Wind rose showing the distribution of wind directions accociating strong winds and snowfall.
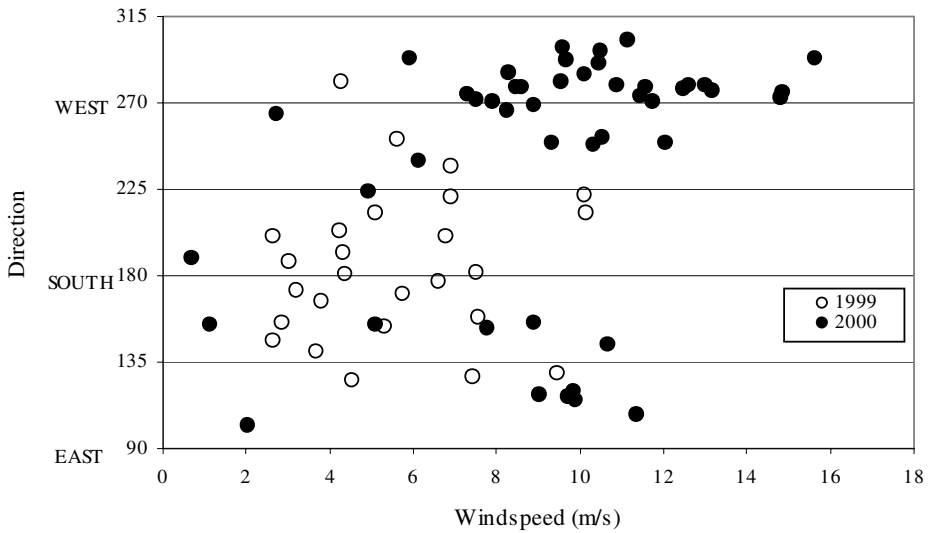
Figure 6.5 The diagram shows wind speed and direction during snow fall events registered in the maintenance crew diary.

Table 2: Point scale for visibility observations.

Visibility (m)	> 100	50-100	25-50	10-25	5-10	< 5
Points	1	2	3	4	5	6
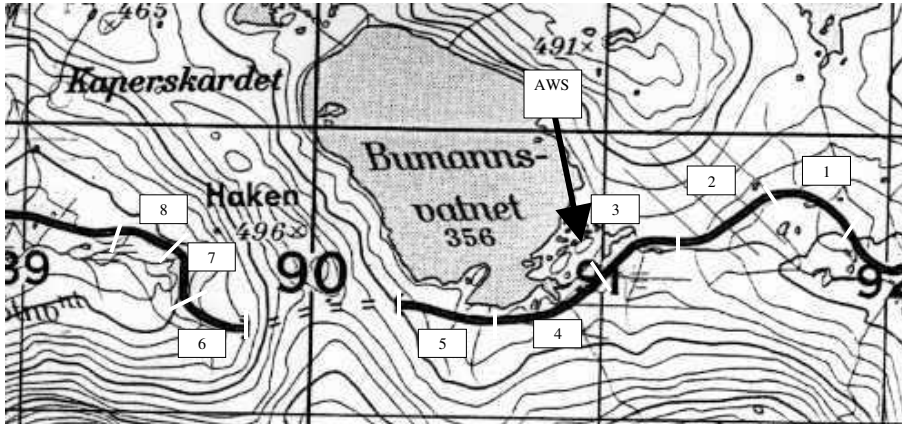
Figure 6.6 Marked road sections for visibility observation. Location of weather station (AWS) indicated by black arrow.

Table 3: Available log entries including visibility observations

	1998-99	1999-00
Number of log entries	48	64
Days with log entries	29	41
Days with snow fall	15	35
Days with convoy driving	2	15
Days with road closure	1	9[a]

a. Additional 20 days of closed road are logged without visibility observation.

reasons; the crew did not always manage to perform the visibility observation and the road was often impassible for several days due to storm.

The averaged point score for each road section was found for different types of weather. These results are presented in Figure 6.7 and show that road sections 3 and 4 are the most vulnerable on the road. The worst conditions are observed during winds from the west, with and without simultaneous snowfall.
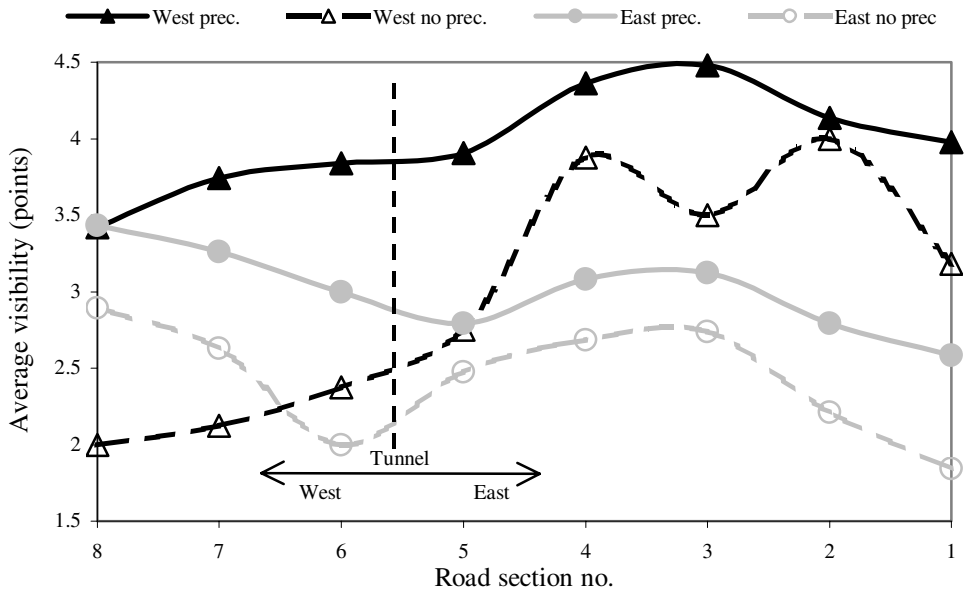
Figure 6.7 Average visibility on all road sections for different weather: Winds from the west or the east, with and without simultanous precipitation
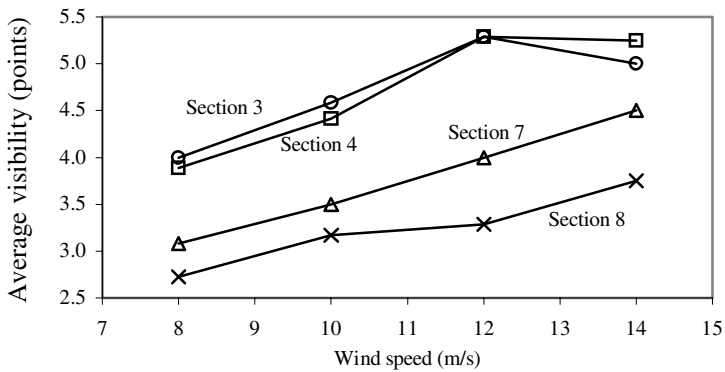
Figure 6.8 Average visibility on selected sections as a function of wind speed for westerly winds.

The visibility was also connected to measured wind speeds from the AWS. In Figure 6.8 it is clearly seen how the visibility decreases (higher point score) when the wind speed increases.

6.2.5 Snow survey

Snow depth was measured in chosen profiles along the road at the end of both winters (Figure 6.9). This gave information about how the snow tends to collect around the road and where the snowbanks on the road shoulder are highest. A selection of the
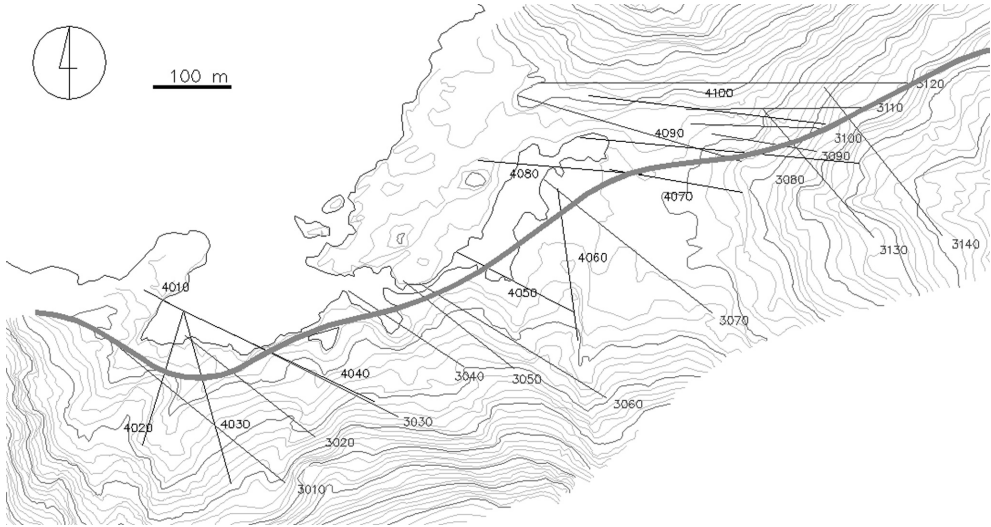
Figure 6.9 Location of profiles for snow survey. Profiles from year 1999 are assigned a 30xx number, year 2000 profiles have 40xx.

Figure 6.10 Snow survey in profiles 3030 and 4040 (above) and 4030 (below).

measured profiles is presented in Figure 6.10 and Figure 6.11. The measurements show that snow amounts on the ground as approximately twice as much in 2000 than in 1999. Snowbanks on the road shoulder in year 2000 were 3.5 m in profile 4020 and 4.5 m in profile 4100. To give a better understanding of the conditions on the road, Figure 6.12 shows a photograph taken in April 1999.
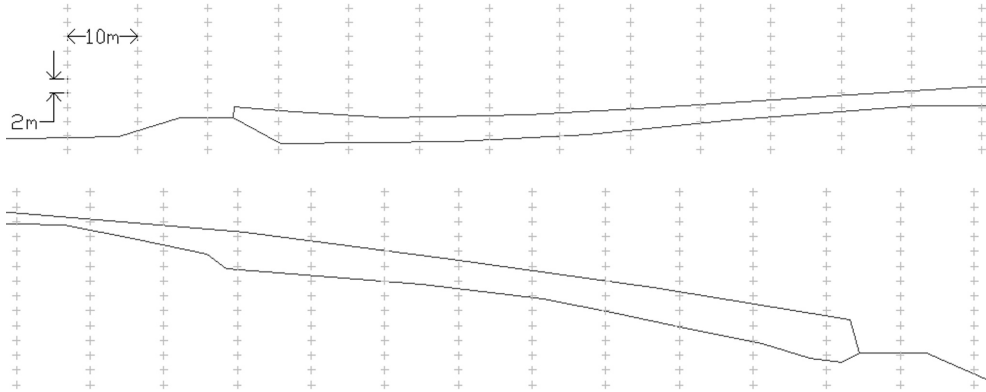
Figure 6.11 Snow survey in profiles 4050 (above) and 4100 (below).

Figure 6.12 Photograph taken in April 1999 in Kaperdalen. The caravan to the right is passing profile 4020. The high snowbanks along the road increase the vulnerability of the road to snow drifting.

6.2.6 Summary and proposed countermeasures

The main conclusions from this field program regarding the driving conditions can be summarized in two paragraphs:

1. Storms from the west with simultaneous precipitation cause the worst problems on the road. These events can be very frequent and last for several days.

2. Road sections no. 3 and 4 are the most vulnerable. This is where the road crosses the valley and is almost perpendicular to the winds from west (see Figure 6.6). These sections should have first priority under planning of countermeasures.

Countermeasures to reduce the snow problems and decrease the number of days with closures can be listed in order of priority:

1. The road should be elevated approximately 1 m on sections 3 and 4. The road width should also be increased from 6 m to approximately 7.5 m to facilitate snow removal and meeting of vehicles, especially snow removal equipment.

2. Auxiliary lanes for use of rotary snow blowers parallel to the traffic lanes should be constructed by widening the road shoulders. This is especially important where the adjacent terrain is high compared to the road surface but should preferably be done along the whole length of road sections 3 and 4.

In Figure 6.13 the proposed countermeasures are located on a map. A large volume of excavation in the vicinity of the road is needed to supply the demand for fill masses according to the countermeasures listed above. These masses should be taken where the terrain is high close to the road, and the excavation area should serve as a widened ditch for the road, enabling rotary blowers to remove snow from the excavated areas. A more detailed description of the proposed countermeasures lettered according to position on Figure 6.13 is:

A to D Excavation: 20 m wide ditch (Figure 6.14).

E Excavation: 50 m wide ditch.

F Excavation: 20 m wide ditch.

G Elevation of road embankment by 1 m. Widen the road from 6 to 7.5 m. (Even an auxiliary service lane should be made)

H Increase road width even where increased elevation is not included.

I This curve should be adjusted from R=120 to R=180 m.

In total, the proposal suggests replacing mass volumes of about 20.000 m^3, all of which has to be excavated in solid bedrock.
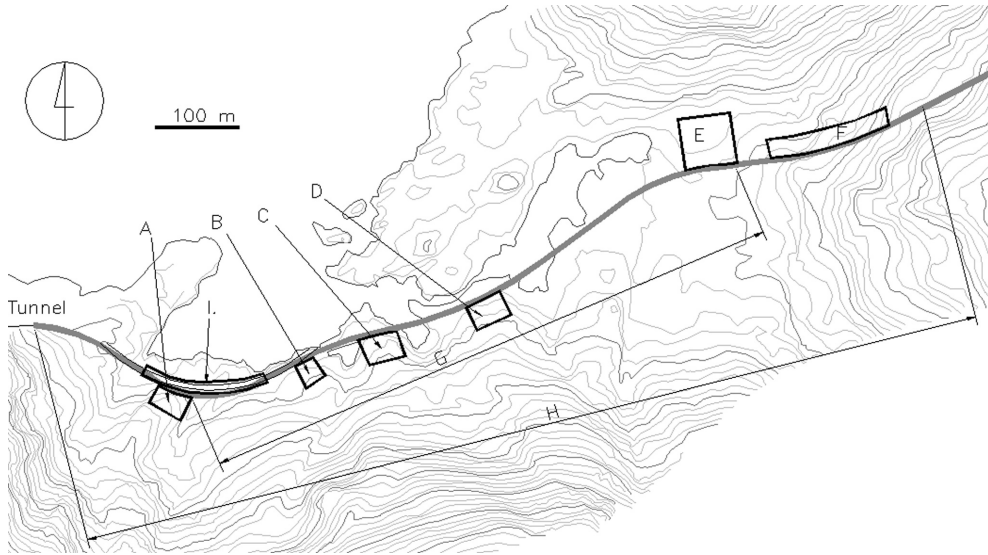
Figure 6.13 A map showing the location of proposed countermeasures in Kaperdalen.

Figure 6.14 Troublesome cut section at location "A" (Figure 6.13) in Kaperdalen.

6.3 Bolstadarhlidarbrekka study site

The Bolstadarhlidarbrekka study site is located on National Road no.1 in the north of Iceland, Figure 6.15. The climate of the site is characterised as a mild maritime climate, with frequent temperature fluctuations around the freezing point. Primary snow drifting exposure is due to strong winds from the north that often bring heavy snowfall.

   The road is located on a southward facing slope (Figure 6.16) and is in part located inside a natural snow sedimentation area which makes the road vulnerable to snow drifting during winters of high precipitation amounts. Besides that, part of the road is built under steep and high rock cuts which also can be troublesome. An automatic weather station was installed in the autumn 1998 at the site. It registered wind speed
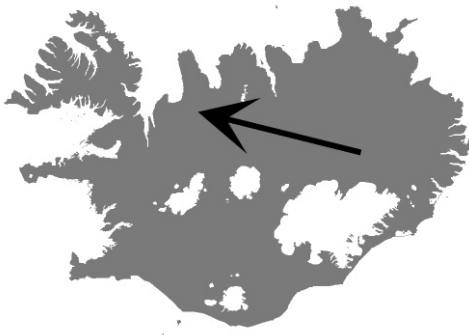
Figure 6.15 Location of the Bolstadarhlidarbrekka study site on National Road no.1 in Iceland.
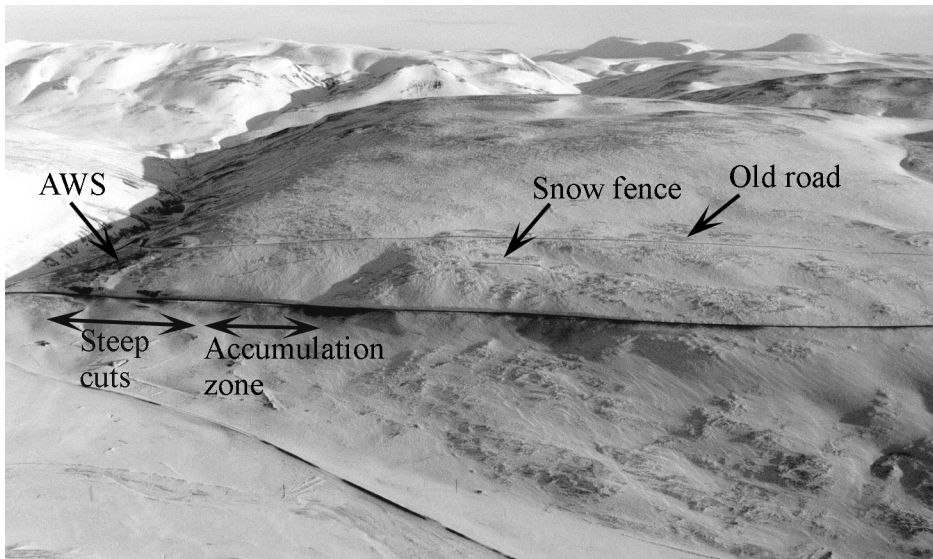
Figure 6.16 A photograph of the road in Bolstadarhlidarbrekka, view to the north.

and direction as well as temperature and relative humidity. Late winter 1999, snow survey was carried out in chosen profiles and snowdrifts were also photographed.

The results from this field investigation form the basis for many of the numerical wind simulations in the included papers in the thesis. Both topographic data and snow survey from the site were utilized in papers I, II, III and IV. Due to the conditions on the site, a visibility observation was not carried out here. The reason is that driving conditions on the road are generally good through the winter, apart from during snow storms from the north, when the road becomes impassible for several hours due to reduced visibility and snowdrifts on the road. More detailed description of the conditions is found in the papers and is not repeated here.

In normal winters, the snow problems on the road are seldom that severe that access to the road is impaired. However, experience has shown that during winters of extreme snowfall amounts and frequent strong winds, the road is unusually vulnerable, and keeping it open can be impossible for longer periods of time. In such cases, it is possible to direct the traffic to the old road (Figure 6.16), an operation that has proved successful before. I therefore suggest that the old road is maintained in good enough condition to allow instantaneous utilization when necessary. Alternatively, to protect the main road from snow drifting in its current path would either demand extensive earthwork or the construction of snow fences upwind from the steep cut sections and the main snow accumulation zone.

Figure 6.17 Heavy snow banks at the road in Bolstadarhlidarbrekka.

7. PAPERS CONTEXT

7.1 Paper I: *Simulation of two-dimensional wind flow and snow drifting application for roads: Part I*

The main objective in this paper is to set up and test the flow solver, Flow3D. Two-dimensional (2D) flow over the Askervein hill was simulated and compared to available data from that site, both measurements and simulations from other investigators. The performance of the model proved satisfactory, and a procedure to extract the wind speed values at a fixed height along the surface was utilized to create diagrams of the wind speed evolution along topographic profiles.

Wind flow in 2D profiles along the prevailing snow drifting wind direction from the Bolstadarhlidarbrekka study site was simulated. Simulations were done for both the terrain in the absence of any snow accumulations (summer conditions) and for the terrain with measured snowdrifts. Wind speed evolution for both cases was plotted in the same diagram, also showing the terrain profile with and without measured snowdrifts. The main conclusion from this work is that the wind speed evolution along 2D terrain profiles gives information about the location of heavy snow sedimentation areas because the wind speed falls considerably there.

7.2 Paper II: *Simulation of two-dimensional wind flow and snow drifting application for roads: Part II*

The simulation results from paper I are used in this paper. The aim was to apply known empirical relations for snow transport, sedimentation and wind speed on the speed evolution curves from the previous simulations. The simulations showed that after the drift had accumulated on the ground, the wind speed (or the friction velocity) along the ground had risen over the sedimentation area. The difference in wind speed before and after drift accumulation showed good correlation with the surface elevation due to snow accumulation. Further, this relationship was used to calibrate an empirical snow transport formula.

The horizontal friction velocity gradient along the snowdrift surface was transformed into a horizontal snow transport gradient, using an empirical snow transport formula. This gradient was then compared to the difference in surface slopes between the ground upwind from the drift and the slope of the drift itself. A linear relationship was found between the parameters (Figure 10). This concept is not adopted in the continuing work with snow drifting on 2D downslopes in paper III. The reason for this is that my understanding of the problem has developed towards the conclusion that equilibrium snowdrift surfaces exist even if the wind speed along the surface is falling. The vertical axis in Figure 10, should therefore have indicated the rate of wind speed reduction and not the reduction of snow transport. In other words, I believe that the snow surfaces in fact were true equilibrium surfaces, with no further deposition possible along the main portion of the drift. The change in snow transport along the surface, dQ/dx, is zero but the horizontal wind speed gradient, du/dx is

depending on the angle between the drift surface and the upwind terrain surface, an assumption that is more in harmony with eq. (6) in paper III.

Although I later partially abandon the conclusions, the work is a step toward defining the flow conditions associated with a fully developed equilibrium snowdrift surface on the ground. For drift free roads, it is essential that the equilibrium surface does not extend onto the road surface.

7.3 Paper III: *Snow sedimentation in gently sloping road cuts*

This paper continues the discussion on snow drifting on downslopes that can be described as a 2D flow. Data from the previous papers is used, as well as new wind field simulations for an idealized terrain slope. The paper has three main objectives: (1) Identification of general criteria for snowdrift sedimentation to initiate at a particular point. (2) Description of the wind speed evolution in gentle sidehill cuts, and definition of the flow criteria for a drift free road. (3) To propose a procedure that allows the use of topographic data only to predict the maximum extension of a fully developed snowdrift surface.

The results suggest that heavy snow deposition does not happen on slopes that are less than 20 % downwards along the wind direction. This assumption is though depending on the character of the upwind terrain, meaning that the critical slope is probably less when the flow has passed a hill top, than when the upwind terrain is a continuous slope or a flat plain. When the local terrain slope exceeds this value, the sudden wind speed reduction can cause heavy deposition. Downwind of such an area, the road should be placed so that the wind speed has increased high enough to provide a snow erosion zone over the road. It is demonstrated how pure wind flow simulations are sufficient to check the performance of a proposed gentle slope cut with respect to snow drifting.

The most important contribution of the paper is a statistical model that creates a streamlined equilibrium snow drift surfaces based on topographic information only. The model is suitable to estimate the validity of a predicted snowdrift extension, and is therefore helpful to design gently sloping cuts that ensure that the road is located in a snow erosion zone.

7.4 Paper IV: *Snow drifting on roads under steep sidehill cuts*

This paper covers snow drifting in steep road cuts. It is probably under this topic where the advances of using Computational Fluid Dynamics are most prominent. Using wind simulations here, it was possible to describe the three-dimensional (3D) flow pattern that generally develops in steep road cuts. The 3D flow pattern results in snowdrift distribution that is not uniform along the cut. An important goal in the paper was to investigate how the cut design should consider this.

The results indicate that a vortex forms under the cut and travels in a direction parallel the road. This vortex is capable of transporting large amounts of drifting snow which are deposited when the vortex migrates into the mean flow at the cut end, or when it's transport capacity is fully utilized. An alternative principle for steep cut

design was proposed. The new design facilitates for higher wind speed under the cut and promotes the deposition of snow outside the road. It is also expected to improve the visibility on the road considerably under snow storm. I find this concept promising for full scale testing.

7.5 Paper V: *Design criteria for roads in snow-drifting areas*

The paper summarizes some of the results that were available during an intermediate stage of the work. Only the discussion of the performance of different guard-rail profiles in snow drifting is not covered by the other papers, and is therefore the most important original contribution of the paper. It was demonstrated how the choice of a guard-rail profile that exhibits low fluid dynamical drag is likely to perform better in drifting snow than a high-drag profile. This fact has been put in practice before, e.g. by the use of wire safety barriers, and narrow pipe guard rails. However, the findings of the investigation suggest that a safety barrier of a relatively large cross sectional area still can be applicable in snow-drifting areas, pending the drag coefficient of the shape. This is specially interesting for the utilization of wood in safety guard rails.

7.6 Paper VI: *Wind tunnel experiments and numerical simulation of snow drifting around an avalanche protecting dam*

Although not directly dealing with road engineering, the work in this paper was important for inspiring the work with steep road cuts, presented in paper IV. The wind tunnel tests on snow-drifting around avalanche dams were initiated by the Icelandic Meteorological Institute. A substantial part of the avalanche protection program in Iceland is the construction of deflecting and collecting dams. Little experience has been collected before on the ability of these dams to intercept drifting snow, and accumulate it around the dam. It is believed that heavy drift accumulations in front of the dam may reduce it's efficiency when snow avalanches occur. What makes this problem specially important is that the same weather conditions cause avalanche hazard and snow accumulation around the dam at the same time.

To imitate a 20 m high and a 300 m long dam in the wind tunnel and maintain the ratio of horizontal and vertical lengths, a model in scale 1:100 was used. This endangers the similitude scaling for snow drifting in the model. The main task of the paper was to compare the wind flow for a prototype avalanche dam with the flow in the scale model and to evaluate the validity of the wind tunnel results.

The main findings suggest that the snow pattern observed upwind from the model dam is probably valid for the prototype. For the downwind situation the wind flow simulations revealed a large difference in turbulence activity and the mean flow pattern between the model and prototype, for a dam that is perpendicular to the wind. Neither did the downwind snowdrifts for the perpendicular dam observed in the wind tunnel appear convincing for prototype interpretation. When the dam was oblique to the wind direction on the other hand, the turbulent quantities and the mean flow was similar for the model and the prototype simulations.

8. CONCLUSIONS

8.1 General

Wind flow in road cuts was analysed with the help of Computational Fluid Dynamics. The wind flow results were compared to snow surveys, to explain the snow drifting in light of the wind pattern. It has been demonstrated that the use of pure wind flow simulations of both 2D and 3D flow can contribute to snow drifting research for roads. The work has resulted in recommendations for the design of road cuts in snow drifting areas. Road cuts were emphasised in this theses, because snow drifting in road cuts presents one of the greatest challenges faced by the drivers, maintenance personnel and road engineers. Also, in light of previous works by other investigators, more knowledge on road cuts is needed.

The original contribution of the thesis to road engineering is of both theoretic and practical character. An important result of the work is the distinction between two- and three-dimensional flow patterns around roads. A 2D flow situation is mainly associated with terrain and road design that exhibits small changes in the direction of the road. Gradually sloping cuts generally develop 2D flow. Where the terrain adjacent to the road changes rapidly, and especially behind sharp edges such as in steep road cuts, the wind and snow drifting is only described adequately as a 3D flow. New findings for road cuts are presented in paper III and paper IV, which treat gradual cuts and steep cuts respectively.

Apart from road engineering, new findings were achieved regarding the modeling process and snow drifting interpretation of wind simulation results. From the work with the avalanche dam, interesting results were found on scaling in physical modeling and for snow accumulation around the dam.

8.2 Results summary

The most important findings of the thesis are summarised in the following section. For convenience, the results are presented in three parts according to their field of interest.

8.2.1 Road engineering in snow drifting areas

1. On leeward facing hillsides, local terrain slopes of less than 20 % are not likely to cause heavy snow deposition. The critical slope is however probably depending on the upwind landscape (Paper III).

2. On downwind slopes prone to sedimentation, where the terrain can be approximated by a straight line, the wind speed falls approximately linearly along the ground or the drift surface (Paper III).

3. The design of a drift free road cross section should facilitate a snow erosion zone on the road surface. If the road is downwind of a sedimentation area, a substantial wind speed rise thus has to occur over the road embankment (Paper III).

4. A mathematical scheme for creating equilibrium snowdrift surfaces by terrain slope weighing was proposed. The method is useful for evaluating the validity of predicted snowdrift extensions in road cuts and natural deposition zones (Paper III).

5. A design for steep road cuts was proposed. The cut should have a curved or streamlined design in the horizontal plane, shifting both cut ends away from the road. The proposed design increases the speed of the vortex under the cut and creates less turbulent flow. The results are promising for both snow accumulation around the road and the visibility. This curved design of the cut also exhibits a more pleasant visual appearance in the landscape than a straight cut following the road direction (Paper IV).

6. A low drag profile for safety guard rails causes less snow deposition on the road and better visibility than a high drag profile. Even a relatively thick or high profile is believed to be applicable if the drag coefficient is low (Paper V).

8.2.2 Model application in snow drifting research

Wind flow simulations give good information on snow drifting conditions. The wind speed curve close to the ground in 2D flow situation can give information on the following:

1. Heavy sedimentation areas are identified by a sharp fall in the wind speed (Paper I).

2. The normalized wind speed curve is the same for any reference wind speed. Only one simulation is therefore needed to get information on the wind speed evolution along the 2D profile for any input wind speed (Paper I and II).

3. The magnitude of the horizontal wind speed gradient close to the ground, du/dx, indicates the relative initial rate of deposition. An area of high negative value of the gradient will therefore extract and accumulate more snow per time unit from the wind than an area featuring a lower gradient (Paper II).

4. The magnitude of the wind speed drop in a sedimentation area is proportional to the total snow accumulation capacity of the terrain feature (Paper II).

Mean flow vortices in 3D flow can be informative on snow transport and sedimentation:

5. A vortex with low tangential velocity with the ground and whose axis makes a large angle with the mean flow direction is likely to deposit more snow than one with high velocity and more parallel direction to the mean flow (Paper IV).

6. The spot of vortex termination, where the vortex motion is dissipated in the mean flow is a potential sedimentation area (Paper IV and VI).

Conclusions for physical scale modeling in full scale snow drifting:

7. Use of model scale 1:100 is successful for upwind drift modeling but less accurate for downwind drifts when using artificial snow as the entrained material (Paper VI).

8.2.3 Wind and snow drifting around large, long and steep earth dams

1. Windward drift accumulation upwind of steep and long structures is large over an upwind distance of 4 times the structure height for a perpendicular wind direction and 2 times the height for a structure aligned 30° to the wind direction (Paper VI).

2. A wind speed increase of up to 20 % was found over a large area downwind of a structure aligned 30° to the wind direction (Paper VI).

8.3 Recommendations for future works

In general, results based on numerical simulations will most often need a further validation. Although the present results are coupled to on site investigations, the final performance of the recommended solutions is yet to be proved. The solutions presented here do neither add considerable additional cost to the design process nor the construction of future road projects, and are therefore feasible for full scale implementation. It is likely that their implementation allows for further development and improvements to the principles.

It has been shown that the use of numerical simulations can lead to new findings for road engineering in snow drifting areas. Other topics of the road design that have not been covered in this work may benefit from such analysis. This could as an example be the study of interactions between road embankment slope and height and the superelevation in curves.

9. REFERENCES

Amundsen, I., 1995. Vegutforming og landskapstilpassing. Visuelle forhold i norsk vegbygging fra 1930 til i dag. Thesis. (In Norwegian). NTH, Trondheim.

Anderson, H.I., 1988. Lecture notes in Subject 76572 Turbulent flow. Dept.of Physics and Math., NTH, Trondheim.

Arya, S.P., 1982. Atmospheric boundary layers over homogeneous terrain. In: Plate, E.(Editor), Studies in Wind Engineering and Industrial Aerodynamics. Engineering Meteorology: Fundamentals of Meteorology and Their Application to Problems in Environmental and Civil Engineering. Elsevier, Amsterdam, pp. 233-267.

Bagnold, R.A., 1941. The Physics of Blown Sand and Desert Dunes. Methuen and Co. Ltd., London.

Baker, C.J. and Dutch, W.G., 1995. An investigation into the potential use of solid snow barriers on the Snake Pass, Derbyshire. Proceedings of The Institution of Civil Engineers 95: 151-160.

Barltrop, N.D.P. and Adams, A.J., 1991. Dynamics of fixed marine structures. Butterworth-Heinemann, Oxford.

Bruland, O., 2002. Dynamics of the Seasonal Snowcover in the Arctic. Thesis. Norwegian University of Science and Technology, Trondheim.

Budd, W.F., Dingle, W.R.J. and Radok, U., 1965. The Byrd Snowdrift Project: Outline and basic results. Studies in Antarctic Meteorology, Antarctic Research Series 9: 71-134.

Cushman-Roisin, B., 1994. Introduction to Geophysical Fluid Dynamics. Prentice Hall, New Jersey.

Dannevig, P., 1968. Fjellboka. (In Norwegian). A/S Nordanger-Bergen & Park Forlag, Bergen.

Duntley, S.Q., 1948. The reduction of Apparent Contrast by the Atmosphere. Journal of the Optical Society of America 38: 179-191.

Gauer, P., 1999. Blowing and drifting snow in alpine terrain: A physically-based numerical model and related field measurements. Mitteilungen des Eidgenössischen Institutes für Schnee- und Lawinenforschung. Eidgenössisches Institut für Schnee- und Lawinenforschung, Davos.

Gerhart, P.M., Gross, R.J. and Hochstein, J.I., 1992. Fundamentals of fluid mechanics. Addison-Wesley Publishing Company, Reading.

Gurer, I., Sato, T., Kosugi, K., Kamata, Y. and Sato, A., 2002. Comparison of the models of different types of snow fences in a cold wind tunnel. Proceedings of the XIth PIARC International Winter Road Congress, 28-31 January 2002, Sapporo, Japan.

Haraldsdottir, S.H., Thordarson, S., Olafsson, H. and Norem, H., 2002. Drifting snow around an avalanche dam in a wind-tunnel. Materiali Glyaciologicheskikh Issledovanii (Data of Glaciological Studies) 93.

Iversen, J.D., 1980. Drifting-snow similitude transport-rate and roughness modeling. Journal of Glaciology 26: 393-403.

Jaedicke, C., 2001. Drifting snow and snow accumulation in complex arctic terrain. Field experiments and numerical modelling. Geophysical Institute, University of Bergen, Bergen.

Kobayashi, D., 1972. Contributions from the Institute of Low Temperature Science. Hokkaido University, Sapporo.

Liljequist, G.H., 1957. Energy exchange of an Antarctic snow-field. Norwegian-British-Swedish Antarctic expedition, 1949-52. Scientific results. Norsk Polarinstitutt, Oslo.

Liston, G.E. and Sturm, M., 1998. A snow-transport model for complex terrain. Journal of Glaciology 44: 498-516.

Male, D.H., 1980. The seasonal snowcover. In: Colbeck, S.C.(Editor), Dynamics of Ice and Snow Masses. Academic Press, New York, pp. 305-395.

Mellor, M., 1966. Light scattering and particle aggregation in snow storms. Research Report 193, CRREL, Hanover

Middleton, W.E.K., 1952. Vision through the atmosphere. University of Toronto Press, Canada.

Naaim-Bouvet, F., 1995. Comparison of requirements for modeling snowdrift in the case of outdoor and wind tunnel experiments. Surveys in Geophysics 16: 711-727.

Nemoto, M. and Nishimura, K., 2001. Direct measurements of shear stress during snow saltation. Boundary-Layer Meteorology 100: 149-170.

Nishimura, K. and Hunt, J.C.R., 2000. Saltation and incipient suspension above a flat particle bed below a turbulent boundary layer. Journal of Fluid Mechanics 417: 77-102.

Norem, H., 1975. Designing highways situated in areas of drifting snow. Draft translation 503. CRREL, Hanover, New Hampshire.

Norem, H., 1994. Snow Engineering for Roads. Handbook no. 174. Norwegian Public Road Administration, Road Research Laboratory, Oslo.

Norem, H., Sætran, L.R. and Thordarson, S., 2002. Measures to reduce the generation of "snow smoke" behind heavy vehicles. Proceedings of the XIth PIARC International Winter Road Congress, 28-31 January 2002, Sapporo, Japan.

Owen, P.R., 1964. Saltation of uniform grains in air. Journal of Fluid Mechanics 20: 225-242.

Pomeroy, J.W. and Gray, D.M., 1990. Saltation of Snow. Water Resources Research 26: 1583-1594.

Pomeroy, J.W., 1989. A process-based model of snow drifting. Annals of Glaciology 13: 237-240.

Richards, P.J. and Hoxey, R.P., 1993. Appropriate boundary conditions for computational wind engineering models using the k-e turbulence model. Journal of Wind Engineering and Industrial Aerodynamics 46 & 47: 145-153.

ROADEX, 2001. Winter Maintenance Practice in the Northern Periphery. Roadex sub project B, phase I. State-of-the-art study report. ERDF article 10, Northern Periphery Programme.

Stull, R.B., 1988. An Introduction to Boundary Layer Meteorology. Kluwer Academic Publishers, Dordrecht.

References

Sundsboe, P.A. and Hansen, E.W.M., 1996. Modelling and numerical simulation of snow drift around snow fences. In: Izumi, M., Nakamura, T. & Sack, R.L.(Editors), Proceedings of the Third International Conference on Snow Engineering. A.A. Balkema, Rotterdam, pp. 353-359.

Sundsboe, P.A., 1997. Numerical modelling and simulation of snow drift. Thesis. Norwegian University of Science and Technology, Trondheim.

Tabler, R.D., 1991. Snow transport as a function of wind speed and height. In: Sodhi, D.S.(Editor), Proceedings of The 6th International Cold Regions Specialty Conference. ASCE, New York, pp. 685-697.

Tabler, R.D., 1994. Design Guidelines for the Control of Blowing and Drifting Snow. SHRP-H-381. National Research Council, Washington, DC.

Tabler, R.D., 1988. Snow Fence Handbook. Tabler & Associates, Laramie, Wyoming.

Tabler, R.D., 1980. Self-similarity of wind profiles in blowing snow allows for outdoor modeling. Journal of Glaciology 26: 421-434.

Takeuchi, M., 1980. Vertical profile and horizontal increase of drift-snow transport. Journal of Glaciology 26: 481-492.

Taylor, P.A. and Teunissen, H.W., 1987. The Askervein Hill Project: Overview and background data. Boundary-Layer Meteorology 39: 15-39.

Thiis, T.K., 2000. Experimental validations of numerical simulations of snowdrifts around buildings and in terrain. Thesis. Norwegian University of Science and Technology, Trondheim.

White, F.M., 1988. Fluid Mechanics. McGraw-Hill Book Company, New York.

Wieringa, J., 1993. Representative roughness parameters for homogeneous terrain. Boundary-Layer Meteorology 63: 323-363.

Wiik, T., 1999. Wind loads on low rise buildings: A numerical and experimental study of effects caused by building details on the external surface pressure. Thesis. Norwegian University of Science and Technology, Trondheim.

Paper I:
Simulation of two-dimensional wind flow and
snow drifting application for roads: Part I

Simulation of two-dimensional wind flow and snow drifting application for roads: Part I

S. Thordarson & H. Norem

Norwegian University of Science and Technology,
Department of Road and Railway Engineering, Trondheim, Norway

ABSTRACT: Snowdrift sedimentation on leeward facing mountain slopes and terrain ridges makes road planning in certain areas very difficult. Problem areas are frequently found on leeward facing slopes where the wind blows perpendicular over the road. We use the commercial computational fluid dynamics code Flow 3D to simulate two-dimensional wind flow, in order to quantify the snow drifting conditions for roads. To evaluate the numerical model, the study includes a comparison to Askervein Hill data. The main idea of the study is to simulate the wind flow over original terrain profiles and the flow over actual observed snowdrifts, and compare the resulting friction velocity profiles. We use this comparison to estimate the snow drifting rate, and the effect and capacity of natural snow sedimentation areas. We propose a relationship between the slope of the terrain upwind from the snowdrift area, the slope of the drift and the horizontal rate of change of the snow drifting rate.

1. INTRODUCTION

Road planning in snow drifting areas is a challenging task, especially where complex terrain influences the sedimentation of drifted snow on the ground. Wind flow in the lowest part of the atmospheric boundary layer is modified by landscape and terrain features, which explains why snow drifting conditions are subject to large spatial variations, even locally. Computational fluid dynamics (CFD) is used in this study to analyse the wind flow around roads with respect to snow drifting conditions.

Several investigators have used CFD to predict snowdrifts around snow fences (e.g. Sundsbø 1997) and buildings (e.g. Thiis 2000, Waechter et al. 1997) or made general models for snow drifting (e.g. Shao & Li 1999, Pomeroy & Gray 1990, Sato et al. 1997, Uematsu et al. 1989). Significantly less has been done with CFD in the area of road and highway engineering and more knowledge and guidelines are needed in this area of work.

In this first part of two of the report, the objective was to test and evaluate the CFD code Flow3D as a tool for simulation of atmospheric boundary layer wind flow over complex terrain, and to simulate wind flow over several two-dimensional terrain

profiles from a study site. The second part of the report deals with snow drifting application of the results from the study site.

The present part of the report includes a simulation of wind flow over Askervein Hill, and a comparison with measured and simulated results from other authors. For details on the Askervein Hill Project, see Taylor & Teunissen (1987). We conclude that this comparison confirms that the numerical procedure in use will simulate the characteristics of the mean wind flow on downslopes of the scale in question up to an acceptable accuracy. The simulations from the study site were done over original ground profiles and over measured snow cover in the same profiles. The results confirm that a plain wind simulation can be an aid to identify areas for large snowdrift sedimentation.

2. METHODS

2.1 Wind field simulation

The simulated area and the terrain height difference on the study site is on such a large scale, that the use of a plain engineering numerical flow model for the wind flow becomes questionable. Wind flow over complex terrain and hills is the subject of boundary layer meteorology and has been simulated numerically by many investigators (e.g Ying 1994, Wood 1995, Davies et al. 1995, Beljaars et al. 1987, Raithby & Stubley 1987).

The code used for the wind field simulation in this study is Flow3D (Flow Science, Los Alamos NM, USA). For post processing of the results we used Field View (Intelligent Light, USA). The code has been customized to account for logarithmic inlet and initial conditions for the wind flow over complex terrain and a feature to trace calculated values along a surface at an arbitrary elevation above the ground has also been added. Flow3D applies a rectangular calculation mesh and uses the FAVOR technique (Flow Science, 1997) to adapt the mesh to the flow geometry, which in this case is two-dimensional terrain profiles. This is done by integrating a volume fraction into the momentum equations to account for partially blocked computational cells at the boundary to geometric objects in the flow field. The FAVOR method makes grid generation a straight forward task and enables complex geometry to be resolved without time-consuming grid generation. Although the FAVOR method is very handy for the integration of terrain in the flow field, one drawback has to be dealt with when tracing computed values along the boundary to a complex geometric feature; the rectangular discretization results in spatially fluctuating gradients in the flow field very close to the boundary. Although these fluctuations may not have serious impact on the flow physics, they make the curve of extracted values along the boundary highly fluctuating and difficult to interpret. As a mitigation, we found that choosing cell aspect ratio, dz_{cell}/dx_{cell}, that follows the slope on the ground smoothens out these fluctuations to a certain degree.

Even when optimizing the grid spacing according to terrain slope, abrupt change in slope and the appearance of minor terrain perturbations gives unphysical

fluctuations as described above, and hence since the shear stress along the ground is of main interest for this study, we had to employ a different method on estimating the surface shear stress. In stead of tracing the shear stress along the surface boundary, we extract the velocity at height dz_{cell} along the surface, where dz_{cell} is the vertical spacing between computational points in the finite difference discretization. Since the velocity calculated at height dz_{cell} is in the vicinity of the surface we find it reasonable to assume a logarithmic decrease in velocity from that point and down to the surface. Hence, we can solve for the friction velocity directly from eq. (1). The resulting curve is relatively smooth and any fluctuations can be explained by the nature of the underlying terrain.

The code solves the Navier-Stokes equations for the mean wind speed together with the mass continuity equation, and turbulence closure is achieved through a standard k-e model. For further information on the features of Flow3D we refer to Sundsbø (1997) or Flow Science (1997).

2.2 Roughness modelling

The roughness height, z_0, can not be modelled directly in Flow3D. In general, solid boundaries are treated as smooth surfaces, and here with a no-slip condition. However, object roughness can be applied by adjusting the fluid viscosity in the first cell row enclosing the object, but we did not get control over this feature and therefore the terrain surface in our model is practically smooth.

In nature, when wind with a certain velocity distribution describing a boundary layer developed over terrain of a certain roughness, travels over to a new surface which has another roughness, an inner boundary layer based on the new surface roughness will develop inside the former (Stull 1988). The information about the new roughness is transported vertically up into the flow by diffusion and the inner boundary layer will grow higher as the wind moves further down the new surface. This will also happen in a numerical model, when the inlet boundary describes a logarithmic boundary layer of certain roughness, but the underlying terrain has another roughness. The growth rate of the inner boundary layer depends on the efficiency of diffusion in the model, which depends on how fine the computational mesh is. High vertical gradients near the surface will not be resolved by a coarse grid, thus disabling diffusion. Choosing a coarser grid will therefore help to sustain the initial roughness through the simulation domain and minimize the disturbing effect of the virtually smooth underlying surface in the model.

2.3 Boundary conditions and domain dimensions

The extension of the two-dimensional profiles at the study site is up to 1000 m and the terrain height difference is about 150 m. This large height difference and the inevitable high simulation domain is on such a scale that the effect from possible thermal stratification has to be discussed. However, assuming neutral stability in the atmospheric boundary layer and a flat upwind terrain, the logarithmic wind profile can be applied (Stull 1988):

$$u(z) \; = \; \frac{u_*}{\kappa} \ln \left(\frac{z}{z_0} \right) \tag{1}$$

where

$u(z)$ = mean wind speed at height z

u_* = friction velocity

κ = von Karman's constant

z_0 = aerodynamic roughness length

It is well documented that atmospheric shear stress on the ground is the governing factor concerning whether snow particles are eroded from the ground or deposited to form drifts. The goal for the wind field simulation is to quantify the shear stress variations along the two-dimensional terrain profiles during strong winds. The friction velocity, u_*, is per definition representing the surface shear stress:

$$u_* \; = \; \sqrt{\frac{\tau_0}{\rho}} \tag{2}$$

where τ_0 is the shear stress at ground level and ρ is the density of air.

The bottom boundary condition applied in our model has been described in the previous section. Probably the most difficult boundary to treat in this simulation is the inlet boundary. Because the terrain upwind from the simulated area is complex, the actual shape of the inlet velocity profile will be different for different locations and we did not have the opportunity to measure the shape of the velocity profile for the individual profiles investigated here. Since the upwind terrain is relatively flat, although complex in nature, a logarithmic inlet boundary based on eq. (1) is chosen. The outflow boundary has been chosen as continuative, that is, forcing all horizontal derivatives to zero at the boundary. This outflow condition is the most common one found in previous studies.

Although located several hundred meters above the bottom of the computational domain, the choice for a boundary condition at the top was found to be critical. When applying a solid lid with free slip, the recirculation zone formed below the steep incline of the road embankment in some of the simulated terrain profiles would gradually move up the hill during the calculation until large portion of the simulation domain would lie in a recirculating zone. By applying a constant pressure boundary condition at the top, this problem was avoided and the point of separation remained at a fixed location in those profiles where separation occurred. The top boundary pressure is set to 990 mbar in all simulations.

The terrain profiles from the test site are about 1000 m long, from top of the hill down to the valley bottom. The computational domain is stretched all the way down to the flat ground to capture the whole height difference in the model. Also when choosing a suitable height for the domain, the total height difference along the terrain profile has to be considered. In their Askervein simulation, Raithby & Stubly (1987) used 700 m domain height, which corresponds to roughly 7 times the terrain height

difference. We tested the domain height in our model to find that the velocity near the ground did not change remarkably when the domain height was in excess of 4 to 5 times the downslope height. This proportion being lower than the one found necessary for isolated hills can probably be explained by the nature of the flow geometry when only a downslope hill is simulated instead of an isolated symmetrical hill.

The computational grid used in our model has 2 m spacing in the vertical up to a level 10 m above the highest portion of the slope and is increased to 10-15 m at the top boundary to save computational costs. The horizontal spacing is varying according to terrain slope, such that dz_{cell}/dx_{cell} roughly equals the terrain slope, dz/dx. However on the upper and flatter portion of the terrain profile the spacing is set more dense than the slope indicates.

3. RESULTS

3.1 Model comparison to Askervein Hill data

To test the numerical code against other atmospheric studies, a simulation was done over a two-dimensional sinusoidal hill. The Askervein Hill has been chosen for this comparison because the topographic dimensions are almost similar to that in the current study. It can be seen on Figure 1 that a sinusoidal hill of 120 m height and 1000 m long approximately follows a slice through the Askervein hill-top at location HT, at least with such an accuracy that main features of the flow can be compared. A description of other models referred to on Figure 1 and Figure 2 can be found in Beljaars et al. (1987) and Walmsley & Taylor (1996). Note that the other simulations are three-dimensional but the current is two-dimensional.

The model was run with z_0=3 cm and u_*=0.60 m/s, the same values as reported for many of the measurement series from the Askervein Hill field project. Fractional speed-up ratio used in this presentation is defined as:

$$FSR = \frac{U}{U_{ref}} - 1 \qquad (3)$$

where U is the measured or simulated wind speed and U_{ref} is the speed at an upwind reference location. On Figure 1, FSR at 10 m height above the ground is compared. The vertical FSR profile at the hill crest, location HT, is shown on Figure 2. We note that our model is failing from 3 m height and down to the ground at the hill top, predicting to high values. The value at 2 m height is 15% higher than the measured one, but the two meter wind speed is the basis for our shear stress estimation for the terrain profiles from the study site. At 1 m height the calculated FSR value is 27% higher than the measured value. This is probably the result of the roughness modelling problem discussed in chapter 2.2. However, the hill summit, which Figure 2 refers to, is located 1000 m downstream from the inlet boundary which is twice as far as the interesting portions of the real terrain simulation from our study site. Even if a slightly
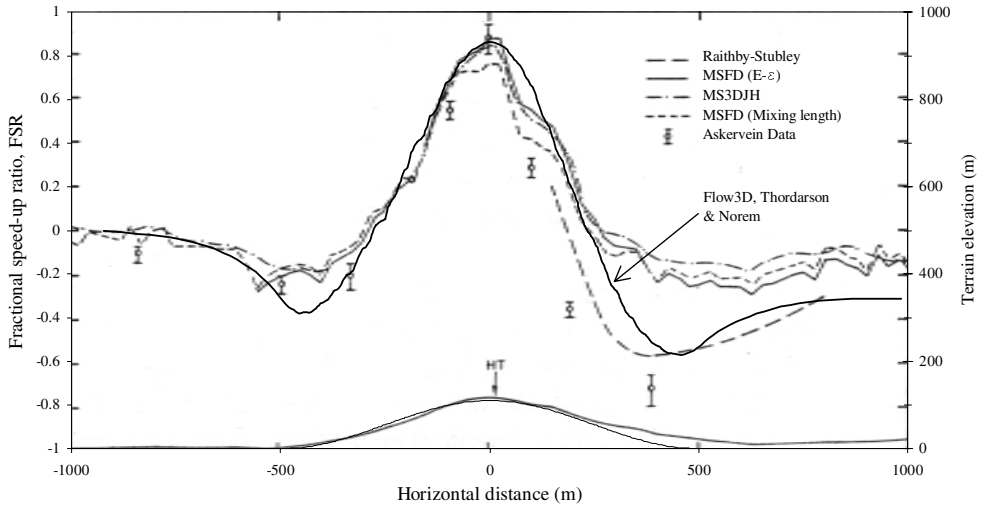
Figure 1 Model comparison to Askervein Hill data, measurements and simulations by other investigators. Number of computational cells is 180 in the horizontal direction and 180 in the vertical. Fractional speed-up ratio at 10 m height, eq. (3).
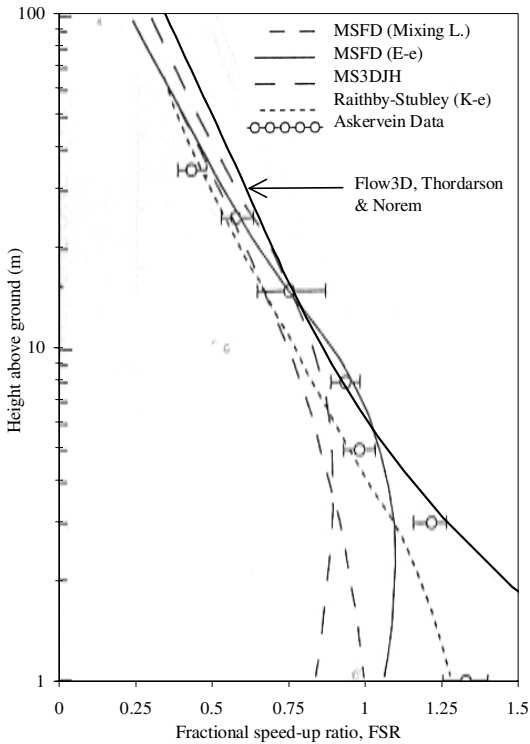

Figure 2 Model comparison to Askervein Hill data. FSR at hill crest.

progressive overestimation of velocity happens along the simulated profiles, the local variations and horizontal velocity gradient will probably be realistic. We will thus conclude that the model is precise enough for the work in this study.

3.2 Study site simulations

The numerical model described in the previous chapter was run on several two-dimensional profiles from the test site. Characteristics of the test site are described in Part II of this report. Two configurations were run for every terrain profile, the first one with original terrain and the second including the late-winter snow cover from the snow survey.

We chose a relatively high input velocity for the model, $u_* = 0.8$ m/s, and a low roughness height, $z_0 = 0.001$ m. According to eq. (1), this gives a wind speed of 18.4 m/s at 10 m height. The model was also run for lower velocity, $u_* = 0.6$ m/s and $z_0 = 0.01$ m, resulting in 10.4 m/s at 10 m height. When the two resulting curves for friction velocity along the terrain surface are normalized by the input friction velocity, the curves fall into each other. This important result indicates that the shape of the friction velocity profile along the terrain is unaffected by the input velocity. This will however not be true if a high velocity suddenly triggers a separation in the flow, but none of the profiles simulated here resulted in separated flow, at least not until downwind from the road.

Figure 3 shows the results for the first profile, numbered 1040. It can be seen that the drift starts to form where an abrupt change in terrain slope occurs about 80 m upstream from the road and is terminated by a sharp 5 m high edge at the road. The sharp edge was made by rotary blowers when re-opening the road after the latest storm. The shear stress curve for the original terrain, u_* ground, falls dramatically where the drift starts to form and maintains almost constant value towards the road. Looking at the curve from the simulation including the snow cover, u_* snow, it can be seen that some of the upstream shear stress is maintained, however the curve has a constant fall towards the drift edge where a sharp drop occurs. Not to any surprise, the simulation reveals a recirculating flow over the road beneath the sharp edge of the drift though the shear stress curve fails to indicate this, since it is based on the velocity at 2 m height. The difference in shear stress along the length of the drift between the two simulations is representing the flow energy gained by the wind by building up the drift.

Figures 4 to 6 show the results for other topographic profiles from the test site. Also here we note that the snowdrift starts where a sudden drop in friction velocity is calculated. These results are treated in Part II of this report.
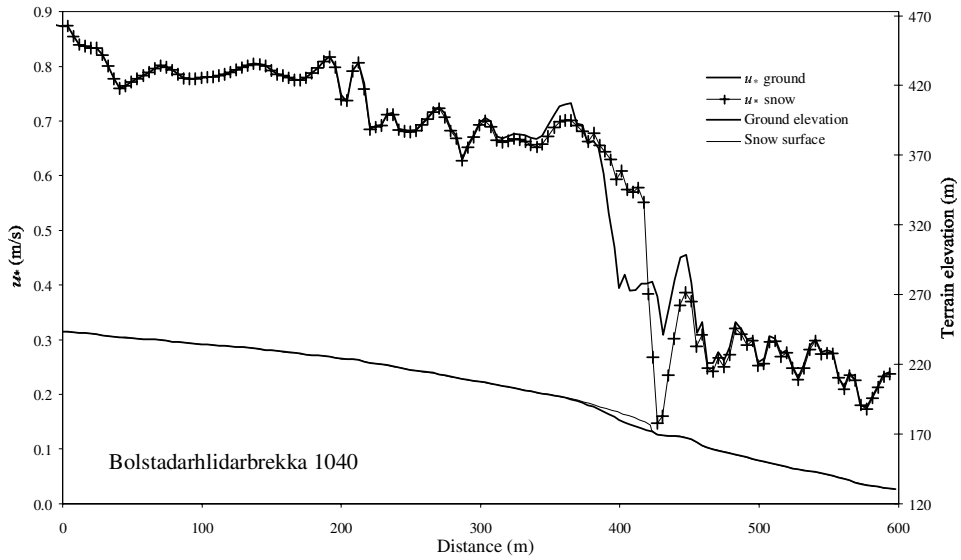
Figure 3 Calculated friction velocity, u_* along profile 1040. Simulation over original terrain and simulation over measured snow cover. The main road is located at distance 430 m. The old road is located at distance 210 m and is providing a moderate snowdrift area downwind. This drift is however not included in the snow cover simulation since only the large snowdrift adjacent to the main road was included in the snow survey.
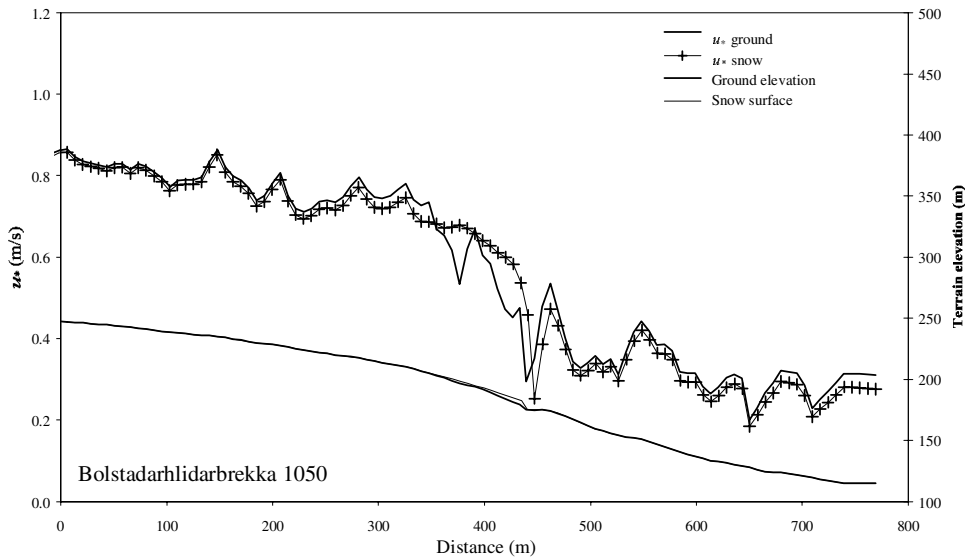
Figure 4 Profile 1050, simulations with and without snow cover present.
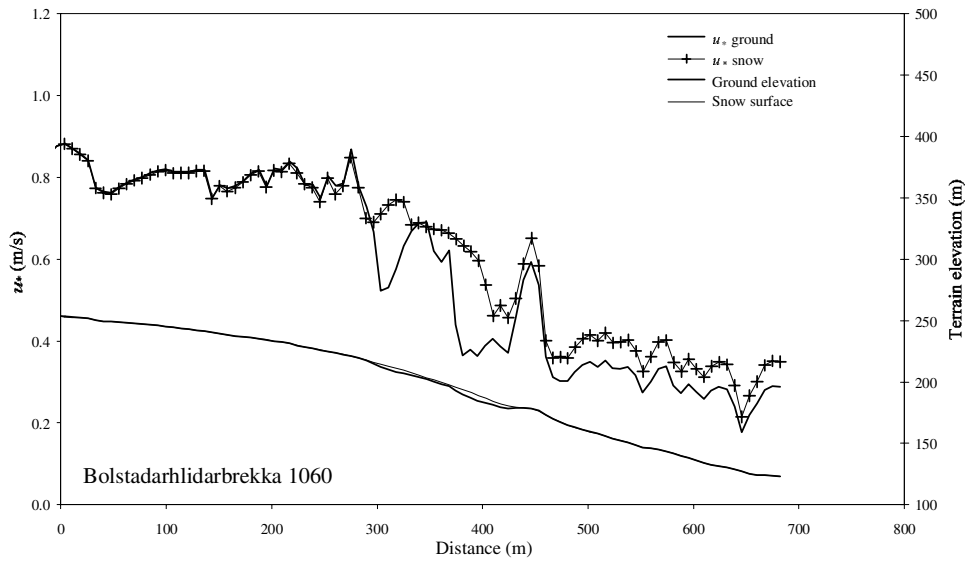
Figure 5 Profile 1060, simulations with and without snow cover present.
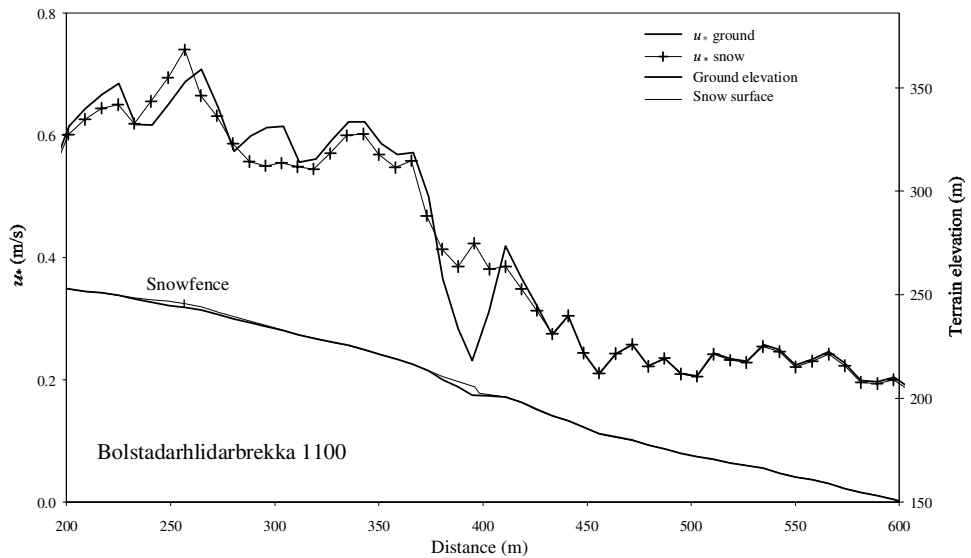
Figure 6 Profile 1100. Note that the snow fence structure is not included in the model, the calculation only takes account for the snow surface and not the 1 m high portion of the fence perturbing through the drift. The drop in u_* across the fence should thus be underestimated here.

4. CONCLUSIONS

Comparison with Askervein Hill data indicates that the model is capable of simulating unseparated atmospheric boundary layer flow over hills. The results show that the velocity at 10 m height is well representative and the vertical velocity profile is quite accurate, at least outside of the inner boundary layer developed adjacent to the ground as a result of the virtually smooth surface applied in the model. For the estimation of shear stress on the ground this inner boundary layer will cause some inaccuracy. Therefore, we see the roughness modelling as a weakness in the model, which in worst case could result in the model not detecting separated flow where it should happen. This factor should be paid attention to in further studies.

In some of the simulated profiles from the study site, the snowdrift area starts where abrupt change in terrain slope occurs, and hence the start point could easily be predicted from looking at the terrain profile alone, but in other profiles the snowdrift start point is found on a gradually increasing slope, where no sharp changes in slope find place. Hence, the study confirms that a plain wind simulation can be an aid to identify areas for large snowdrift sedimentation in two-dimensional profiles.

ACKNOWLEDGEMENTS

REFERENCES

Beljaars, A.C.M., Walmsley, J.L. & Taylor, P.A. 1987. A mixed spectral finite-difference model for neutrally stratified boundary-layer flow over roughness change and topography. *Boundary-Layer Meteorology* 38: 273-303.

Davies, T.D., Palutikof, J.D., Guo, X., Berkofsky, L. & Halliday, J. 1995. Development and testing of a two-dimensional downslope model. *Boundary-Layer Meteorology* 73: 279-297.

Flow Science, Inc. 1997. *Flow3D, Users Manual.* Los Alamos, NM: Flow Science Inc.

Pomeroy, J.W. & Gray, D.M. 1990. Saltation of Snow. *Water Resources Research* 26: 1583-1594.

Raithby, G.D. & Stubley, G.D. 1987. The Askervein Hill Project: A finite control volume prediction of three-dimensional flows over the hill. *Boundary-Layer Meteorology* 39: 247-267.

Sato, T., Uematsu, T. & Kaneda, Y. 1997. Application of a random walk model to blowing snow. In Izumi, Nakamura & Sack (ed.), *Snow Engineering: Recent Advances*: 133-138. Rotterdam: Balkema.

Shao, Y. & Li, A. 1999. Numerical modelling of saltation in the atmospheric surface layer. *Boundary-Layer Meteorology* 91: 199-225.

Stull, R.B. 1988. *An Introduction to Boundary-Layer Meteorology*. Dordrecht: Kluwer Academic Publishers.

Sundsbø, P.A. 1997. *Numerical modelling and simulation of snow drift*. Ph.D. thesis. Narvik: Norwegian University of Science and Technology.

Taylor, P.A. & Teunissen, H.W. 1987. The Askervein Hill Project: Overview and background data. *Boundary-Layer Meteorology* 39: 15-39.

Thiis, T.K. 2000. A comparison of numerical simulations and full-scale measurements of snowdrifts around buildings. *Wind and Structures* (in press).

Uematsu, T., Kaneda, Y., Takeuchi, K., Nakata, T. & Yukumi, M. 1989. Numerical simulation of snowdrift development. *Annals of Glaciology* 13: 265-268.

Waechter, B.F., Sinclair, R.J., Schuyler, G.D. & Williams, C.J. 1997. Snowdrift control design: Application of CFD simulation techniques. In Izumi, Nakamura & Sack (ed.), *Snow Engineering: Recent Advances*: 511-516. Rotterdam: Balkema.

Walmsley, J.L. & Taylor, P.A. 1996. Boundary-layer flow over topography: Impacts of the Askervein study. *Boundary-Layer Meteorology* 78: 291-320.

Wood, N. 1995. The onset of separation in neutral, turbulent flow over hills. *Boundary-Layer Meteorology* 76: 137-164.

Ying, R., Canuto, V.M. & Ypma, R.M. 1994. Numerical simulation of flow data over two-dimensional hills. *Boundary-Layer-Meteorology* 70: 401-427.

Paper II:
Simulation of two-dimensional wind flow and
snow drifting application for roads: Part II

In Hjorth-Hansen et al. (ed.), Snow Engineering: Recent
Advances and Development. Proceedings of the 4th
International Conference on Snow Engineering. A.A
Balkema, Rotterdam.

Simulation of two-dimensional wind flow and snow drifting application for roads: Part II

S. Thordarson & H. Norem

Norwegian University of Science and Technology,
Department of Road and Railway Engineering, Trondheim, Norway

ABSTRACT: Snowdrift sedimentation on leeward facing mountain slopes and terrain ridges makes road planning in certain areas very difficult. Problem areas are frequently found on leeward facing slopes where the wind blows perpendicular over the road. We use the commercial computational fluid dynamics code Flow 3D to simulate two-dimensional wind flow, in order to quantify the snow drifting conditions for roads. To evaluate the numerical model, the study includes a comparison to Askervein Hill data. This comparison is presented in Part I. The present report presents field observations of wind and snow from Iceland and numerical simulations of snow drift sedimentation. The simulations are compared to Tabler's equation for equilibrium snowdrift and the field observations.

1. INTRODUCTION

In the area of road design and drifting snow, Tabler and Norem have written engineering guidelines (Norem 1975, 1994, Tabler 1988, 1994). However, any guidelines developed with the help of CFD have not yet found its way into design codes and standards. It is therefore of interest to road planning that the effect of terrain characteristics on the wind flow and snow drifting conditions is investigated in order to develop guidelines for designers. In the present study, the commercial fluid dynamics code Flow3D (Flow Science, Los Alamos, NM USA) is used to calculate two-dimensional wind field in several profiles through a roadway section. In a two-dimensional application, terrain characteristics refer to terrain slope and change in slope. The study is supported by wind measurements and snow surveys from the same road section.

The goal in this latter part of the report is to use the results from the wind field simulations from the study site, described in Part I of this report to evaluate the drifting snow conditions.

On roads in mountainous areas, the most difficult sites with respect to heavy snowdrift sedimentation are frequently found where prevailing wind direction blows downslope, resulting in retarded wind speed and thus a lower atmospheric shear stress

at the surface. Typical problem areas of this kind are where the road is aligned perpendicular to the wind on the leeward side of terrain ridges and mountain sides. Under these conditions there is a great risk for the road being placed in natural deposit areas for snow. On the other hand, this may also lead to a very favourable road align in the case that the road is situated downwind from the area of equilibrium snowdrift development.

Regardless of turbulence that is present in all high Reynolds number flows and always has a three-dimensional nature, fluid flow in all applications can be categorized as either flow with two-dimensional nature or flow featuring three dimensional interactions in the mean flow. With respect to this, we suggest that a roadway exposed to drifting snow can be spatially divided into sections of either two-dimensional or three-dimensional character. This paper deals with road sections where the wind flow can be described two-dimensionally.

Our simulations were done over original ground profiles and over measured snow cover in the same profiles. The difference between the two simulations is used to establish a relationship between terrain slope, drift slope, drifting snow transport rates and snow trapping efficiency of terrain features.

The study confirms that a plain wind simulation can be an aid to identify areas for large snowdrift sedimentation, and to evaluate the snow-trapping efficiency and capacity of these. We propose a relationship between the terrain slope upwind of the drift and the drift slope itself, and the horizontal gradient of the snow drifting rate. This can be considered when choosing road path near leeward sloping terrain features and when choosing appropriate cross sectional profile for the road. The model developed in the study is a potential addition to the tools already known for road and highway engineering in snow drifting areas, although further testing and generalization is necessary.

2. METHODS

2.1 Field observations

The study site, national road no.1 at Bolstadarhlidarbrekka in Iceland is situated on a mountain slope where strong winds and heavy snowfall occur during the winter, Figure 1. The data collected and used as a support for numerical work in this paper consists of measurement series from an automatic weather station (AWS) and a snow survey. Additionally, information from maintenance personnel on road closures and sight distance along the road during storm periods is available. The data from the test site was collected during the winter 1998-1999.

Norem (1975, 1994) has classified weather conditions for snow drifting problems on mountain roads. According to this the data from the AWS was used to identify the prevailing direction for strong winds.

The snow survey was done at the end of the winter. Snow depths were measured in profiles parallel to the prevailing wind direction, the same profiles as chosen for the numerical simulation, Figure 1. The measured snow profiles extend up to the erosion
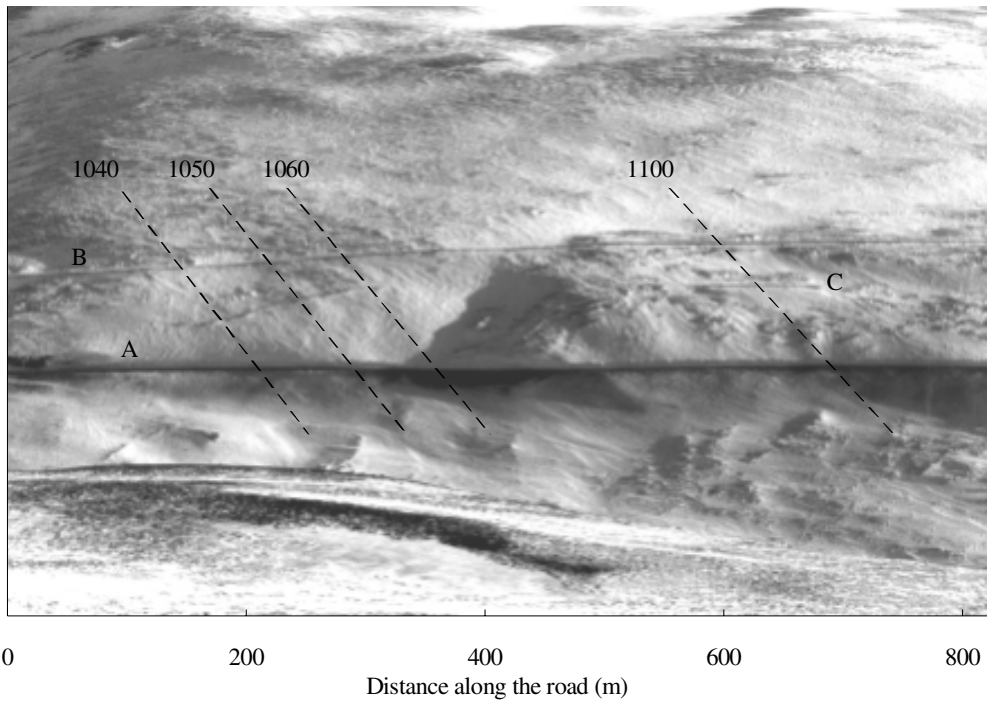
Figure 1 Photograph showing the study site at Bolstadarhlidarbrekka. The marked profiles are investigated in the study. Other symbols: A, the main road. B, an older generation road. C, a snowfence. The snowfence is 3 m high and 100 m long.
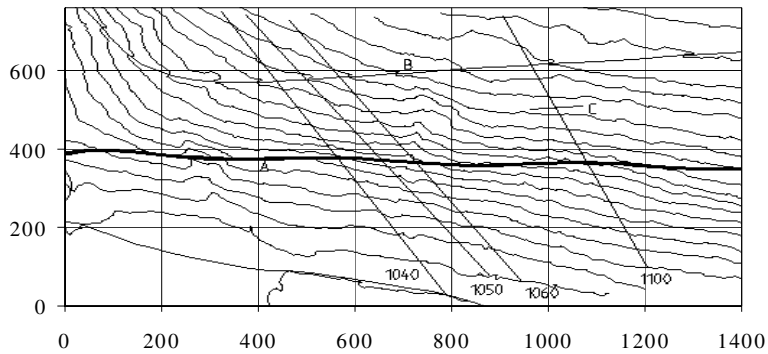
Figure 2 Topographic map of the study site, 10 m equidistance curves. Scale along the edges is in meters. The valley bottom is at the lower edge, governing wind direction from the top along the marked profiles. Profiles are aligned roughly 10° clockwise from true north. A, B and C are the same as in Figure 1.

area where no snow was registered on the ground, and are superimposed on topographic profiles taken from a digital map, Figure 2.

2.2 Wind field simulation

The method and tools for the wind field simulation is documented in Part I of this report.

3. RESULTS

3.1 Field observation

The road site chosen for the field observations has the typical characteristics of maritime climate. The worst drifting snow problems on the road are usually encountered when strong northerly winds blow from the ocean with simultaneous precipitation, which results in enormous quantities of drifted snow. A typical storm may last from few hours to several days and will occasionally lead to closure of the road. Between storms, periods of higher temperatures accompanied by rain or wet snowfall harden the snow cover and consequently few events of drifting snow are registered between the events described above. These cycles of snowstorms and mild weather result in large spatial variations of the snow cover thickness and even leave the wind eroded areas completely snow-free throughout the winter, making the deposition areas for drifted snow easy to identify. This fact together with a monotone wind direction for drifting snow due to the surrounding landscape, makes the site very favourable for this kind of investigation.
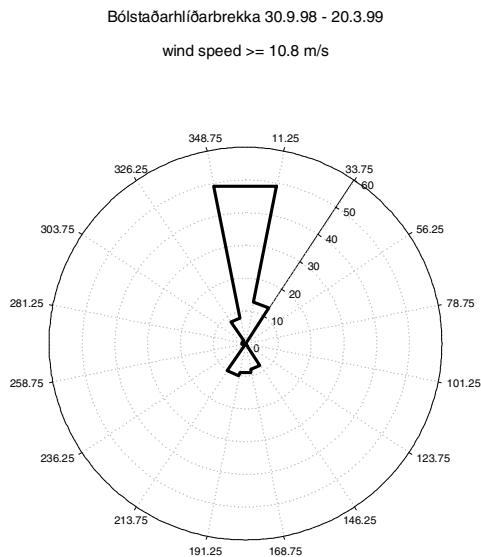
Figure 3 Wind rose of strong winds only for the winter months at Bolstadarhlidarbrekka. Note the dominating frequency of strong winds from the north, 50%. Total frequency of strong winds for the period was 17%.

Wind rose for wind speeds exceeding 10.8 m/s during the winter months shows that the strong winds are appearing in a narrow sector from north, Figure 3. The wind speed registered during a snow storm is generally between 15 m/s and 25 m/s and the highest 10 minute mean wind speed registered during the winter was 35 m/s, including a 48 m/s gust.

3.2 Model results and snow drifting application

3.2.1 Shear stress and snow transport

We refer to the wind field simulations for the study site in Part I. A closer view of the results for profile 1040 is found on Figure 4. Figure 5 shows the shear stress difference, *(u$_*$ snow) - (u$_*$ ground)* for profile 1040, plotted together with the measured snow cover thickness at running intervals along the drift. Apparently, there is a strong correlation between these two curves. We use this correlation to create a relationship between the shear stress gain and the deposited snow masses in order to quantify the snowdrift rate and estimate the trapping efficiency of the terrain depression. Many authors have reported on the relationship between the friction velocity, u_*, or wind speed at a certain height above the ground and the snow transport capacity of the wind. The simplest form for these models is:

$$Q = a(U - b)^{\alpha}$$

(1)

where *a*, *b* and α are constants, *a* and α found by regression analysis on experimental data and *b* denoting a threshold wind speed for drifting snow. *U* (m/s) is the wind speed or friction velocity and *Q* [kg / (s m)] is the snowdrift rate per unit width. The constant *a* is usually replaced by (ρ/g C), where ρ is the density of the fluid, *g* is gravitational acceleration and *C* is an experimental constant (Pomeroy & Gray 1990, Schmidt 1986). In general, this kind of model indicates that a change in wind speed in horizontal direction results in a change in the observed snowdrift rate. When integrated into a fluid flow model, this relationship can be used to calculate drift sedimentation and erosion (Uematsu et al. 1989):

$$\frac{\partial h}{\partial t} = -\frac{1}{\rho_s}\frac{\partial Q}{\partial x}$$

(2)

This model adjusts the snow surface elevation, *h*, in a computational cell according to change in drift rate, *Q*, along the surface. ρ_S is the density of sedimented snow on ground.

We use this relationship to calculate the total change in drift rate caused by elevating the surface from ground level to the observed drift surface. The change in transport rate, ΔQ, is a result of drift growth, ΔV (m^3/m), when divided by estimated drift density ρ_S (kg/m^3), and multiplied by a time ΔT (s) for the duration of the drift build-up. For simplicity the threshold velocity for snow transport, *b*, is neglected here. This should not result in large error since the threshold value for snow transport is
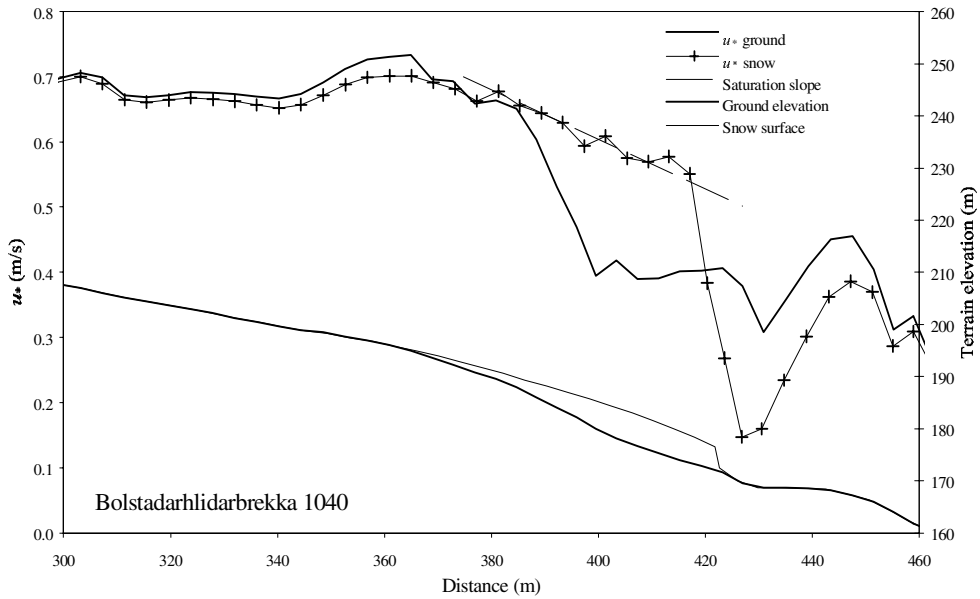
Figure 4 Closer view over the calculated friction velocity, u_* along profile 1040. The friction velocity keeps a constant drop along the drift surface. Further we note that the friction velocity is lowered on a section upstream from the drift.
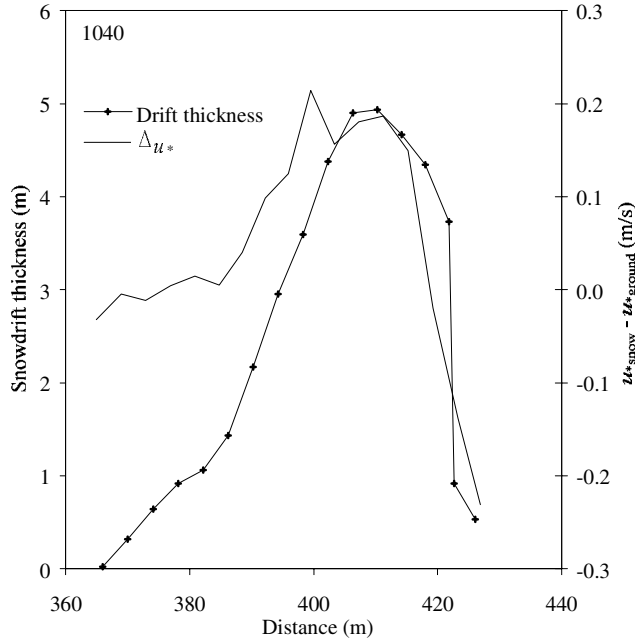
Figure 5 Profile 1040. Difference between calculated friction velocity for ground and snow cover, and measured snowdrift thickness.

very low for a fresh loose snow cover (Kind 1981) and the snow drifting at the observation site is mainly occurring with simultaneous precipitation. The snow drifting rate formula is:

$$Q = C \frac{\rho}{g} u_*^{\alpha} \tag{3}$$

For conservation of snow-mass in the model we get:

$$\frac{\Delta V}{\Delta T} = \Delta Q \frac{1}{\rho_S} \tag{4}$$

where $\triangle Q = (Q \text{ snow} - Q \text{ ground})$, according to eq. (3). This model was applied in stepwise increments, dx, along the drift length to calculate the drift volume from the gain in u_*. Note that this calculation is not integrated in the fluid flow model but is done after the wind flow has been simulated over the two surfaces, ground and snow cover. Figure 6 shows the relationship between the accumulated measured drift volume on the ground for profile 1040 against the calculated drift volume from eq. (3) and eq. (4) in running intervals along the drift. The unknown parameters, ρ_S, $\triangle T$, C and α have to be determined. We use profile 1040 to calibrate the equation, since it has the most smooth ground surface. The drift density is chosen as $\rho_S = 400$ kg/m^3
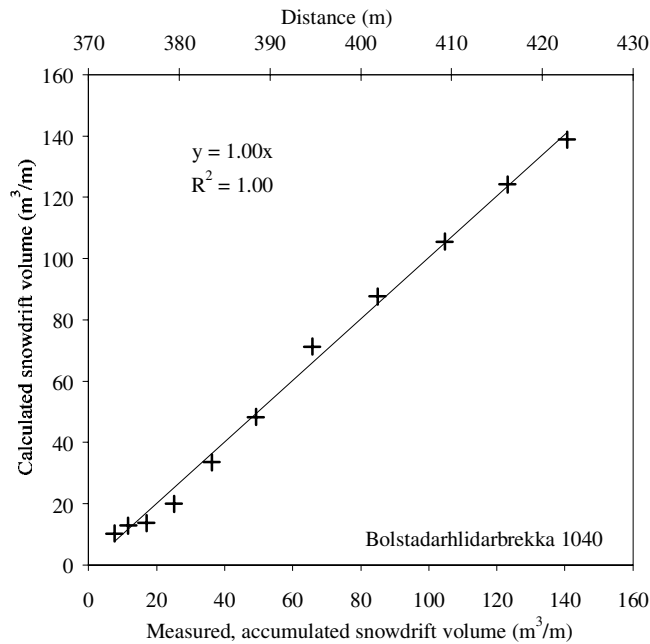
Figure 6 Profile 1040. Measured drift volume, accumulated in stepwise increments along the drift, and computed drift volume according to eq. (3) and eq. (4). Best linear fit results in α = 2.85 and C = 2.30.

and the build-up duration, $\triangle T$, is set to two days. The values for ρ_S and $\triangle T$ are actually arbitrary chosen, as a part of scaling the equation. The exponent α is adjusted to find the least squares difference for a linear fit between the calculated and measured drift volumes, and finally, the constant C is modified until the slope of the line equals one. This gives the constants $C=2.30$ and $\alpha=2.85$, and the transport rate equation becomes:

$$Q = 2.30 \frac{\rho}{g} u_*^{2.85} \tag{5}$$

Of course, since we neither know the actual ρ_S nor $\triangle T$, the absolute drifting rate calculated here is not likely to be correct. Anyhow, this will not matter in this application, since the exponent α, is the parameter that really describes the changes in drifting rate due to changes in friction velocity. The exponential relationship found here, $Q \sim u_*^{2.85}$ is close to the most commonly reported relationship, α of about 3 (Pomeroy 1989, Kind 1981, Kobayashi 1972). Takeuchi (1980) reported on $\alpha=2.7$ for old firm snow and $\alpha=4.16$ for settled dry snow. This model was applied to profiles 1050 and 1060 with the same value for all parameters found for profile 1040. The resulting diagrams are displayed on Figure 7 and Figure 8.
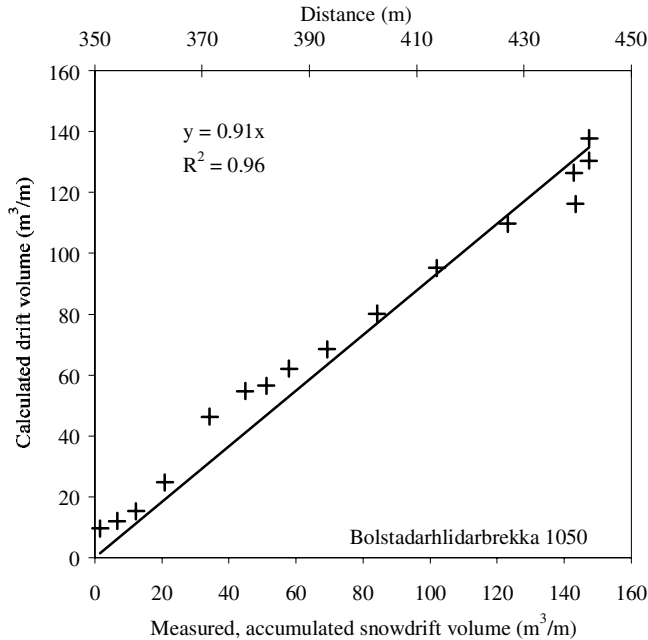
Figure 7 Profile 1050, results from applying eq. (4) and eq. (5) on the u_* difference between ground and snowcover.
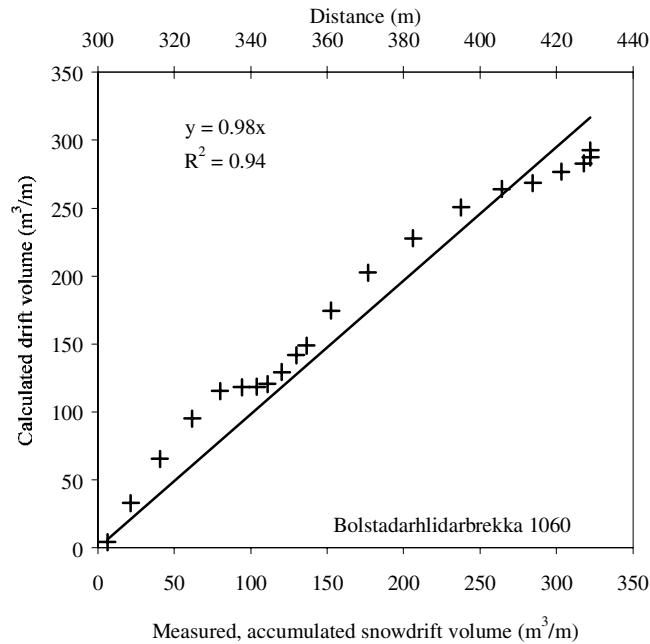
Figure 8 Profile 1060, same as for Figure 7.

3.2.2 Terrain slope and snow transport

The friction velocity diagrams displayed in Part I indicate that there is a tendency towards a constant u_* value along terrain sections of constant slope on the moderate sloping sections. This is reasonable considering that in nature, we do not observe snowdrifts starting suddenly on a constant slope, but we relate the starting point to a change in slope. However, when the terrain slope exceeds a certain value, there is a sudden drop in the u_* curve.

To test this effect, we built an ideal terrain profile from constant slope segments and imported into the wind flow model. Figure 9 shows that u_* indeed keeps a constant value along each section, until the terrain slope changes from 30% to 40% where a steep descend in the friction velocity profile occurs, at distance 300 m. This slope could be in the vicinity of the critical terrain slope for flow separation, but this critical slope can be related to the proportion between horizontally length scale of the hill and the roughness height, λ/z_0 (Wood 1995). Separation is a sufficient condition for snow drift sedimentation in two-dimensional flow, but according to our results, not necessary for sedimentation. Diagrams on the shear stress variations along the profiles from the study site show that the large snowdrifts observed start where a sudden and continuous decrease in shear stress is calculated. Hence, this must be a feasible start point for a large snowdrift sedimentation on the ideal terrain profile and we applied Tabler's model for equilibrium drift growth here. Tabler (1994) has suggested equilibrium shape for snowdrifts, given that the start point of the drift is
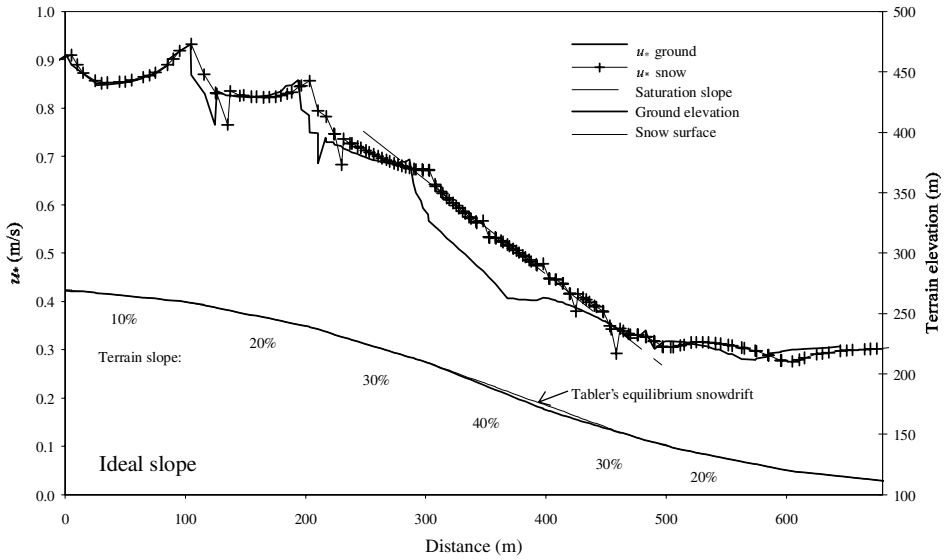
Figure 9 Model run over ideal terrain of constant sloping segments. Tabler's equilibrium drift formula, eq. (6), is applied at distance 300 m, where a sharp drop in the u_* curve occurs, and the model was run again over the new snow cover.

known. His model is based on regression analysis of measured snowdrifts in the field and uses the terrain slope upwind and downwind of the prediction point as input parameters:

$$Y_S = 0.25\,X_1 + 0.55\,X_2 + 0.15\,X_3 + 0.05\,X_4 \tag{6}$$

where

Y_S = snow slope (%) over the main portion of the drift

X_1 = average ground slope over a distance of 45 m upwind of the catchment lip

X_2 = ground slope from 0 to 15 m downwind of the trap lip

X_3 = ground slope from 15 to 30 m downwind of the trap lip

X_4 = ground slope from 30 to 45 m downwind of the trap lip

The resulting drift starts at distance 300 m and has a 35.5% slope. The wind flow model was now run again over this new artificial snow cover and the u_* curve plotted on Figure 9. The u_* curve now has a constant slope and lies above the curve for the ground simulation as one will expect. However, we see that the relationship of constant terrain slope and constant friction velocity is not valid here. Either this could mean that the relationship is not valid for steeper slopes than about 30%, or that the

distance required to establish a constant friction velocity is longer, the steeper the slope is. We note that this is also the case for the profiles from the study site.

The relationship between upwind terrain slope and drift slope, and the constant slope of the u_* curve was found worth a further study. This is because according to snow transport theory, the drift will still be growing as long as the shear stress along the drift surface is decreasing.

For the next diagram plotted, the friction velocity was replaced by calculated drift rate according to eq. (5). Considering drift rates calculated from the u_* values, these must be considered as maximum possible drift rate and not the actual drift rate, at least until the point of sedimentation is reached. We know that at the point where snow sedimentation starts, the transport capacity of the wind is fully exerted and no further decrease can occur without snow particles being deposited on the ground. We can thus normalize the drift rate curve, such that the drift rate at the point where the sedimentation starts is set to 100%. The slope of the curve will hence give a reduction in percent per meter travelled from the initial point. On Figure 10, the difference between the upwind terrain slope and the surface slope of the drift is plotted against the slope of the friction velocity curve along the drift surface which has been modified to percent reduction per unit length as written above. The terrain slopes are average slopes along a 50 m long path. The data used to derive this relationship comes from profiles 1040, 1050, 1060 and the ideal slope profile with Tabler's equilibrium drift.

We find a linear relationship passing through the origin, Figure 10, which is in accordance with the rule that no sedimentation can be initiated if no drop in friction velocity and no change in slope happens. Besides we see that the larger the difference between upwind terrain slope and drift slope, the higher is the rate of drop in transport capacity along the drift surface and hence, the faster the drift growth or the more efficient is the natural snow trap.

For the model derived here, it is assumed that a decrease in u_* or maximum possible transport rate immediately results in a drift growth on the spot. This is really a crude simplification, since it will take some distance for the snow particles to be deposited on the ground. As a simplified example, considering a terminal fall velocity of 0.5 m/s for a snow particle transported by the wind at 15 m/s. This particle will be transported 15 m downwind if initially at 0.5 m height when the drop in u_* encourages this particle to be sedimented. Despite this, it is tempting to state that a theoretical equilibrium drift surface will actually have the same slope as the upwind terrain, though it will seldom reach it because how slow the last stages of drift growth towards equilibrium happen. Supporting this, we can refer to small scale terrain depressions in nature that are easily filled with drifting snow and smeared out in the landscape, but larger depressions take longer time to fill. In engineering application, the definition of an equilibrium snowdrift surface, which still allows a certain fall in friction velocity along it is thus feasible. Norem (1994) has used a 10% to 15% slope difference as a reference value for equilibrium drift surfaces in road planning applications.
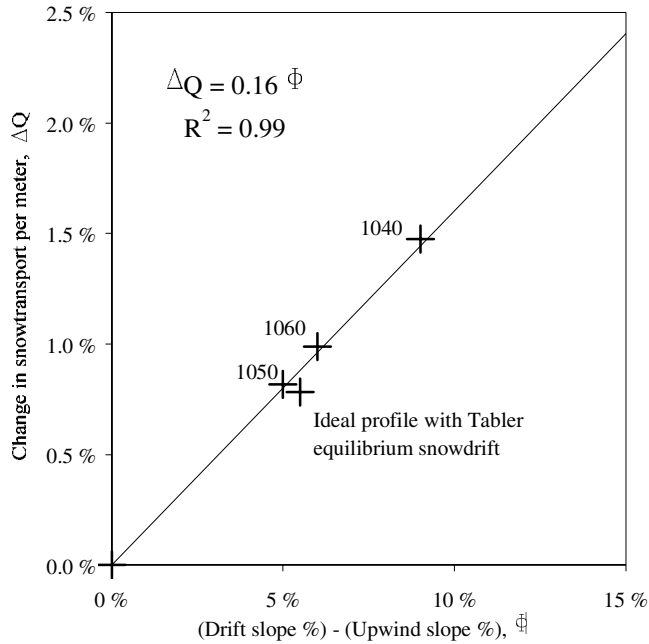
Figure 10 Calculated relationship for upwind slope and drift slope, and relative drop in transport rates per meter along the drift.

3.2.3 Profile 1100, snow fence

The last terrain profile from the study site is taken through an existing snow fence. This snow fence is 3 m high and is made of fabrics of about 50% porosity. By the time of the snow survey, the windward- and leeward drifts had grown together, leaving only one meter of the fence standing above the surface.

The following example is an effort to evaluate the location of the snow fence and its effect to reduce snow problems on the road. First, the model was run on the original terrain, without considering the snowfence, then the model was run with the measured snowdrifts included. The part of the fence still active, the topmost meter, is not included in the simulation, and hence the effect of the fence is underestimated here. The two resulting u_* curves are plotted on Figure 6 in Part I.

The u_* curve for the snow surface falls steeply across the drift around the fence, the equivalent drop in drifting rate is about 29% or 1% per meter, according to eq. (5). Figure 10 suggests that 1% drop per meter is close to being a practical equilibrium state for the drift development. In the meanwhile, the fall of the u_* curve along the drift adjacent to the road corresponds to a change in drift rate from 71% of the original flux down to 24%. This equals that about 3% of the flux at the start of the drift is sedimented per meter of length along the drift. Compared to the other profiles investigated, where the drop in drift rate was from 0.8% to 1.5% along the snow

cover, it is evident that the fence has delayed the development of the drift next to the road significantly.

4. CONCLUSIONS

From Part I of this report we recall that the normalized shape of the friction velocity curve along the two-dimensional profiles is unaffected by the input velocity. This is important for the general application of the model developed here.

The study confirms that a plain wind simulation can be an aid to identify areas for large snowdrift sedimentation in two-dimensional profiles, and to evaluate the snow-trapping efficiency and capacity of these. We use a new method to establish a relationship between the friction velocity and the snow drifting capacity of the wind, by using the difference in calculated friction velocity between simulations with and without the snow cover present. We propose a relationship between the terrain slope upwind of the drift and the drift slope itself, and the horizontal gradient of the snow drifting rate. This can be considered when choosing road path near leeward sloping terrain features and when choosing appropriate cross sectional profile for the road.

The model developed in the study is a potential addition to the tools already known for road and highway engineering in snow drifting areas.

ACKNOWLEDGEMENTS

REFERENCES

Flow Science, Inc. 1997. *Flow3D, Users Manual.* Los Alamos, NM: Flow Science Inc.

Kind, R.J. 1981. Snow drifting. In Gray, D.M. & Male, D.H. (ed.), *Handbook of snow*: 338-360. Toronto: Pergamon Press.

Kobayashi, D. 1972. *Studies of snow transport in low level drifting snow*. Contributions from the Institute of Low Temperature Science. Sapporo: Hokkaido University.

Norem, H. 1975. *Designing highways situated in areas of drifting snow*. Draft translation 503. Hanover, New Hampshire: CRREL.

Norem, H. 1994. *Snow Engineering for Roads*. Handbook no. 174. Oslo: Norwegian Public Road Administration, Road Research Laboratory.

Pomeroy, J.W. 1989. A process-based model of snow drifting. *Annals of Glaciology* 13: 237-240.

Pomeroy, J.W. & Gray, D.M. 1990. Salutation of Snow. *Water Resources Research* 26: 1583-1594.

Schmidt, R.A. 1986. Transport rate of drifting snow and the mean wind speed profile. *Boundary-Layer Meteorology* 34: 213-241.

Tabler, R.D. 1988. *Snow Fence Handbook*. Laramie, Wyoming: Tabler & Associates.

Tabler, R.D. 1994. *Design Guidelines for the Control of Blowing and Drifting Snow*. SHRP-H-381. Washington, DC: National Research Council.

Takeuchi, M. 1980. Vertical profile and horizontal increase of drift-snow transport. *Journal of Glaciology* 26: 481-492.

Wood, N. 1995. The onset of separation in neutral, turbulent flow over hills. *Boundary-Layer Meteorology* 76: 137-164.

Paper III:
Snow sedimentation in gently sloping road cuts

(Submitted to Cold Regions Science and Technology)

Snow sedimentation in gently sloping road cuts

Skuli Thordarson[1]

Norwegian University of Science and Technology,
Department of Road and Railway Engineering,
7491 Trondheim, Norway

ABSTRACT: Wind speed evolution and snow drifting conditions on leeward facing hillsides and in gently sloping road cuts were investigated. The aim of the study was threefold: (1) Identification of general criteria for snowdrift sedimentation to initiate at a particular point. (2) Description of the wind speed evolution in gentle sidehill cuts, and definition of the flow criteria for a drift free road. (3) To propose a procedure that allows the use of topographic data only to predict the maximum extension of a fully developed snow drift surface. The work is based on previous recommendations for road and highway engineering in snow-drifting areas. Numerical wind flow simulations and snow surveys were used, together with statistical methods. The results indicate that the initiation of snowdrift sedimentation on the ground is depending on the upwind landscape as well as on the local slope. To prevent snowdrifts to extend onto the road surface, the relative wind speed over the road has to be high enough to provide an erosion zone on the road. This is achieved when an extrapolated extension of the wind speed curve on the upwind terrain intersects the speedup curve around the road, over the ditch area. A mathematical scheme that generates equilibrium snowdrift surfaces was proposed. The method is useful for evaluating the validity of a predicted snowdrift extension toward the road.

Key words: Drifting snow, gentle cut, road engineering, snow control.

1. INTRODUCTION

On roads in snow drifting areas, one of the most common reasons for snow encroachment onto the road surface is inappropriate location and design of the road in leeward facing hillsides. Both shortcoming cross section design of the road or simply the location of the road inside a natural snow deposition area can result in snowdrifts extending onto the road surface. This requires frequent snow removal, or may otherwise leave the road impassable to most vehicles.

It was previously shown by Thordarson and Norem (2000, 2002) that snow drifting is substantially different in steep road cuts than in gently sloping cuts. Steep

---

1. Fax: +47 7359 7020; E-mail: thordars@stud.ntnu.no

cuts usually exhibit wind flow that must be described three-dimensionally. Wind flow in gentle slope cuts on the other hand can usually be described as a two-dimensional flow, even if the boundary layer separates from the surface and recirculation of air occurs. Thordarson (paper submitted for publication in Cold regions sci. and techn.) has analysed the flow in steep road cuts, and proposed design alternatives for snowdrift control. The current report focuses on snow drifting in gently sloping cuts with two-dimensional snow drifting and wind flow pattern.

The objective of the study reported here is to analyse the wind flow and snow drifting conditions in leeward facing hillsides and gently sloping road cuts and to extend previously published recommendations for the design of gentle slope road cuts. The work had three main goals:

1. Identification of general criteria for snowdrift sedimentation to initiate at a particular point.

2. Description of the wind speed evolution in gentle sidehill cuts, and definition of the flow criteria for a drift free road.

3. To propose a procedure that allows the use of topographic data only to predict the maximum extension of a fully developed snow drift surface.

The study is based on the previous work by the author and on design recommendations by Norem (1975, 1994) and Tabler (1994), respectively. This includes snow drift measurements, numerical wind flow simulations and statistical methods. The most important result is a statistical model to calculate a streamlined equilibrium surface for snowdrifts, which can be used to estimate the validity of a predicted drift extension. I conclude that proper use of topographic data together with climatic information should enable engineers to identify critical road sections in leeward facing hillsides, and in many situations, to design a drift free road.

2. WIND FLOW AND SNOW DRIFTING ON LEEWARD FACING HILLSIDES

2.1 Wind flow on downslopes

Wind flow over complex terrain is a very complicated phenomenon and is widely investigated in the field of boundary-layer meteorology. The purpose of the following overview is to achieve a simplified picture of the wind speed evolution close to the ground on downslopes, which in turn is most important to snow drifting. The wind speed development and vertical distribution on leeward facing slopes is depending on the upwind landscape and surface roughness and other factors such as atmospheric stability and the presence of temperature inversions. These factors have e.g. been described by Stull (1988) and other authors. During snow drifting events of interest to this study, wind speed is usually so high that temperature inversions are eliminated by turbulent mixing (Liljequist, 1957), and the air mass in the lowest part of the
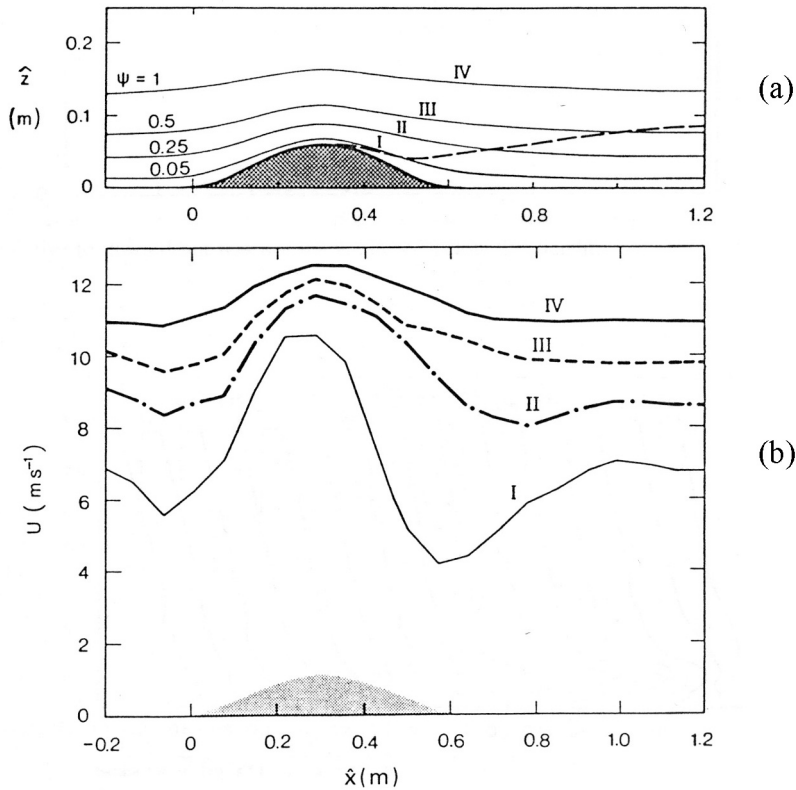
Figure 1 Wind tunnel results, unseparated flow over a two-dimensional hill. Reprinted from publication by Finnigan et al. (1990). Figure (a) shows four streamlines over the hill and in (b) the mean wind speed along these streamlines is plotted (height of hill not to scale).

boundary layer can be assumed to be of uniform temperature and density. Flow response due to topographic features can therefore be predicted according to that.

Leeward facing slopes of isolated hills and ridges usually develop continuous wind speed reduction. Besides that, if the slope is steep enough the flow may separate and form a reversing flow close to the surface. Unseparated flow over a hill was documented by Finnigan et al. (1990) in their wind tunnel experiment of the flow over a 50 mm high and 600 mm long hill. Figure 1 (a) shows the streamline pattern from this experiment. In Figure 1 (b), the horizontal mean wind speed is plotted along each of the streamlines from Figure 1 (a). The main features of the wind speed evolution can be summarised as:

1. The flow response is stronger close to the surface than higher up in the flow.

2. Wind speed is retarded in front of the hill and reaches a peak value at the summit.

3. An approximately linear decrease in the mean wind speed is observed close to the ground on the leeward facing slope.

4. Wind speed on the leeward side reaches a stable value at some distance from the hill foot.

Similar flow behaviour was observed over Askervein Hill, which is an isolated 126 m high ridge with approximately sinusoidal cross section. Both measurements (Taylor and Teunissen, 1987) and simulations (Beljaars et al., 1987; Raithby and Stubley, 1987; Thordarson and Norem, 2000) for the Askervein hill confirm the features listed above. From these results it can be concluded that on the leeward slope, the mean wind speed u, at a fixed reference height above the surface is a function of the location along the slope, x, the degree of the slope, θ, and an upstream reference wind speed, u_{ref}. For a particular section of approximately constant terrain slope, this can be formulated as

$$u = u(u_{ref}, x, \theta, F) \qquad (1)$$

where the parameter F gives room for including the effect of the overall geometry and possible thermal effects (atmospheric stability and the presence of temperature inversions).

Hillsides connected to large scale landscape features such as mountain sides and plateaus can maintain a constant wind speed when the slope is moderate and slope changes are gradual. This is according to results from the study of Bolstadarhlidarbrekka mountain side by Thordarson and Norem (2000). The hillside in their study is a descend from a larger mountain plateau and thus does not present the characteristic flow profile of a wind passing a mountain top or hill summit as discussed above. Their results indicated that the wind speed adjusted to a new and lower constant value when terrain slope increased and kept this value along that particular section of constant terrain slope. This implies that eq. (1) loses the x-dependency and becomes, $u = u(u_{ref}, \theta, F)$. These conditions result in little overall wind speed reduction and do not promote heavy deposition of snow. Deposition of drifted snow in the Bolstadarhlidarbrekka mountain side happens mainly where terrain slope exceeds 20-25 %, on locations where the wind speed starts to fall along the surface. This result suggests that any hillside prone to snow drift accumulation on the ground features a wind speed evolution that can be described by eq. (1). The upwind landscape, either a plateau or in case of an isolated hill, may possibly determine where snow starts to deposit.

This simplified description of the wind speed development on downslopes is in many ways analogous to pipe or channel flow through cross section expansions. Figure 2 illustrates the flow through a conduit expansion. Flow enters a control volume through border of area A_1 at mean velocity V_1. The equation of continuity for fluids of constant density (Gerhart et al., 1992):

$$A_1 V_1 = A_2 V_2 \qquad (2)$$
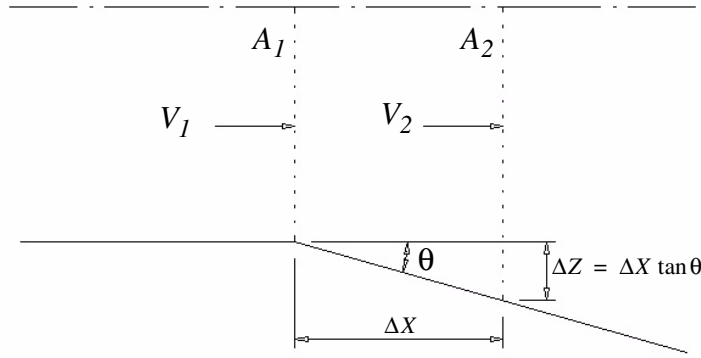
Figure 2 Conduit flow through an expansion. Flow direction from left to right.

confirms that the mean flow velocity must decrease as the flow exits the control volume at boundary of a larger area, A_2. From eq. (2) and Figure 2, the mean velocity in cross section A_2 is found:

$$V_2 = V_1 \left[\frac{A_1}{A_1 + \Delta X \tan \theta} \right] \tag{3}$$

According to the equation, the mean velocity at position A_2 has changed inversely proportional to the relative expansion of the available flow area. This relative expansion is strictly speaking not valid for wind flow on terrain slopes since the total flow height is only limited by the height of the boundary layer. Nevertheless, it can be said that the apparent effect of increased slope is increased available flow area, resulting in lower wind speed. The purpose of the parameter F in eq. (1) is to account for the relative cross section expansion, which will vary according to the overall geometry and atmospheric conditions. In eq. (3), when A_1 is large compared to the additional flow space provided by the downslope, the value inside the parentheses can be approximated as $[1 - \Delta X \tan \theta / A_1]$. Interpreting Figure 2 as a topographic downslope, A_1 takes the role of the total boundary layer depth, approximately 400 - 1000 m, or a number that can be defined as $O(10^2)$. With this information, eq. (1) can be rewritten on the following form:

$$u = u\left(u_{ref}, F, 1 - \frac{x \cdot \tan \theta}{O(10^2)} \right) \tag{4}$$

However, the relationship in eq. (4) only estimates the average wind speed in a very high vertical column on a leeward slope. This wind speed is not interesting for the conditions close to the ground, where snow drifting occurs. A better approximation for the wind speed evolution in the very lowest layers is needed. Referring back to

Figure 1, we recall that the flow speed reduction is stronger close to the ground than higher up in the flow. Consider the flow region confined by streamline no. I and the surface. Since no flow will cross the streamline nor the surface boundary, this region can be treated as a closed conduit. Now, taking A_1 as the flow area between streamline I and the hill top, and A_2 between the streamline and the hill foot on the leeward side, we see that the additional flow area provided by the downslope is determined by the difference in slope of the ground, θ, and the slope of the reference streamline, θ_I. Even if A_1 is small, it is still large compared to the rate at which A_2 grows. The approximation behind eq. (4) is still valid in this case and the wind speed close to the ground should be proportional to -x. The functional relationship that determines the wind speed close to the ground on downslopes should therefore look like:

$$u = u\left(u_{ref}, 1 - \frac{x \cdot \tan(\theta - \theta_I)}{F_I}\right)$$ (5)

where x is the distance travelled from top of the slope, $(\theta - \theta_I)$ is the difference between ground slope and slope of a reference streamline close to the ground and F_I is the flow area between the reference streamline and the ground at top of the slope. The principle is illustrated in Figure 3. For the wind speed to fall linearly along the slope, F_I and $(\theta - \theta_I)$ must be linearly related. This allows for modifying eq. (5) to a computable expression:

$$u(x) = u_{ref}(1 - Bx)$$ (6)

where

$u(x) =$ wind speed close to the ground at distance x from the beginning of the slope

$u_{ref} =$ wind speed close to the ground at top of the slope

B = a constant depending on ground slope and upwind and downwind landscape, as well as atmospheric conditions
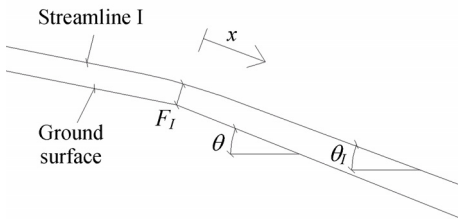

Figure 3 Explanation to eq. (5).

This relationship should be valid when the ground surface along the flow direction can by approximated by subsequent straight lines. The same description applies even if the wind direction is not aligned perpendicular to the slope gradient. A non-perpendicular wind direction will result in less effective slope of the hill or the road cut. On the other hand, where the slope gets so steep that boundary layer separation occurs, this description does not apply. The critical slope angle for flow separation to occur is depending e.g. on the ratio of roughness height and the hill height (Finnigan, 1990; Wood, 1995). With snow drifting it can be assumed that flow separation from the surface is a sufficient criterion for sedimentation but not a necessary criterion.

2.2 Snow drifting on downslopes

In the following text, the importance of the wind speed for snow drifting is emphasised. Over a flat ground, the boundary layer flow in the lowest part of a neutrally stable atmosphere is commonly described by the logarithmic wind profile (Stull, 1988):

$$u(z) = \frac{u_*}{\kappa} \ln\left(\frac{z}{z_0}\right) \tag{7}$$

where u is the wind speed at height z. The aerodynamic roughness height, z_0, is a measure of the surface roughness on the ground and gives the theoretical height at which the wind speed is zero. The letter κ stands for the von Karman constant, equal to 0.4 (Stull, 1988). The shear stress in the flow at ground level is an important parameter for snow drifting. The friction velocity in eq. (7), u_*, is a measure of the shear stress, τ_0, caused by the surface wind on the ground:

$$u_* = \sqrt{\frac{\tau_0}{\rho_0}} \tag{8}$$

Here, ρ_0 is the density of air and τ_0 designates the sum of turbulent and molecular shear stresses on the ground. If the roughness height, z_0, and wind speed at a given height, $u(z)$, is known, the friction velocity, u_*, can be calculated by eq. (7).

Many investigators have presented formulas describing the quantity of snow transport in terms of the friction velocity or wind speed at a reference height. Amongst these are Kobayashi (1972), Pomeroy and Gray (1990) and Schmidt (1986). The snow drifting capacity of the wind is generally found to have approximately third power relationship with the wind speed or the friction velocity. The empirical transport formulas can be on the form:

$$Q = a(u_* - u_{*\mathrm{th}})^3 \tag{9}$$

where the constant a is found by regression analysis on experimental data and $u_{*\mathrm{th}}$ represents a threshold friction velocity for snow drifting to initiate. The friction velocity is u_* (m/s) and Q (kg/s m) is the snowdrift rate per unit width.

Over an erodible snow cover and if sufficient wind speed is present ($u_* \geq u_{*\mathrm{th}}$), transport of snow is initiated. Measurements by Takeuchi (1980) showed that the amount of transported snow increases along the fetch until a steady state situation is achieved. The snow transport can then be described by eq. (9). Assuming steady state snow drifting, a terrain section that gives lowered wind speed should then naturally accumulate snow, since the snow transport capacity of the wind has decreased. In any snow accumulation area, the snowdrift surface elevates gradually as snow particles deposit. The elevated snow surface results in increased local wind speed and the criteria for deposition is thus no longer fulfilled.

On downslopes, the same qualitative description should apply. However, it should be noted that the logarithmic wind profile, eq. (7), is not valid unless the ground is flat. This is evident from Figure 1. Another thing is that little is known about the validity of eq. (9) on downslopes. In a previous study by Thordarson and Norem (2000), the wind speed evolution along fully developed equilibrium snowdrifts on the ground, still showed a continues wind speed reduction according to the relationship in eq. (6). Referring to eq. (9), this results in a dilemma. Under steady state snow drifting, a continuous wind speed reduction along a particular surface should result in snow deposition according to eq. (9). The results by Thordarson and Norem showed that the wind speed reduced by 17 % along a particular equilibrium drift surface, which in terms of eq. (9) equals about 40 % reduction in snow transport capacity along the drift surface, and still the sedimentation had stopped. This indicates that snow drifting on downslopes is more effective than over a flat ground and that the same form of eq. (9) can not by applied. It can further be argued that less wind speed is needed to transport the same quantity of snow on a downslope than over a flat surface. Consider the gravitational force experienced by a snow particle. On a downslope, part of this force acts in the direction of the wind along the ground surface, and thereby contributes to the forward movement. It is possible that the decreasing wind speed and shear stress is balanced out by this gravitational contribution.

The above is in contrast with previous assumptions by Thordarson and Norem (2000) on one hand, and by Tabler on the other hand (1994). These investigators have previously stated that drift sedimentation continues until the ground shear stress is the same as immediately upwind. It has been shown here that steady state snow drifting conditions can exist on downslopes with simultaneous wind speed reduction, without sedimentation to occur. It is important that this applies both to solid ground surfaces as well as equilibrium snowdrift surfaces.

3. GENTLY SLOPING ROAD CUTS

In gently sloping cuts, a uniform cross-section design can serve for drifting snow control along the whole cut section, as long as terrain variations upwind and downwind of the road are small. In the following text, previous snow control
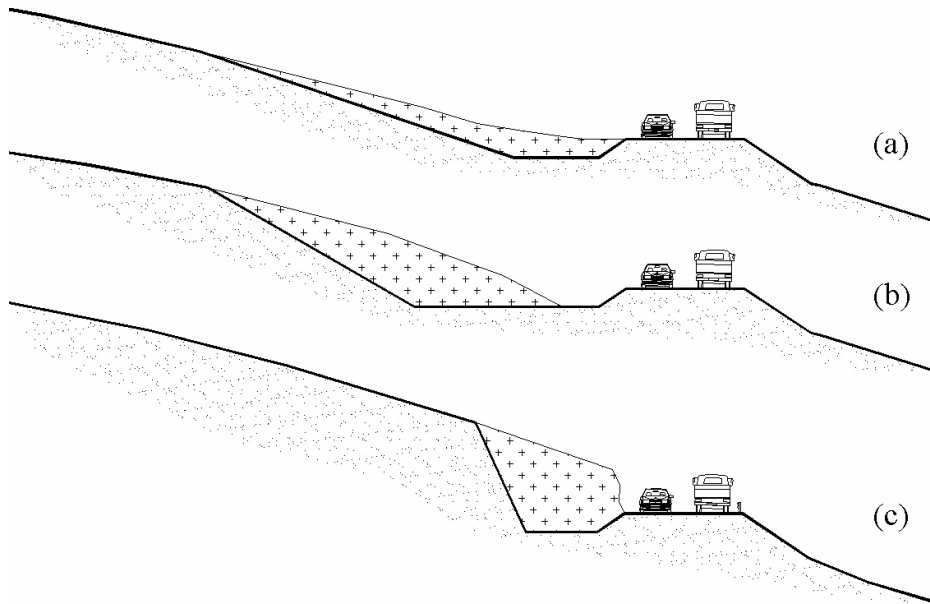
Figure 4 Three possible approaches for snowdrift control, (a) equilibrium snowdrift, (b) large storage capacity and (c) maintenance based snowdrift control.

recommendations for gently sloping road cuts by Norem (1975, 1994) and Tabler (1994) are reviewed.

Although neither listed explicitly by Norem or Tabler, three approaches can be identified in their work to achieve snow drift control in road cuts. A road cut should provide at least one of the following (see Figure 4):

(a) *Equilibrium snowdrift.* The cut is designed to provide a snow erosion zone on the road and thereby preventing drifts to accumulate on it. Snowdrifts in the cut create an equilibrium surface outside the road.

(b) *High storage capacity.* The cut is designed to accumulate large amounts of drifted snow away from the road. Depending on the storage volume and the total annual drifting snow quantities, the drift should not reach the road until late winter.

(c) *Maintenance based snow control.* The cut provides limited storage capacity and demands frequent snow removal. The cut should keep the road free of snow during the first hours of a storm and it should allow the use of snow clearing equipment outside the driving lanes. This solution should be carefully applied due to visibility problems during storm and avoided where large amounts of drifting snow are expected.
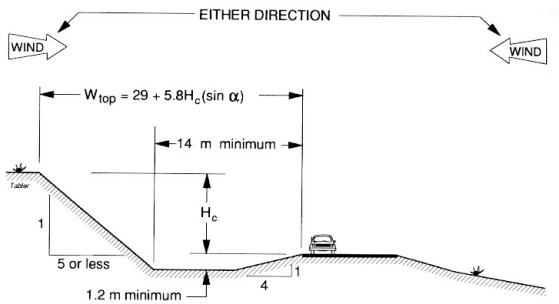
Figure 5 Recommended design for sidehill cuts to ensure a drift free road (Tabler, 1994). The distance W_{top} is reduced according to the sine of the angle of the prevailing wind direction to the road.

Different climatic and topographic conditions on the site may result in different choice of approach towards snowdrift control. In general, the three approaches listed above apply to increasing terrain slope in the respective order. The work in this report is focused on the first approach, snow control by facilitating for equilibrium snowdrift surface that terminates before it reaches the road.

Tabler (1994) suggested a standard cross-section for sidehill cuts that is valid for two-dimensional flow. A sketch of this cross-section is displayed in Figure 5. The design is valid when the terrain upwind from the cut edge is horizontal, and is therefore conservative for an upwind terrain sloping downward toward the cut. Tabler found that the single most important parameter is the distance from the road shoulder to the top of the cut. The principle presented in Figure 5 is intended to create an equilibrium drift that tails out on the road foreslope, below the road shoulder, and thereby ensuring a drift free road. However, it also provides huge storage capacity for drifted snow. Alternatively, Tabler suggest that earthwork volumes can be reduced by using a terraced cut on the expense of snow storage capacity. Finally, Tabler states that the necessary cut length is the same for the opposite wind direction, an assumption that may seem conservative. One serious drawback is associated with the method: Consider a hillside whose slope is equal to or exceeds 1:5.8 (17.2 % or 9.8°). After drawing the 29 m horizontal line upwind from the road edge (any distance results in the same dilemma), the 5.8 H_C line does not intersect the terrain surface at all. This prohibits the use of the method in many situations on long hillsides.

Tabler's proposal presented above is based on his model for equilibrium snow drift surfaces (1994). The snowdrift prediction model is based on regression analysis of measured snow profiles in the field, and utilizes weighing of slopes upwind and downwind of the snowdrift starting point (trap lip).
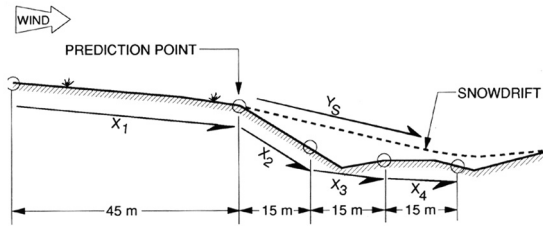
Figure 6 Tabler's snowdrift prediction model, slopes and distances used in eq. (10). (Tabler, 1994).

The model is as follows:

$$Y_S = 0.25\,X_1 + 0.55\,X_2 + 0.15\,X_3 + 0.05\,X_4 \qquad (10)$$

where

Y_S = snow slope (%) over the main portion of the drift

X_1 = average ground slope over a distance of 45 m upwind of the trap lip

X_2 = ground slope from 0 to 15 m downwind of the trap lip

X_3 = ground slope from 15 to 30 m downwind of the trap lip

X_4 = ground slope from 30 to 45 m downwind of the trap lip

Slopes upward in the direction of the wind are taken as positive, and downward slopes as negative. Following limit applies: If measured X_2, X_3 or $X_4 < $ -0.20, set these equal to -0.20. The model is further illustrated in Figure 6. For more exact application, Tabler suggests using the model in an incremental way by shifting the prediction point along the newly calculated surface and repeating the calculation until the predicted surface terminates at the ground. Examining this model, it can be seen that it is not suitable for very steep terrain. The slope limit of -20 % (-11.3°) and the fixed reference distance of 15 m (especially for X_2) results in the predicted surface to extend at a to high elevation, resulting in to long predicted drift. In many mountainous situations, the terrain slope exceeds the range of this model and further development is thus necessary to adapt the model to steeper terrain. The model has however been applied successfully in many appropriate terrain situations from Colorado, Wyoming and New York state (Ronald D. Tabler, private communication).

Norem (1994) recommended a cross-section presented in Figure 7. His field measurements have indicated that the equilibrium drift surface often will follow a line that intersects the upwind terrain slope by an angle of 1:6.5. The model is adjusted according to expected local snow depth on the upwind terrain. Like Tabler, Norem suggests that the distance between the cut edge and the road can be reduced proportional to the sine of the prevailing wind attack angle. Where large snow amounts are expected, Norem recommends a 20-30 m wide ditch to provide high

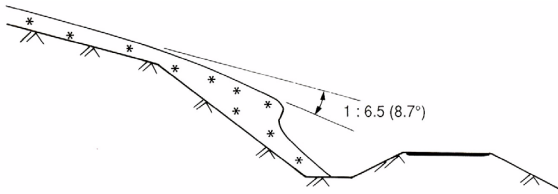Figure 7 Measurements have shown that the drift surface often follows a line that intersects the upwind terrain slope at an angle of 1:6.5 (Norem, 1994).

storage capacity for deposited snow. However, he does not find it necessary to apply the same rule or the principle of Figure 7 for the opposite wind direction. In that case, Norem suggests that the ditch width on the cut side of the road is set to 3-5 m and does not specify the distance to the top of the cut.

4. WORKING METHODS AND MATERIALS

In the current study, both results from elsewhere and new works were analysed. The methods used to achieve the three main goals stated in section 1 were as follows:

1. *Criteria for snowdrift sedimentation.*
   Five terrain profiles with heavy sedimentation areas were used. The actual terrain profiles were divided by the trap lip in two sections. The terrain surface in each section was approximated by straight lines whose slope was measured. Profiles were then categorized according to the landscape far upwind that can either be a hill summit, flat plain or a continuous slope. Four of the profiles (B1030, B1040, B1050 and B1060) are from Bolstadarhlidarbrekka study site at National Road no. 1 in Iceland, previously published by Thordarson and Norem (2000) and one profile (FL14520) is from National Road no. 50 at Flokadalsa river in Iceland (Orion Consulting, Reykjavik. Unpublished material).

2. *Wind speed evolution on downslopes and in road cuts.*
   Results from wind flow simulations were used to access the wind speed curve close to the ground. This was done for both original ground surface and for snowdrifts present on the ground.
   Idealized terrain profiles of constant slope (-20 %) with a road and a gentle sidehill cut (slope -40 %) were modelled. The geometry for the first simulation (Case 1) was constructed to generate a continuous wind speed reduction according to eq. (6). The role of the second (Case 2) was to demonstrate slopes that exhibit constant wind speed. The simulations were done with the flow solver Flow3D (Flow Science, NM USA), which has been applied in several wind flow and snow drifting studies before (Thordarson and Norem, 2000; Sundsbø, 1997; Thiis, 2000). The code solves the Reynolds-averaged Navier-Stokes equations on a finite difference scheme. A standard $k - \varepsilon$ model for turbulence was used. Grid point spacing for Case 1 and Case 2 was the same, 1 m in the vertical and 2

m in the horizontal direction. Height of the simulation domain was eight times the slope total height. Inlet wind conditions are determined by eq. (7) with $z_0 = 0.001$ m and $u_* = 0.7$. The top boundary has a constant pressure, outflow boundary is continuative (all derivatives in the flow direction set to zero) and the bottom is set with a no-slip condition.

3. *Prediction of equilibrium snowdrift surface.* For this task, a mathematical or a statistical approach was used. The main difference between the model developed here and Tabler's model is that the current model is not empirically-derived. The model is inspired by the fact that the upper portion of an equilibrium snowdrift has a slope similar to the upwind terrain, and the drift gradually curves so that the lower portions have a slope similar to the downwind terrain.

5. RESULTS AND ANALYSIS

5.1 Criteria for snowdrift sedimentation

The five terrain profiles together with measured snow surfaces are presented in Figure 8 through Figure 12. Terrain surface immediately upwind and downwind from the snowdrift starting point (trap lip) was approximated by straight lines and the measured slopes given as $\tan\theta \cdot 100\%$.
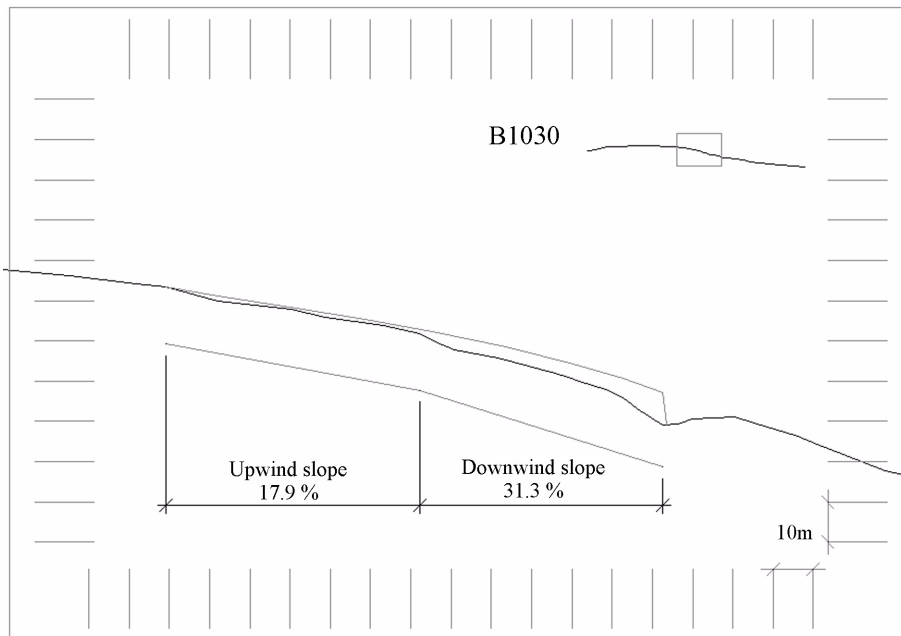
Figure 8 Terrain profile no. 1030 from Bolstadarhlidarbrekka, black line. Measured snowdrift surface indicated by gray line. Terrain slopes next to the snowdrift starting point indicated in terms of $\tan\theta \cdot 100\%$.
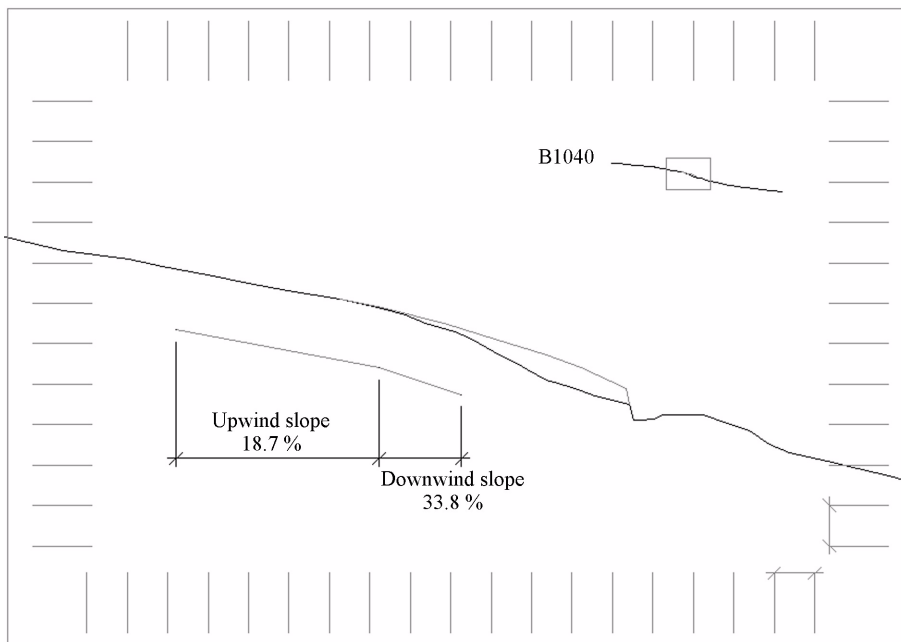
Figure 9 Terrain profile no. 1040 from Bolstadarhlidarbrekka.
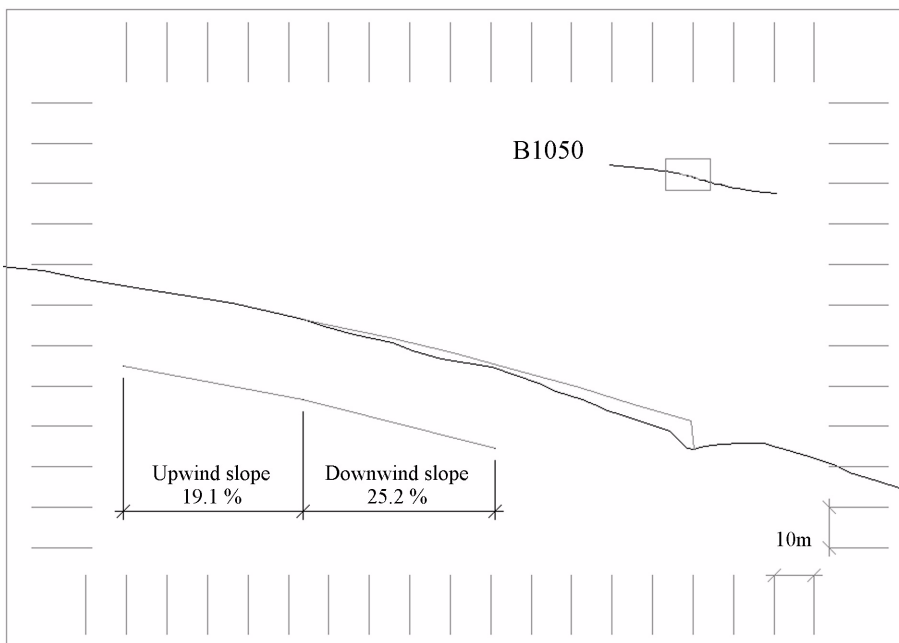
Figure 10 Terrain profile no. 1050 from Bolstadarhlidarbrekka.
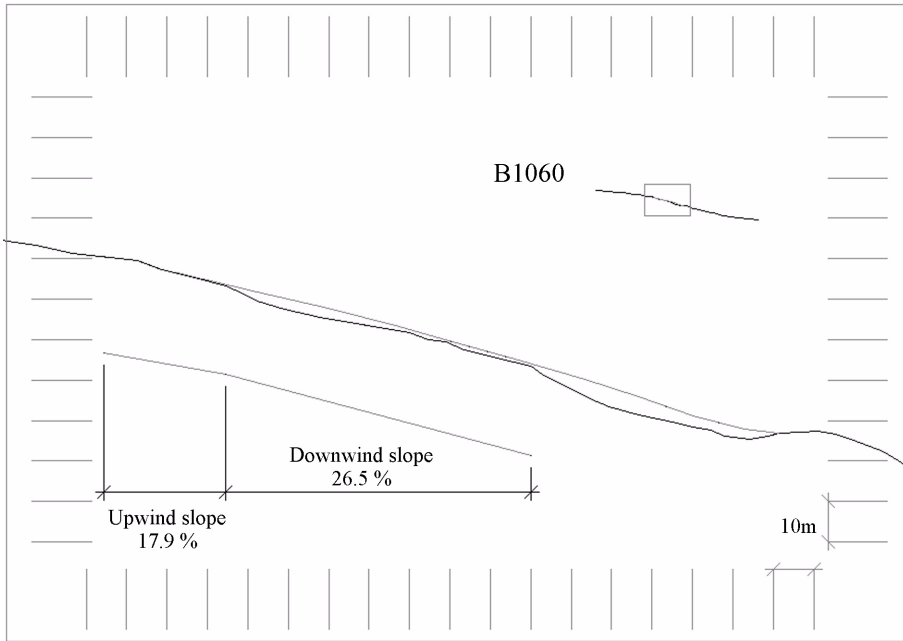
Figure 11 Terrain profile no. 1060 from Bolstadarhlidarbrekka.
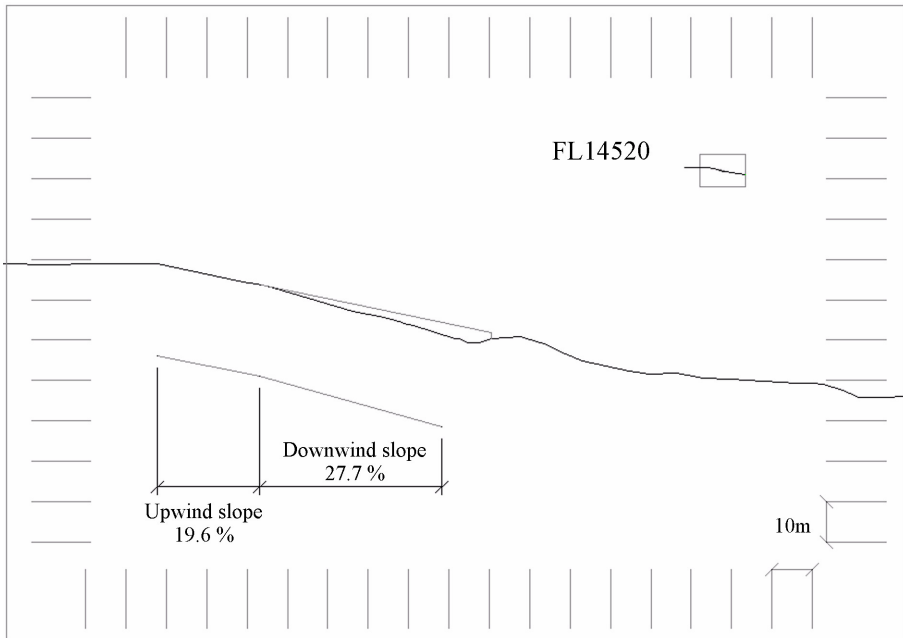
Figure 12 Terrain profile from National Road no.50 at Flokadalsa river in Iceland (location 14520 m). Orion Consulting, unpublished material.

The respective slopes are listed in Table 1. Although more profiles would be needed in order to give reliable criteria for the initiation of snowdrift sedimentation on downslopes, the following information can be extracted from the results:

1. Slopes of up to 20 % do not cause deposition. A possible exception from this is in the case of a slope descending from a hill summit (as B1030 in Table 1).

2. Abrupt slope changes toward 25 % slope or more cause snowdrifts on the ground.

3. A road cut edge will in most cases result in snowdrift sedimentation, depending on the backslope deviation from the upwind terrain slope.

Table 1: . Terrain slopes around the snow sedimentation area.

Profile ID	Terrain slope around trap lip, %		Upwind landscape specification
	Upwind	Downwind	
B1030	17.9[a]	31.3	Hill top
B1040	18.7	33.8	Continuous slope
B1050	19.1	25.2	Continuous slope
B1060	17.9	26.5	Continuous slope
FL14520	19.6	27.7	Plateau

a. Shallow deposits upwind of trap lip

5.2 Wind speed evolution in road cuts

Before presenting the results for the simulations for the idealized slope, two real terrain profiles with different conditions are presented (Figure 13 and Figure 14). The simulated wind speed evolution in these profiles was previously published by Thordarson and Norem (2000).

Figure 13 (B1040) shows the typical wind speed evolution when the equilibrium snowdrift surface extends beyond the road. Wind speed over the road is very low, and will not provide erosion of snow from the road surface. Figure 14 (B1060) presents a situation where the equilibrium drift most likely does not reach the road. Wind speed over the road is relatively high compared to the previous example, as a speedup happens over the road. The fall in the wind speed curve for the drift tail (dashed line, location 400-420 m on the horizontal axis) suggests that the drift was still developing at the time of the survey. However, an imaginary extension of the straight part of the dashed line (360 - 400 m) toward the speedup zone over the road, crosses the speed curve around the road embankment where it is still rising, and therefore the drift is
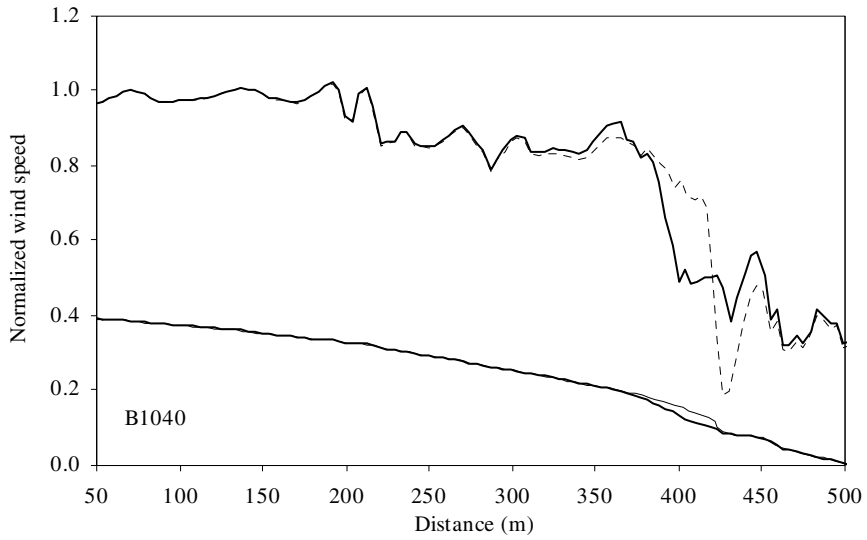
Figure 13 Simulated wind speed evolution along the ground for profile B1040. Normalized wind speed close to the surface ($z = 2$ m) plotted on the vertical axis. Results for wind flow over measured snow cover as dotted line. (Thordarson and Norem, 2000).
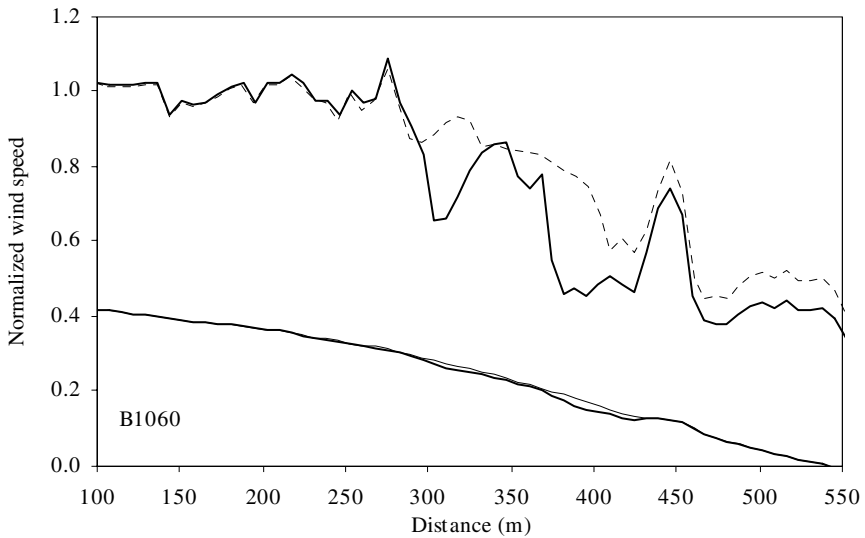
Figure 14 Simulated wind speed evolution along the ground for profile B1060. Normalized wind speed close to the surface plotted on the vertical axis. Results for wind flow over measured snow cover as dotted line. (Thordarson and Norem, 2000).
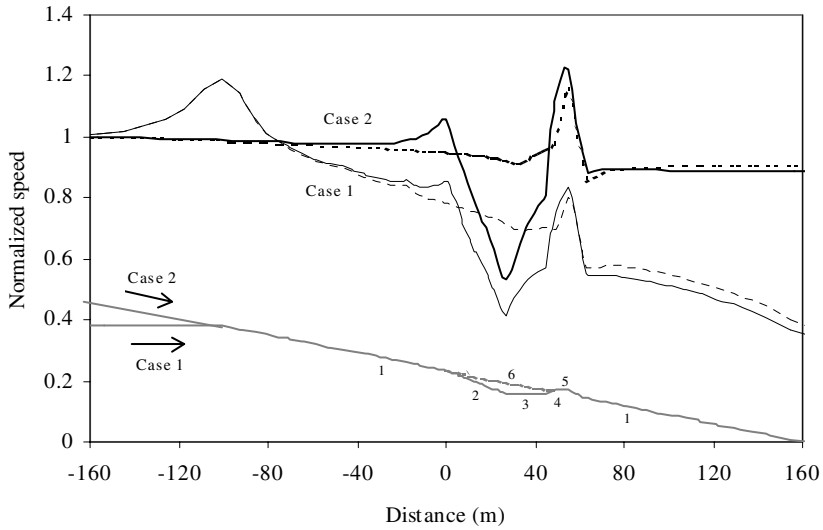
Figure 15 Wind flow simulation for road cut in an idealized sidehill of 20 % slope, wind speed evolution close to the ground. Results for Case 1 and Case 2. Terrain elements marked with numbers; 1 original ground, 2 cut backslope, 3 ditch bottom, 4 road foreslope, 5 road surface and 6 predicted snowdrift surface (simply an extension of the upwind slope that tilts slightly upward close to the road shoulder).
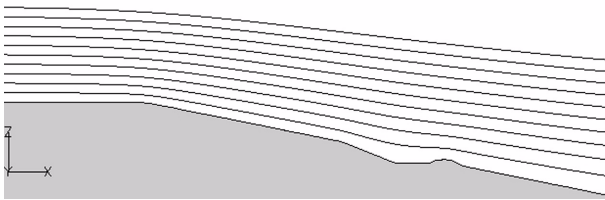
Figure 16 Wind flow simulation, Case 1, streamlines.
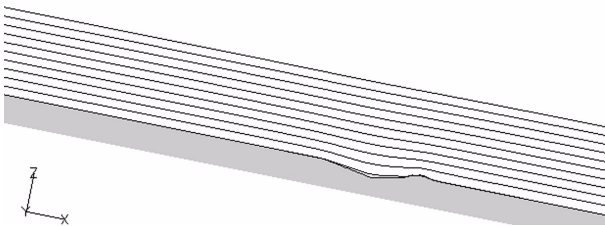
Figure 17 Wind flow simulation, Case 2, streamlines.

likely to terminate on the road shoulder. In other words, the road surface will most likely lie in an erosion zone both before and after the drift has reached its equilibrium stage. In both Figure 13 and Figure 14, it is observed how the wind speed adjusts to a constant value along the gradually sloping upper portions of the profiles, as was discussed in section 2.1.

Figure 15 shows results from the idealized slope. Case 1 shows the wind speed evolution that would apply in most situations as discussed in section 2.1, and Case 2 shows results when the upwind landscape generates a constant wind speed along the slope. Looking at the wind speed curve for Case 1, it shows an increased wind speed around the edge where the slope starts (-100 m). This behaviour is commonly observed where sharp slope changes occur. The same happens at the road cut edge in both cases (0 m). Apart from this speedup observed around the abrupt slope changing points, the wind speed evolution over the backslope (2) of the road cut in both cases, and on the upwind slope for Case 1 behaves according to eq. (6). Table 2 shows the resulting estimates for the constant *B* from eq. (6).

Table 2: . Results from Figure 15 fitted against eq. (6).

Terrain portion		Terrain slope, %	*B* in eq. (6)
Case 1	Upwind of road cut	20	0.0025
	Cut backslope	40	0.018
Case 2	Upwind of road cut	20	0[a]
	Cut backslope	40	0.020

a. Model setup predefined to maintain a constant speed upwind of the road cut.

The wind speed reaches a minimum at the foot of the backslope and starts to speed up over the ditch bottom (3). A sharp rise in the speed is observed over the embankment foreslope (4) and over the road surface (5). It is important that the speedup over the road is the same whether the snowdrift is present or not. Results for Case 1 and Case 2 suggest that the drift continues to develop until the wind speed curve along it has the same gradient as the curve over the ground upwind from the cut edge. This is also observed in Figure 14. In Figure 13 the situation is different, and the terrain downwind of the road is dominating the gradient of the wind speed curve along the equilibrium drift. Profile B1040 exposes an unusually large change in terrain slopes between the upwind and downwind sections of the trap lip and the conditions are quite far from offering a drift free road. I therefore believe that in most cases, the criterion for a drift free road can be represented by Case 1 in Figure 15 and summarised as follows:

- Equilibrium snowdrift surface results in a wind speed evolution that follows the same horizontal wind speed gradient along the surface as that immediately upwind of the trap lip.

- An extension of the wind speed curve upwind of the trap lip (or cut edge), drawn downwind towards the road, should intersect the speed curve around the road no closer to the road than on the foreslope.

These results are important, since they allow the use of pure wind flow simulations or physical model experiments to test the quality of a given design with respect to snow drifting. In other words, to test this principle, no snowdrift simulation is necessary, only wind speed information. In general, the results above show that the equilibrium drift surface tends to adjust both to the terrain surface upwind and downwind of the drift area. In the same way, the wind speed curve adjusts according to the new surface created by the drift deposits. It can be said that the objective of the wind is to deposit snow particles on the ground until an equilibrium stage represented by least possible loss in kinetic energy is reached. Also, the transition from the upwind terrain and over to the drift surface and from the drift surface to the downwind original terrain is smooth, and both the wind speed curve and the drift surface are tangents to the respective elements outside the drift area.

5.3 Equilibrium snowdrift prediction

In the pursuit for a statistical model for generation of snowdrift surfaces, results from the previous section are utilised, together with the fact that any surface boundary (such as the ground or a snowdrift surface) in the flow is a streamline. The predicted surface thus has to resemble a streamline that is tangent to the upwind ground slope and the downwind ground. Thinking of the equilibrium drift as an aerodynamic optimal surface with respect to minimum loss of kinetic energy from the wind, it should be "streamlined". Even if the drift is deposited due to flow separation in the actual area, the equilibrium drift surface is supposed to have eliminated flow separation, and the method is thus both valid for separated and unseparated flow.

The calculation scheme presented below, creates a surface based on upwind and downwind weighing of terrain slopes. Before applying the scheme, two points have to be defined in advance: The drift starting point and an assumed drift length. The scheme then creates a streamlined surface along the estimated drift area. The appearance of the calculated drift surface, especially in relation with the downwind terrain can then be used to evaluate if the predicted drift length is likely or not. The procedure is complete in the following steps, together with Figure 18 and Table 3:

1. Draw the terrain cross section including the proposed road construction, along the prominent snow drifting wind direction.

2. Identify the trap lip (starting point of drift growth). Refer to the criteria in section 5.1

3. Define the most likely maximum extension of the drift (drift length from the trap lip). This length can be defined e.g. according to Norem (1994),

with a line that intersects the downwind terrain at an angle of 1:6.5 from the upwind terrain (Figure 7), or the first guess could otherwise be a drift that is to terminate at the road foreslope. The predicted drift length is assigned the symbol L_p, in Figure 18.

4. Divide the drift area into ten segments of equal length, $L_p/10$. Each segment or step is assigned a number, $n \in [1;10]$. Define imaginary points on the drift surface to be calculated, point 0 is the trap lip and point n is at the right hand end of step n.

5. Starting on step $n = 1$, calculate the slope from point $(n - 1)$ to a point on the ground at distance $L_p/2$ upwind: $\varphi_n = \Delta Z/(L_p/2)$, where ΔZ is the vertical distance between the respective points. On steps 6 to 10, this point is on the newly calculated drift surface, point $(n\text{-}5)$, not on the original ground. (All slopes involved are given as $\Delta Z/\Delta X$. Slopes downward in the wind direction are negative, upward slopes are positive).

6. Calculate the slope from point $(n - 1)$ on the calculated drift to the ground at distance $L_p/2$ downwind: $\psi_n = \Delta Z/(L_p/2)$.

7. Now the estimated drift slope over step n becomes:

$$S_n = \varphi_n \left[1 - \frac{n}{10}\right] + \psi_n \left[\frac{n}{10}\right] \tag{11}$$

8. Draw the slope segment S_n in the terrain profile, extending $L_p/10$ downwind from point $(n\text{-}1)$, and repeat the procedure for the next step until the ten segments have been drawn and Table 3 is complete. Note that in each step, the reference point, $(n\text{-}1)$, is always located on the calculated drift surface (unless $n\text{=}0$, then the reference point is on the original ground where the drift starts).

9. A calculated drift that ends in mid-air and points along the downwind slope suggests that the initial L_p is to short. Drift that reaches the ground surface or tails out close to the ground suggests that the chosen L_p is probably informative about the maximum drift growth in the actual terrain cross section.

The method has been successfully tested on several different terrain profiles. It gives a useful check on the validity of drift lengths estimated by other methods, e.g. Norem's or Tabler's. An example of the application is in Figure 19, where L_{p1} (predicted drift intersecting the ground at an angle 1:6.5 from the upwind terrain slope) turned out to be to short and the most likely drift extension is in the vicinity of L_{p2} (angle 1:9 from the upwind terrain slope).
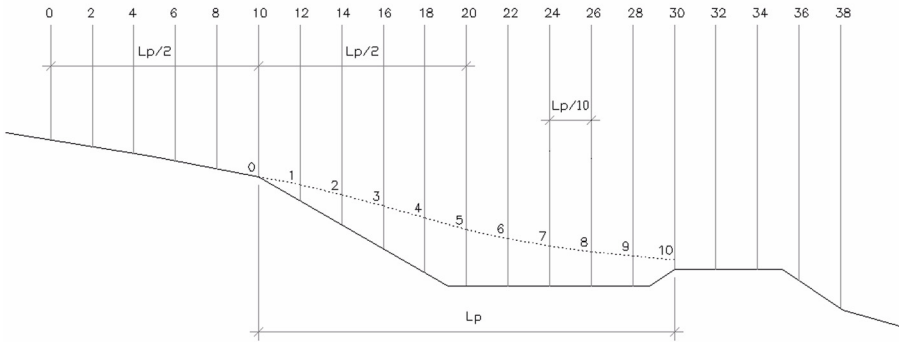
Figure 18 Explanation to the method for equilibrium snow surface prediction by incremental slope weighting. L_p is first guess for drift length prior to using the calculation scheme. The vertical lines are numbered for convenience. As an example, the upwind slope from segment 7, U_7, is the slope from point 6 (line 22) to the intersection of line 12 with the newly calculated drift surface (point 1), and the downwind slope, D_7, is from point 6 to the intersection of line 32 with the ground.

Table 3: . Calculation scheme for incremental equilibrium slope prediction.

Step no.	Upstream		Downstream		Weighed slope eq. (11)
	Slope	Factor	Slope	Factor	
1	φ_1	0.9	ψ_1	0.1	S_1
:	:	:	:	:	:
n	φ_n	$1 - \dfrac{n}{10}$	ψ_n	$\dfrac{n}{10}$	S_n
:	:	:	:	:	:
10	φ_{10}	0	ψ_{10}	1.0	S_{10}
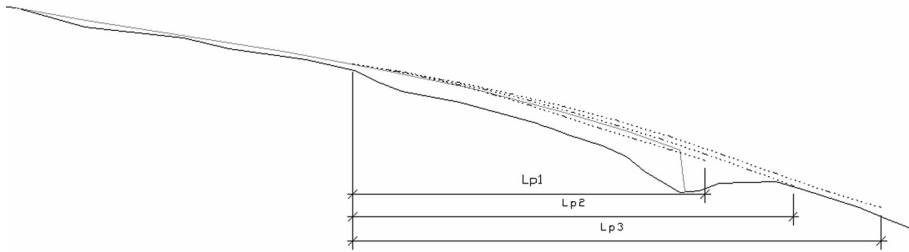
Figure 19 Results from testing of the drift prediction method for profile B1030. The figure shows results for three different distances for the initial L_p together with the measured snow surface in gray. In this example L_{p1} equals 80 % of L_{p2} and L_{p3} equals 120 % of L_{p2}.

6. DISCUSSION

The wind flow and snow drifting conditions on downslopes and in gradual road cuts were studied. The results can be summarised as follows:

1. Even though gradual road cuts do in most cases initiate sedimentation, it is crucial to know in advance if sedimentation will be triggered upwind of the cut, as this will result in a longer equilibrium drift extension. The maximum terrain slope that sustains high enough wind speed to prevent heavy snow deposition was estimated to be around 20 %. However, the results indicate that snow sedimentation is likely to occur at a less slope (< 20 %) downwind from hill summits than when the upwind landscape is flat or descending in the wind direction. The sparse number of measured snow profiles available for the current study prevents the generalization of these results. Future works should include the compilation of a database with a large number of terrain profiles with snow measurements, in order to identify the influence of the upwind landscape on the snow sedimentation potential at different slopes.

2. Wind speed evolution on downslopes prone to snowdrift sedimentation shows a rapid decrease in wind speed. When the terrain surface can be approximated by straight lines, the wind speed falls approximately linearly along the slope and the horizontal wind speed gradient is depending on the slope angle and the upwind landscape.

3. A drift free cross section design of a road should ensure that the road is located in an erosion zone downwind of an equilibrium drift surface. This is achieved when an extension of the wind speed curve upwind from the trap lip, drawn downwind towards the road, intersects the speed curve around the road in the ditch, or no later than on the foreslope. This principle can be

verified for any proposed cross section with wind flow simulations or physical experiments.

4. A statistical method for predicting equilibrium snowdrift surfaces was proposed. The method does not give the drift extension explicitly, but is relying on a reasonable initial guess for the drift extension. The appearance of the calculated drift surface indicates the validity of the predicted drift extension, and the method can be repeated for different distances to seek the most likely equilibrium snowdrift surface. The advances of the model compared to Tabler's model is that it is applicable in any geometric scale, regardless of terrain slope. The calculation scheme has not been calibrated with survey data, but simply creates a streamlined surface over a given distance. It is very likely that the performance of the scheme can be improved by selecting other scaling procedures or by altering the relative difference over which the upwind and downwind reference slopes are evaluated. However, the author believes that any calibration with respect to measured snow profiles should be done with care, so the scheme is not "locked" to certain landscape types. Especially should the distances over which the slopes are measured be related to the overall length scale (the current proposal is $L_p/2$), instead of being locked to a fixed distance (as in Tabler's equation, 15 and 45 m). On the other hand, it might be the case that different scaling is necessary for different landscape types in order to optimize the results from slope weighing models.

ACKNOWLEDGEMENTS

REFERENCES

Beljaars, A.C.M., Walmsley, J.L. and Taylor, P.A., 1987. A mixed spectral finite-difference model for neutrally stratified boundary-layer flow over roughness change and topography. Boundary-Layer Meteorology 38: 273-303.

Finnigan, J.J., Raupach, M.R., Bradley, E.F. and Aldis, G.K., 1990. A wind tunnel study of turbulent flow over a two-dimensional ridge. Boundary-Layer Meteorology 50: 277-317.

Gerhart, P.M., Gross, R.J. and Hochstein, J.I., 1992. Fundamentals of fluid mechanics. Addison-Wesley Publishing Company, Reading.

Kobayashi, D., 1972. Contributions from the Institude of Low Temperature Science. Hokkaido University, Sapporo.

Liljequist, G.H., 1957. Energy exchange of an Antarctic snow-field. Norwegian-British-Swedish Antarctic expedition, 1949-52. Scientifig results. Norsk Polarinstitutt, Oslo.

Norem, H., 1975. Designing highways situated in areas of drifting snow. Draft translation 503. CRREL, Hanover, New Hampshire.

Norem, H., 1994. Snow Engineering for Roads. Handbook no. 174. Norwegian Public Road Administration, Road Research Laboratory, Oslo.

Pomeroy, J.W. and Gray, D.M., 1990. Saltation of Snow. Water Resources Research 26: 1583-1594.

Raithby, G.D. and Stubley, G.D., 1987. The Askervein Hill Project: A finite control volume prediction of three-dimensional flows over the hill. Boundary-Layer Meteorology 39: 247-267.

Schmidt, R.A., 1986. Transport rate of drifting snow and the mean wind speed profile. Boundary-Layer Meteorology 34: 213-241.

Stull, R.B., 1988. An Introduction to Boundary Layer Meteorology. Kluwer Academic Publishers, Dordrecht.

Sundsbø, P.A., 1997. Numerical modelling and simulation of snow drift. Thesis. Norwegian University of Science and Technology, Narvik.

Tabler, R.D., 1994. Design Guidelines for the Control of Blowing and Drifting Snow. SHRP-H-381. National Research Council, Washington, DC.

Takeuchi, M., 1980. Veritcal profile and horizontal increase of drift-snow transport. Journal of Glaciology 26: 481-492.

Taylor, P.A. and Teunissen, H.W., 1987. The Askervein Hill Project: Overview and background data. Boundary-Layer Meteorology 39: 15-39.

Thiis, T.K., 2000. Experimental validations of numerical simulations of snowdrifts around buildings and in terrain. Thesis. Norwegian University of Science and Technology, Trondheim.

Thordarson, S. and Norem, H., 2000. Simulation of two-dimensional wind flow and snow drifting application for roads: Part I & II. In: Hjorth-Hansen, E., Holand, I., Løset, S. & Norem, H.(Editors), Snow Engineering. Recent Advances and Developments. Proceedings of the fourth International Conference on Snow Engineering, Trondheim, Norway, 2000. A.A. Balkema, Rotterdam, pp. 437-452.

Thordarson, S. and Norem, H., 2002. Design criteria for roads in snow-drifting areas. Proceedings of the XIth International Winter Road Congress, 28-31 January 2002. PIARC, Sapporo.

Wood, N., 1995. The onset of separation in neutral, turbulent flow over hills. Boundary-Layer Meteorology 76: 137-164.

Paper IV:
Snow drifting on roads
under steep sidehill cuts

(Submitted to Cold Regions Science and Technolgy)

Snow drifting on roads under steep sidehill cuts

Skuli Thordarson[1]

Norwegian University of Science and Technology, Department of Road and Railway Engineering, 7491 Trondheim, Norway

ABSTRACT: Snow drifting on roads is a major concern in many areas. Both terrain characteristics and road design in addition to climatic factors influence the severity of snow drifting problems. Road sections with terrain cuts are the most vulnerable both concerning visibility and snow depositing on the road. The aim of the study was to analyse the flow of air and drifting snow under steep road cuts and to propose new design principles that may reduce the snow problems. Numerical wind flow simulations and a field study from an existing road were applied in this work. Wind flow studies allow for a qualitative comparison of different cut designs. The results confirm that snow drifting under steep cuts is governed by three-dimensional flow pattern, in contrast to two-dimensional flow through gently sloping cuts. Secondary vortex flow is generated at the sharp edges of the steep cut. Modifications to the cut shape affect the vortex flow and can be used for snow control in order to minimize problems on the road. New design principles for steep road cuts were tested, and the most promising principle suggests a cut that expands in width toward the cut ends. This modification increases the speed of the secondary vortex and facilitates for smoother flow pattern and less turbulence. The design is expected to improve visibility and reduce snow sedimentation on the road, without much additional construction costs.

1. INTRODUCTION

1.1 General

Snow drifting on roads affects both accessibility and safety. The hazard can be divided into two main categories; (1) high snow concentration in the air reduces the visual range for the drivers and (2) the deposition of snowdrifts on the road. Road sections with terrain cuts are the most vulnerable both concerning visibility and snow depositing on the road. Therefore are roads in mountainous and hilly terrain more frequently exposed than roads in an open landscape. Although problems may arise under every wind direction, the most vulnerable cut sections are usually found where

---

1. Fax: +47 7359 7020; E-mail: thordars@stud.ntnu.no

the prevailing snow drifting wind direction is perpendicular to the road and the cut is on the windward side of the road.

The main goal of this work is to propose design alternatives that might reduce the snow problems on roads under steep sidehill cuts. To achieve this, the wind flow under steep road cuts was analysed with numerical simulations and the snow drifting behaviour was explained from a fluid-dynamical point of view. The paper demonstrates how numerical wind flow simulations allow a qualitative comparison of the expected visibility and snow sediment conditions for different wind directions and road design. Although not giving exact results for snow drifting, wind simulations can be used to predict the most likely snow behaviour, due to theoretical and experimental relationships between wind flow and snow drifting.

The basis for the current work is following:

1. Previous publications on design principles for steep road cuts by Norem (1975, 1994) and Tabler (1994).

2. Theoretic and experimental relationships between wind flow and snow drifting.

3. Field observations from National Road no.1 at Bolstadarhlidarbrekka in Iceland.

4. Numerical wind flow simulations with the commercial engineering flow solver Flow3D (Flow Science, NM USA).

With these resources, new design alternatives were proposed and tested in the flow solver. The advantage of the current study compared to previous work of Norem and Tabler is the opportunity to investigate the importance of three-dimensional flow behaviour in road cuts.

The most promising design proposal introduces a steep cut design with variable ditch width, wherein the foot of the backslope follows a curve in the horizontal plane. I expect this design to cause less snowdrift sedimentation on and around the road in addition to improved visibility. The principal conclusion is that snow drifting problems on roads under steep rock cuts can be reduced by controlling the wind flow with alternative geometric design without greatly increasing the construction costs.

2. ROAD CUT PRINCIPLES

The requirements to road design in snow-drifting areas have previously been summarized by Norem (1975,1994). According to this, the most important goals are; (1) to avoid snow deposits on the road, (2) to ensure little snow transport across the road for better visibility and (3) to facilitate for the maintenance of the chosen design. In practice, the road design often has to compromise between construction costs, safety, accessibility and maintenance costs. The requirements are important to keep in mind when designing cut sections.
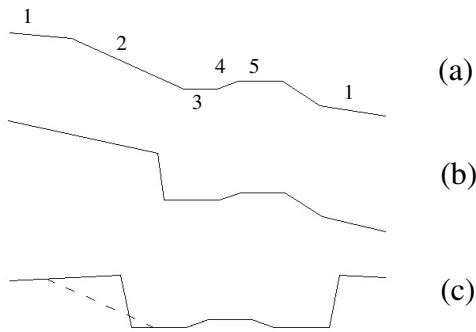
Figure 1 The three types of road cuts.(a) Gentle backslope cut, (b) steep cut, generally used when rock is excavated and (c), a double cut, can have either a gentle or a steep backslope. Typically used when cutting through hilltops. The numbers refer to: 1 original ground, 2 backslope, 3 ditch, 4 foreslope and 5 road surface.

According to different terrain conditions and requirements to road cuts, they differ in height and slope. Roads in steep hillsides claim high cuts and so can roads passing over hilltops do. Soil stability demands gentle sloping cuts in loose soil, whereas high blasting and excavation costs for rock often lead to steep cuts in rock. In general, the most important factors that influence the size and shape of road cuts are:

- Terrain slope
- Soil stability
- Water drainage
- Visual range in curves
- Aesthetics
- Ice- and rock-fall protection
- Snow control

The chosen design has to compromise between these factors and of course the construction and maintenance costs. A sketch of the three main cut types is shown in Figure 1. Different cut types result in different flow pattern around the road with subsequent different snow drifting behaviour.

In a previous publication, Thordarson and Norem (2000) have distinguished between road sections featuring two- and three-dimensional flow. Sidehill cuts with gentle backslope (Figure 1 a) generate wind flow and snow drifting conditions that can be described two-dimensionally. That is because the main flow does not change direction substantially when passing through the cut. Consequently, a uniform cross-section design can serve for drifting snow control along the whole cut section, as long as terrain variations upwind and downwind of the road are small. Steep cuts on the contrary, develop secondary flow motion directed parallel the road and thus the wind flow and snow drifting can only be described three-dimensionally. In the following text, previous snow control recommendations for both gently sloping cuts and steep rock cuts by Norem and Tabler are reviewed.

Although neither listed explicitly by Norem or Tabler, three approaches can be identified in their work to achieve snow drift control in road cuts. A road cut should provide at least one of the following:

1. *Equilibrium snowdrift.* The cut is designed to provide a snow erosion zone on the road and thereby preventing drifts to develop on it. Snowdrifts in the cut create an equilibrium surface outside the road.

2. *Snow storage capacity.* The cut is designed to accumulate large amounts of drifted snow away from the road. Depending on the storage volume and the total annual drifting snow quantities, the drift should not reach the road until late winter.

3. *Maintenance based snow control.* The cut provides limited storage capacity and demands frequent snow removal. The cut should keep the road free of snow during the first hours of a storm and it should allow the use of snow clearing equipment outside the driving lanes.

2.1 Gentle slope cuts

Tabler (1994) suggested a standard cross-section for sidehill cuts that is valid for two-dimensional flow. A sketch of this cross-section is displayed in Figure 2. The design is valid when the terrain upwind from the cut edge is horizontal, and is therefore conservative for an upwind terrain sloping downward toward the cut. Tabler found that the single most important parameter is the distance from the road shoulder to the top of the cut. The principle presented in Figure 2 is intended to create an equilibrium drift that tails out on the road front slope, below the road shoulder, and thereby ensuring a drift free road. However, it also provides huge storage capacity for drifted snow. Alternatively, Tabler suggest that earthwork volumes can be reduced by using a terraced cut on the expense of snow storage capacity. Finally, Tabler states that the necessary cut length is the same for the opposite wind direction, an assumption that may seem conservative.
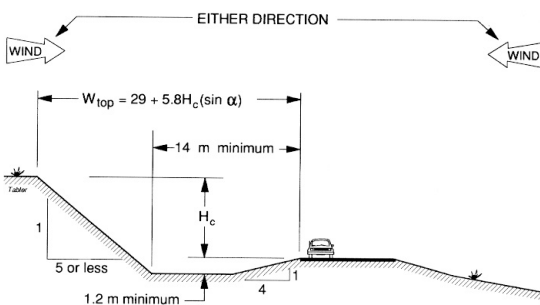

Figure 2 Recommended design for sidehill cuts to ensure a drift free road (Tabler, 1994). The distance W_{top} is reduced according to the sine of the prevailing wind direction.
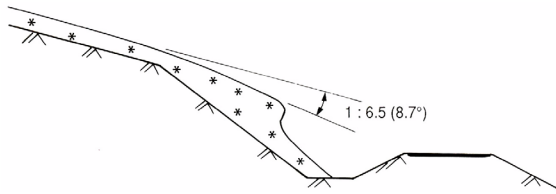
Figure 3 Measurements have shown that the drift surface often follows a line that intersects the upwind terrain slope at an angle of 1:6.5 (Norem, 1994).

Norem (1994) recommended a cross-section presented in Figure 3. His field measurements have indicated that the equilibrium drift surface often will follow a line that intersects the upwind terrain slope by an angle of 1:6.5. The model is adjusted according to expected local snow depth on the upwind terrain. Like Tabler, Norem suggests that the distance between the cut edge and the road can be reduced proportional to the sine of the prevailing wind attack angle. Where large snow amounts are expected, Norem recommends a 20-30 m wide ditch to provide high storage capacity for deposited snow. However, he does not find it necessary to apply the same rule or the principle of Figure 3 for the opposite wind direction. In that case, Norem suggests that the ditch width on the cut side of the road is set to 3-5 m and does not specify the distance to the top of the cut.

In a later study, Thordarson and Norem (2000) used numerical wind flow simulations to associate wind speed development, intermediate stage of drift growth and terrain characteristics around the road. Results from their numerical experiments indicate that drift growth will in theory continue until the drop in wind speed along the drift surface is very small. This is in accordance with Tabler's assumption, that the drift surface will elevate until the surface shear stress is the same as that immediately upwind. The current author is preparing another paper intended as a supplement to snow drifting theory in gently sloping road cuts with two-dimensional flow conditions.

2.2 Steep cuts

For sidehill cuts in rock, a steeper backslope or even a vertical cut is usually applied for practical and economic reasons (Figure 1 b and c). Previous recommendations for steep cut design suggest that an extra wide ditch should be provided wherever snow drifting is expected. By excavating a wider ditch in combination with steep cuts the following benefits are achieved according to Norem (1994):

1. Moving the drift area a certain distance away from the road causes the snow to deposit before it reaches the road, and visibility is substantially improved.

2. At the beginning of a storm, snow will collect outside the road and the number of snow removal duty cycles can therefore be reduced. If the ditch is wide enough, the use of a rotary blower can be postponed until after the storm.
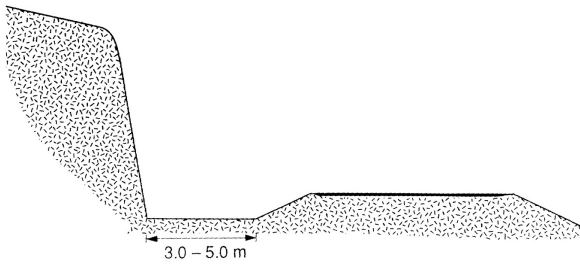
Figure 4 Steep road cut. Norem (1994) recommends a minimum ditch width of 3-5 m.

3. The snow in a 3-5 m wide ditch is easily cleared with a rotary blower working parallel the road and it is therefore possible to use the blower during good weather periods to prepare for the next storm.

A sketch of Norem's proposal is displayed in Figure 4. His physical model experiments (Norem, 1975) indicated that a 5 m wide ditch increases the visibility for wind speeds up to approximately 20 m/s.When the wind direction is almost parallel the road or if the cut is on the leeward side of the road, a relatively narrow ditch would suffice.

Tabler (1994) also proposed a wider ditch for use with steep cuts in snow drifting areas in addition to a 2.5 m wide paved shoulder lane (Figure 5). The main benefits outlined by Tabler are:

1. A minimum ditch width of 3.7 m provides space to contain snow sliding off backslopes, and to store snow removed from the inside lane, over the course of a storm lasting several days.

2. The 2.5 m wide paved shoulder facilitates for snow ploughing and serves four important functions:

   • provides extra width to allow highway users to pass snow removal equipment and slower traffic,

   • allows high-speed ploughs to remove snow from the shoulder (keeping the shoulder ploughed provides a buffer against snow encroachment in the travelled way, thereby allowing more time between snow removal duty cycles),

   • displaces snow berm farther away from travelled way, which reduces the tendency of snow to accumulate on travel lanes,

   • provides better rock fall protection.

3. The 1:6 front slope allows off-road equipment, such as front-end loaders and graders to remove snow from the ditch during clean-up operations between storms.
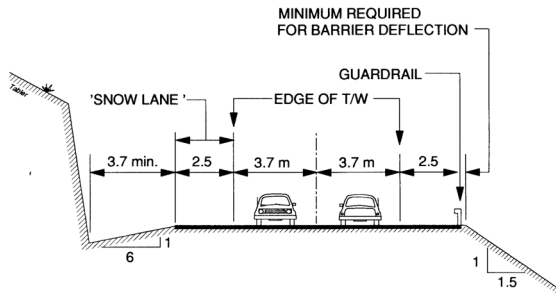
Figure 5 Tabler's proposal for a steep cut design (1994).

The above lists by these two investigators do not reflect identical problems in every aspect, possibly due to different climatic conditions and road standards at where their experiences are gathered. Anyhow, the resulting design proposals for steep cuts from these two investigators are very similar. In Figure 4, assuming a 1 m deep ditch and a foreslope of 1:2, the minimum recommended distance between the travelled lane and the backslope is 5 m, practically the same as the minimum demand in Figure 5.

The recommendations from both Norem and Tabler treat the steep cut as a two-dimensional phenomena. In reality, the observed snowdrifts and driving conditions seldom appear uniform along a steep cut section, and these should consequently by studied three-dimensionally.

3. WIND FLOW AND SNOW DRIFTING THEORY

3.1 Snow transport and sedimentation

The process of snow drifting depends on several physical factors regarding the air and the snow. Regarding the amount of drifting snow in the air, the most important factors are:

- *Wind speed*. Amount of drifting snow increases with increased wind speed.

- *Snow cover hardness*. The history of the snow cover, e.g. temperature and humidity development, determines the threshold wind speed for snow drifting to initiate. A hardened snow cover needs a higher wind speed to erode than a loose snow cover.

- *Precipitation*. Simultaneous snow fall both supplies higher snow concentration directly in the air and provides fresh, easily eroded snow on the ground.

In the following text, the importance of the wind speed is emphasized. Road location with respect to terrain features and modification of the terrain adjacent to the road determines the wind speed distribution in the road cut. The local wind speed is thus the only factor listed above that the engineer partially can control through the choice of design.

The movement of air over the ground exerts an atmospheric shear stress on the surface which is responsible for the erosion of snow particles from the snow cover. The magnitude of turbulent and molecular shear stress at the surface, τ_0, is convenient to describe by the friction velocity, u_*, defined as

$$u_* = \sqrt{\frac{\tau_0}{\rho}}$$
(1)

where ρ is the density of air. Over a relatively flat ground and under statically neutral conditions, the friction velocity has a linear relationship with the wind speed. This is a result of the logarithmic wind speed profile that develops over the ground. The logarithmic wind profile is written as:

$$u(z) = \frac{u_*}{\kappa} \ln\left(\frac{z}{z_0}\right)$$
(2)

where $u(z)$ is the wind speed at height z. The aerodynamic roughness height, z_0, is a measure of the ground roughness and gives the theoretical height at which the wind speed is zero. The letter κ stands for the von Karman constant, usually equal to 0.4 (Stull, 1988). For constant surface roughness, z_0, a known wind speed at a certain height above the ground, either measured or simulated, will therefore give an estimate on the shear stress at the surface, by combining equations (1) and (2).

Per definition, eq. (2) is only valid on flat ground. When the ground is not flat however, the vertical velocity profile departs from the logarithmic relationship and the friction velocity, u_*, loses it's linearity to the wind speed at a given height. Over a rolling or more complex terrain, $u(z)$ will thus only give a rough estimate of the friction velocity. The closer to the ground $u(z)$ is known, the more accurate will the prediction of u_* be.

In mountainous or hilly terrain the mean wind speed close to the ground varies spatially. Wind speed tends to increase on crests and decrease in depressions. Sharp edges in the landscape or even progressive downslopes often trigger boundary layer separation, which results in a reversed mean flow direction close to the ground, high turbulence activity and often lowered wind speed. The variable wind speed explains the uneven distribution of snowdrifts in complex terrain. A simple rule of thumb states that snow is eroded from the ground in high speed areas and deposited in low speed areas.

Through numerous observations and theoretical considerations it has been found that the total amount of snow transported by the wind is roughly a function of the third power of the friction velocity or the wind speed (Schmidt, 1986; Pomeroy and Gray, 1990; Kobayashi, 1972). A simple estimate on the amount of blowing snow can be written as:

$$Q = a(u_* - u_{*\text{th}})^3$$
(3)

where Q (kg/s m) is the snowdrift rate per unit width, $u_{*\text{th}}$ (m/s) represents a threshold friction velocity to initiate snow drifting and the constant a is found by regression analysis on experimental data.

In their two-dimensional simulations of the wind flow across the road in Bolstadarhlidarbrekka mountain side, Thordarson and Norem (2000) showed that the simulated wind field is useful for evaluating the snow drifting conditions. They showed how the horizontal wind speed gradient, du/dx, can be transformed to a vertical snow transport gradient, dQ/dx. A negative value of this gradient results in snowdrift sedimentation, given that the wind is fully saturated with snow particles. A high negative value will cause high rate of snowdrift build-up on the ground. Some of their results which are relevant here can be summarised:

- Major drift areas are identified by a high drop in wind speed.

- Snow is deposited until the elevated drift surface eliminates the sharp wind speed drop (du/dx approaches zero).

- The faster the wind speed decreases along the terrain (the higher negative value of du/dx), the higher is the rate of deposition of snow.

- The higher the total drop in wind speed, the more is the total volume of snow that can be deposited before state of equilibrium (a high storage capacity of the terrain feature).

In three-dimensional flow however, the criteria for snow sedimentation are more complicated. The concentration of snow in the air can be very high in some areas, and sedimentation can occur at relatively high wind speeds. Consequently, care must be taken when using wind speed measurements or simulations to predict snowdrifts in three-dimensional flow.

3.2 Wind speed and visibility in drifting snow

Streamline plots are used together with wind speed plots in the present study to evaluate the snow drifting conditions. Per definition, streamlines are curves that are tangents to the velocity vector everywhere at any given instant (White, 1988). Therefore, in a steady flow, streamlines follow the paths travelled by fluid elements and can be used to identify vortices in the mean flow and track their migration.

A vortex is a flow structure that is identified by rotational movement around an axis. In two-dimensional flow, the streamlines of a vortex form concentric closed paths, and in three-dimensional flow the streamlines take a spiral form. Vortices formed behind sharp edges in a flow have the nature of so called forced or bound vortices. Their tangential velocity is at maximum in the circumference and decreases inwards to the vortex core (White, 1988). Due to turbulent and molecular diffusion, vortices expand their volume and velocity is decreased as they migrate downstream. A vortex is capable of eroding snow from the ground and transport large quantities of drifting snow. Special vortex generating fences have been used for snow removal purposes (Lang and Blaisdell, 1999).

The concentration of snow particles in the air determines the visual range or the visibility. Measurement data from Budd et al. (1966) suggested that during snow storm, the visibility at a certain height, *z*, is:

$$S = \frac{100}{\eta_z} \tag{4}$$

In this equation, *S* is the visibility in metres and η_z is the snow concentration in g/m^3 at elevation *z* over the ground. Rotating or chaotic flow, including vortex formations, generates turbulence, which in turn is the most important factor for the spreading of snow particles in the air. Snow particles, which normally have the highest concentration immediately over the ground are thus elevated to higher levels. Worse visibility is therefore expected inside a vortex than in a more smooth and regular flow.

3.3 Theory application to steep road cuts

Snowdrifts observed in the ditch along steep rock cuts are often surprisingly small, but on the other hand can concentrated drifts form at both ends of the cut. The wind flow and snow drifting around an avalanche protection dam was examined by Haraldsdottir et al. (paper in preparation) and Thordarson (paper accepted for publication in Environmental Fluid Mechanics). That flow configuration has many similarities to the flow under steep rock cuts. The study showed how a wind passing over a wall that was aligned non-perpendicular to the wind direction, created a strong vortex at the leeward side which accumulated and transported high concentrations of snow. The vortex kept the area immediately under the wall almost free of snowdrifts, but drifts were deposited where the vortex mixed with the main flow at the end of the wall. Similar flow phenomena has been observed around buildings. In Figure 6, the wind speed in the leeward transverse travelling vortex can reach a value of 1.4 times the free stream wind speed. Concerning steep road cuts, it seems likely that similar
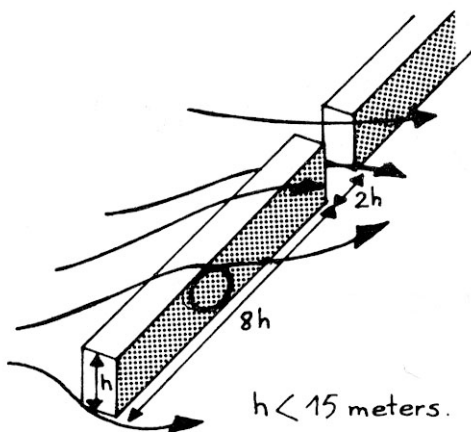

Figure 6 Wind flow over a low, thin, long building separates from the top and upwind edge of the building and creates a vortex at the back where the amplification factor can reach a value of 1.4. The incident angle here is 45°. From Blevins (1984.)

conditions govern the flow, that part of the air tends to form a vortex that travels along the steep backslope in a direction almost parallel the road. This tendency should however depend on the wind attack angle, because a steep road cut will probably generate two-dimensional recirculating flow when the wind direction remains completely stable perpendicular to the cut edge.

3.4 Wind flow simulation

A commercial flow solver is used in this study to simulate the wind flow (Flow3D: Flow Science, NM USA). The author tested results from the solver against field measurements and other simulation work (Thordarson and Norem, 2000). Results for wind flow over complex terrain proved to be in agreement with results from the Askervein Hill Project (Taylor and Teunissen, 1987), which has been used before to validate numerical simulations (Raithby and Stubley, 1987; Beljaars et al. 1987). Others who have done numerical wind flow simulations are e.g. Wood (1995) and Davies et al. (1995). Preparation of wind speed and streamline plots was done with the flow visualisation system Field View (Intelligent Light, NJ USA).

The wind flow around roads appears on such a small scale that thermal effects can be left out in the simulation, and the air is treated as a homogeneous fluid of constant density. The current flow solver solves the Reynolds-averaged Navier-Stokes equations in three dimensions (RANS). This implies that instead of resolving the turbulent motions in the flow, the averaged values of the flow variables (velocity and pressure) are calculated and the remaining unknown turbulent stresses are related to the mean flow by the eddy-viscosity concept. The effect of turbulence on the mean flow is thus accounted for by replacing the turbulent stresses with artificially increased viscosity in the fluid. This turbulent or eddy-viscosity is calculated with an algebraic relation between the simulated mean kinetic energy of the turbulent motion, k, and the turbulent energy dissipation, ε, which are calculated by a standard $k-\varepsilon$ two-equation model for turbulence. Overview over turbulence and the modelling of turbulent flows is found in Gatski et al. (1996) and Tennekes and Lumley (1972).

When reading the results of the current study, it is important to bear in mind that they present mean flow structure and flow speeds. In the strongly swirling and recirculating flows appearing behind sharp edges, turbulence activity is very high and causes snow particles to migrate through the flow. Streamlines drawn in a simulated mean flow field will thus only represent likely average paths of air parcels and snow particles.

Due to the complex physics of snow drifting, the modelling of snow erosion, transport and sedimentation is very difficult. Several investigators have worked with numerical simulations on this subject and great advances have been achieved. Amongst these investigators are Liston & Sturm (1998), Uematsu et al. (1989), Gauer (1999, 2001). Sundsbø (1997) developed a snow drifting model based on the commercial flow solver used here and also Thiis (2000) used drift-flux simulations in Flow3D to indicate initial sedimentation areas around buildings. For engineering applications including complex flow geometry, numerical snow drifting simulations have however not proved very accurate. For the design engineer, understanding of the

wind flow and how it is modified by terrain and structures is a valuable knowledge when working in snow drifting areas and probably more important than obtaining calculated drift pattern with limited reliability. Therefore, only pure wind simulations were chosen for the current work.

3.5 Basis for interpretation of the results

Based on the preceding reviewed theory, a key to the interpretation of the wind flow simulations herein was developed. The following list presents the criteria used for estimating the snow drifting conditions from the simulation results:

1. Areas of relatively low wind speed near the ground suggest possible snowdrift sedimentation. Low wind speed is however not a necessary criterion for sedimentation in three-dimensional flow. The size and number of low speed areas on the road should be minimal.

2. Vortices located over the road or crossing the road reduce the visibility.

3. The more the vortex axis (travelling direction) deviates from the mean flow direction, the less tendency it has to deposit snow in its path. The point at where the vortex terminates is however always considered as a heavy sedimentation area. Under steep road cuts, this phenomena is likely to present the worst hazard.

4. Two-dimensional flow around the road is positive for both sedimentation and visibility, only if snow storage space is adequate to prohibit drifts to extend onto the road surface.

5. Three-dimensional vortex formation upstream and off the road can create better conditions than found on adjacent sections, but can create hazard spots where a vortex terminates close to or crosses the road.

4. EXPERIMENTAL

4.1 Cut sections at Bolstadarhlidarbrekka

Part of this work is from a study site on National Road no.1 at Bolstadarhlidarbrekka in Iceland. The road is situated on a mountain slope where strong winds and heavy snowfall occur during the winter. The site has the typical characteristics of a maritime climate with winter temperatures fluctuating around 0° C. The worst snow problems on the road are usually encountered when strong northerly winds blow from the ocean with simultaneous precipitation, which can result in enormous quantities of drifting snow. Both two- and three-dimensional flow conditions are present at the site, which proved to have almost solely wind from a narrow sector aligned about 45° from the road direction. A monotone wind direction is very favourable for snow drifting studies because the interpretation of drift formations is more accurate.
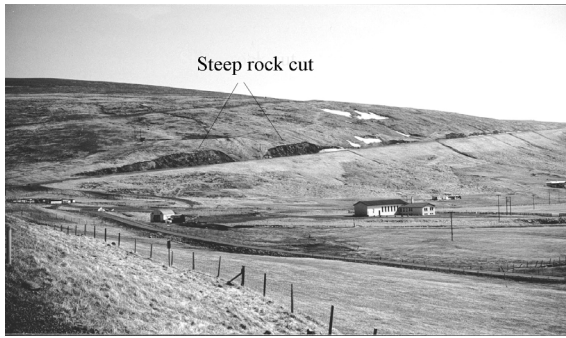
Figure 7 The experimental site at Bolstadarhlidarbrekka. The two steep rock cuts are approximately 10 m high, the first one is approximately 200 m long and the second is 120 m long.

During a normal winter, this road section gets impassable due to snow storms only a handful of times. Although strong winds are frequent at the site, also in absence of precipitation, the temperature fluctuations around the freezing point ensure that the upwind snow cover does usually not feed the wind with snow particles. The driving conditions are accordingly good in-between storm periods. However, experiences from the winter 1994-1995 show that the road section is unusually vulnerable during winters with extremely high snowfall amounts.

The two-dimensional sections of the road were treated by Thordarson and Norem (2000) to establish a connection between wind speed and drift development, as described in the previous chapter. For the current study, the appropriate road section is displayed in Figure 7. The two nearly vertical rock cuts are the subject of the first part of the current study. Late winter 1999 the snowdrift pattern in the cuts was photographed.

Geometry for the wind flow simulation in Bolstadarhlidarbrekka was adopted from a topographic map and in-situ survey. Dimensions are explained in Figure 7. The wind flow model was run for the observed prevailing snow transport wind direction. This simulation is referred to as B0-W45.

4.2 Idealistic double cut

To investigate double sided cuts and to give an idea of the flow in simple sidehill cuts as well, a model ridge of idealized geometry was applied. The situation is yet without any full scale field reference available and originates from a preliminary route selection for a new National Road no.1 at river Thjorsa in southern Iceland.

Six different cut alternatives which claim different amount of earthwork and give different wind flow conditions were tested, all for a nearly perpendicular wind attack angle of 95° and three of them for 30° also. Table 1 lists the excavation volumes and the referring name for each experiment. Plan sketches of the design alternatives are displayed in Figure 8 which also includes a perspective view of design A0. The corresponding cross section profiles taken midway through the cut are displayed in Figure 9.
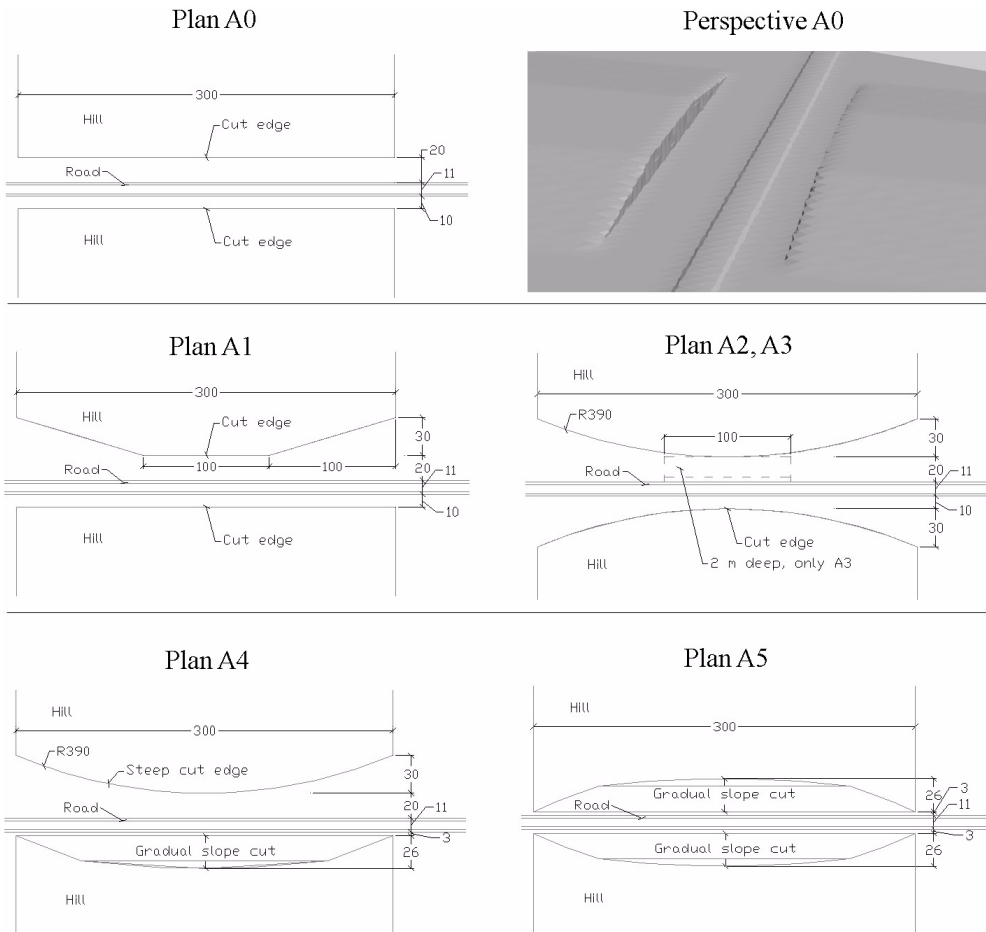
Figure 8 Geometry for the tested design alternatives, planar view. Dimensions in meters.

The objective of the different designs is to answer the following three questions with respect to visibility and snow sedimentation, compared to that of alternative A0:

What is the effect of

- expanding the cut width toward the ends?
- interaction between upwind and downwind cut edges in double cuts?
- gentle cut slopes compared to steep cuts?

Cross section for A0 to A3 features a steep cut on both sides where each meter width of ditch corresponds to 1400 m^3 of additional rock excavation. Midway through the cut, the horizontal distance between top of the cut and the road shoulder is 3.8 H_C (definition in Figure 2). The gentle backslope cut on the right hand side of profile A4 and both sides in profile A5 provides a distance of 5.2 times H_C.

Cross section A0, A1, A2, A3
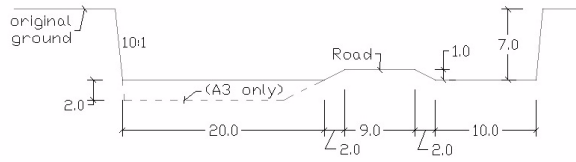
Cross section A4
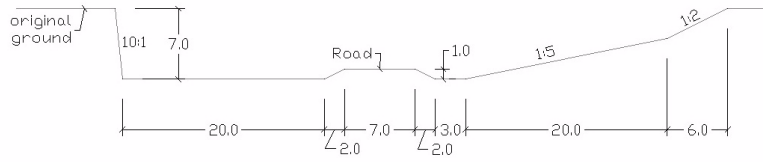
Cross section A5
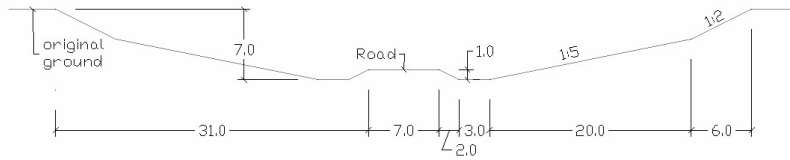
Figure 9 Cross section profiles taken midway through the cut. Dimensions in meters.

Table 1: Earthwork volumes for the different design alternatives in the study and the referring names of experiments.

Cut design	Excavation volume[a]		Experiment	
	m^3	Relative	Wind 95° [b]	Wind 30°
A0	55 600	100 %	A0-W95	A0-W30
A1	63 225	114 %	A1-W95	A1-W30
A2	71 373	128 %	A2-W95	(-)[c]
A3	74 973	135 %	A3-W95	(-)
A4	71 487	129 %	A4-W95	(-)
A5	57 595	104 %	A5-W95	A5-W30

a. The total volume of solid matter removed from the idealized hill due to the road construction.
b. Attack angle of the simulated wind flow with respect to the road center line.
c. No experiment for this configuration.

4.3 Simulation parameters

For all the experiments, model inlet velocity profile was defined by eq. (2) with $u_* = 0.8$ m/s and $z_0 = 0.001$ m. These values correspond to wind speed of 18.4 m/s at 10 m height. The bottom boundary (ground) had a no-slip condition, top boundary was set to constant pressure and the outflow boundary was continuative (all horizontal derivatives set to zero). Mesh spacing in the models was variable, with the finest spacing at ground level in order to better resolve the vertical velocity gradient and flow structure around the road. The smallest mesh cell dimension in experiment B0-W45 was $\Delta x / \Delta y / \Delta z = 2 / 2 / 2$ m and for the idealized cut experiments the dimension was 4 / 4 / 0.5 m.

5. RESULTS

5.1 Cut sections at Bolstadarhlidarbrekka

For simpler terminology, define the upwind end of a cut as the entrance and the downwind end as the exit. This definition is used in the following text. A photograph of the snow accumulation late winter 1999 at Bolstadarhlidarbrekka is presented in Figure 10. The main drift accumulations are found at the entrance and exit of each cut, as well as in the cleft between them. Far right in Figure 10, a section presenting moderately sloping upwind terrain shows the normal behaviour of drifts that develop according to the two-dimensional flow structure in that area.

Results from numerical experiment B0-W45 are presented in Figure 11. The areas of retarded wind speed can to some extent explain the drift pattern in Figure 10, especially the large drift area to the right from the cuts. Low-speed area is found at the exit of the first cut. The same is not true for the entrance part of the same cut, although substantial drifts are located there according to Figure 10. At the second cut, the low-speed area is larger, but again the entrance drift is not indicated by lower wind speed. In Figure 12, an attempt is made to map the flow structure by streamline analysis. The four streamlines traced through each of the cuts indicate the lateral flow deflection that happens, even though the flow does not separate at the top of the cut.

The results suggest that snow is deposited at higher wind speed at the cut entrance (upwind end) than at the exit (downwind end). It is also evident that strong flow deflection occurs at the cut edges and the wind is directed in a rotating motion along the road. No distinct vortex formation is though observed, possibly due to the relatively short length of the cuts and coarse mesh spacing in the computational model.
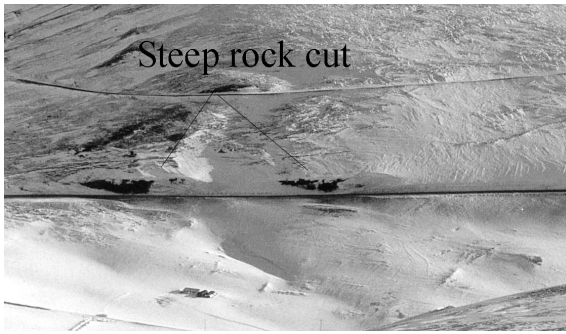
Figure 10 Bolstadarhlidarbrekka, rock cuts. Snow pattern photographed late winter 1999.
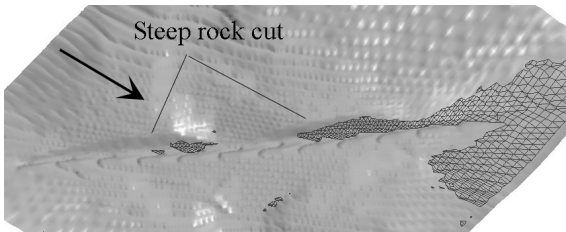
Figure 11 Experiment B0-W45, results from wind flow simulation.Wind direction indicated by arrow, approximately 45° to the road. At ground level, areas of wind speed less than 40 % of reference value are marked with black squares. Reference wind speed value is 15.5 m/s, the speed at elevation 2.3 m above the ground in the free stream flow according to eq. (2).
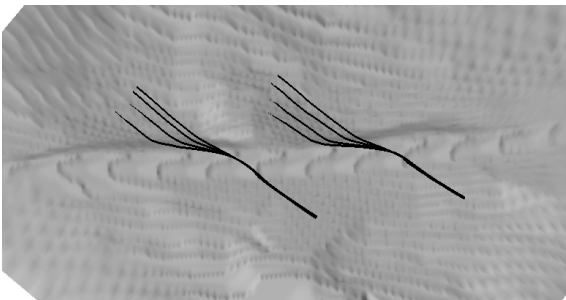
Figure 12 (a) Chosen streamline paths through the steep cuts at Bolstadarhlidarbrekka. The streamlines pass through a vertical column over the ditch at elevation 0, 2, 4 and 6 m above the surface (b).

5.2 Idealistic double cut

5.2.1 Incident angle 95°

The simulation results for the 95° incident are presented in Figure 13. Ten streamlines are traced through each of the figures. The actual streamline seeding is the same for all experiments, the streamlines pass at equal intervals through a line that lies 2 m above the road surface. The streamlines can thus give an idea about the history of the air that vehicles on the road encounter. To keep the graphics as simple as possible, some details of the flow structure are not visualized by streamlines, and are therefore

A0-W95

A1-W95

A2-W95

A3-W95

A4-W95

A5-W95
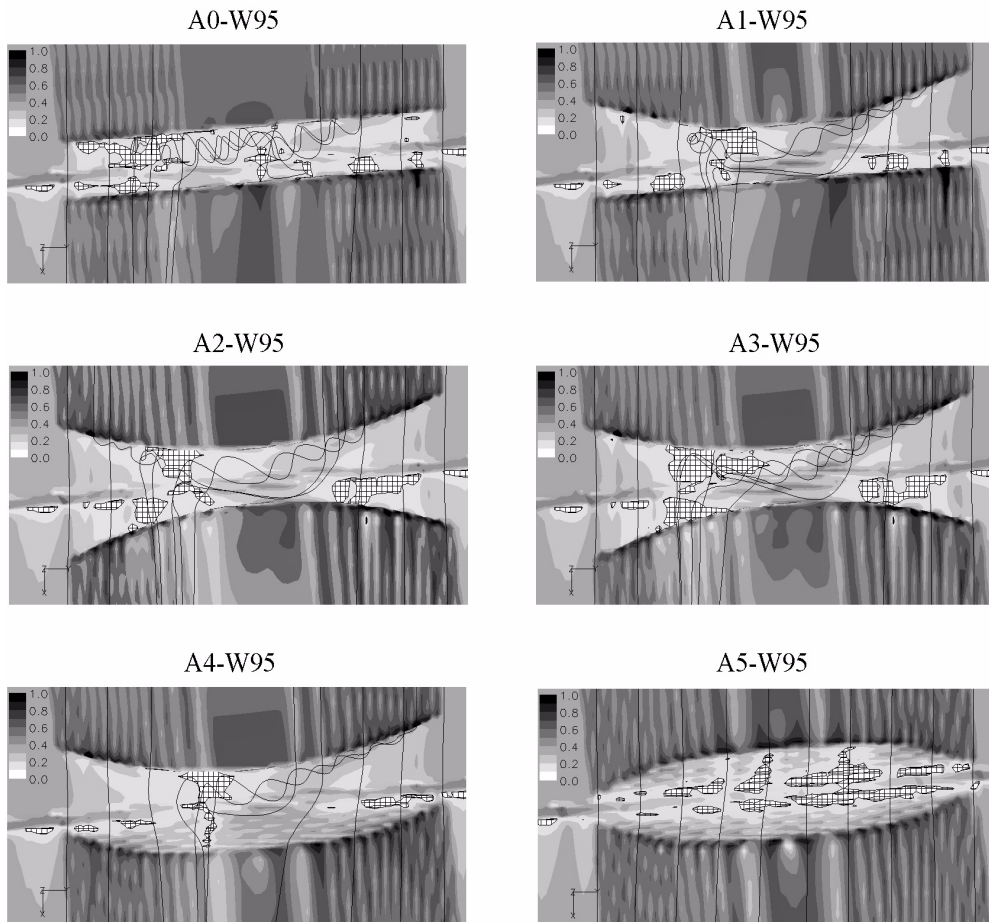
Figure 13 Results from wind flow simulations, wind angle 95° to the road. Wind direction from top to bottom. Gray scales indicate relative wind speed distribution measured close to the ground. The areas of 10 % relative velocity and less are emphasised with black squares. Reference wind speed value is 15.5 m/s, the free-stream speed at elevation 2.3 m above the ground according to eq. (2). Chosen streamline paths in black.

added in the verbal description of the results below. Additionally, the relative wind speed at 1 m elevation above the road is traced along the road for alternatives A0, A4 and A5 in Figure 14.

A0-W95

A vortex forms at the cut entrance (right hand end) and travels from right to left. Midway through, the vortex terminates and a low-speed area forms on the road. Another vortex formation happens at this point, but close to the steep backslope. This second vortex is terminated close to the cut exit with a large low-speed area. The flow of air in the cut is mainly fed from the entrance, little mixing with air from the top of the cut occurs.

A1-W95

The entrance vortex now has a higher speed and spreads less far from the backslope. Higher speed is maintained over the road and the ditch area compared to case A0-W95. The left end of the cut now serves as an entrance for air that is deflected to the right, and meets the main vortex in a concentrated low-speed area.

A2-W95

Similar flow behaviour as in case A1-W95 is experienced here. The main low-speed area is moved farther to the left though. Large low-speed areas form in the widened ditch at the downwind cut edge.

A3-W95

The 2 m deep ditch that was added here (see Figure 8) results in a lower local wind speed. Apparently, the low-speed area on the opposite side of the road is more concentrated than in A2-W95. Considering turbulence, it is likely that this difference is not significant.

A4-W95

Replacing the downwind steep cut with a gentle slope cut alters the flow pattern. Air is more easily drained away from the cut, and the extension of the low-speed area where the main vortex terminates is minimum. Wind speed downwind from the road is also higher, since the gentle downwind slope does not introduce a stagnation in the flow as the steep downwind slope does in A0 through A3.

A5-W95

This double sided gentle slope cut causes two-dimensional flow as expected. No transverse vortices form and the wind speed pattern close to the road is nearly uniform along the whole cut.
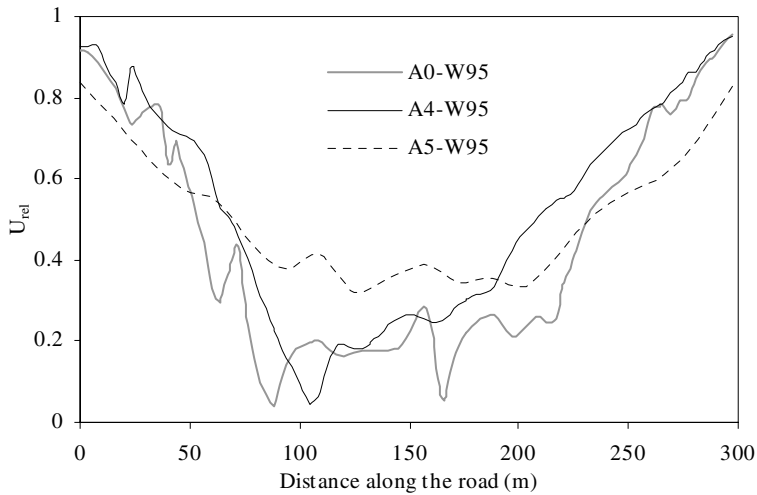
Figure 14 Relative wind speed, U_{rel}, along the road, measured at 1 m elevation above the road center line surface. Distance measured from left to right with respect to the orientation of the cut in Figure 13.

In general, the expanded ditch width alters the effective wind attack angle at the cut edge and results in higher wind speed in the transverse vortex. In addition, the low speed areas are fewer and more concentrated. The flow in A5 is totally different from the other designs as expected, since the gentle upwind slope is designed to give two-dimensional flow over the road.

5.2.2 Incident angle 30°

Results from the experiments with the 30° wind attack angle are presented in Figure 15. In A0-W30 and A1-W30, the streamline paths are chosen to inform about the flow behaviour in the upwind ditch but in A5-W30 the streamlines cross the road with equal intervals at 2 m height. Note that areas marked with white rectangles designate wind speed of 35 % reference speed or lower. The main difference from the 95° incident is higher wind speed below the cut and less vortex tendency.

A0-W30

The flow is deflected parallel the road, first to be captured by the free-stream flow at the cut exit. A low-speed area forms at the exit where the vortex from underneath the upwind cut intersects the road. This area defines the actual termination of the vortex. The largest low-speed area is however found underneath the downwind cut edge, where some of the air is deflected along the wall and some is elevated over the cut edge.

A0-W30

A1-W30

A5-W30
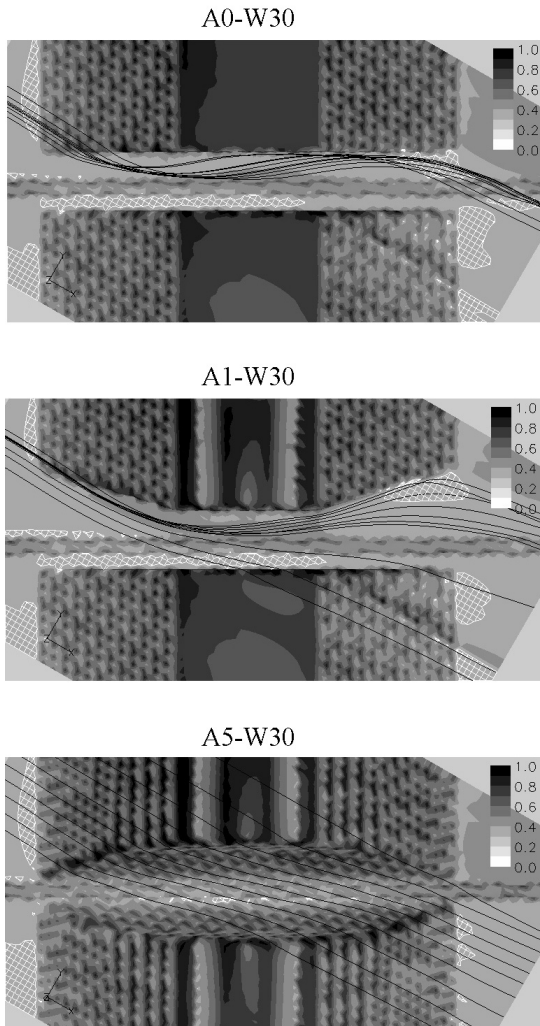
Figure 15 Results from wind flow simulations, wind angle 30° to the road. Wind direction from upper left corner. Gray scales indicate relative wind speed distribution measured close to the ground. White squares designate areas of 35 % relative speed and less. Reference wind speed value is 15.5 m/s, the speed at elevation 2.3 m above the ground according to eq. (2). Chosen streamline paths are visualized by black lines.

A1-W30

Less air is deflected along the upwind cut edge and it shows almost no rotational behaviour. The expanded cut exit spreads the air before it is captured by the free-stream flow and the lowest wind speed area has moved from the road.

A5-W30

In this gentle slope alternative, the flow behaves almost two-dimensionally. Only a slight flow deflection occurs at the upwind edge.

6. DISCUSSION

6.1 Snow drifting prediction

The basis for evaluating the snow drifting conditions is presented in section 3.5. Starting with the 95° incident (Figure 13), both the visibility and the deposition of snow are a potential problem for all the alternatives presented, despite the generous basic width of 20 m for the upwind ditch in A0 through A4. Compared to alternative A0, the introduction of a widened entrance and exit parties to the upwind cut (A1 through A4) results in:

- Higher wind speed on and around the road. On Figure 14, A4 has substantially higher velocity than A0, from midway through the cut (150 m) and the following 100 metres to the right along the road. This suggests less sedimentation of snow and fewer critical points for drifts on the road.

- Smoother flow and less turbulence, also the vortices interfere less with the road. This suggest better visibility on the road.

The apparent effect on the visibility is very promising. Regarding the snowdrift formations, it is possible that the expanded ditch width at the cut ends results in fewer or even only one critical point on the road. However, by widening both ends of the cut, under a nearly perpendicular wind direction, both ends of the cut serve as inlets and generate vortices that travel in opposite directions. As a result, two vortices collide approximately midway through the cut and heavy snow deposition can be expected on that spot. The idea of design A3, with the increased ditch depth is to account for this concentrated sedimentation area and provide more storage space for snow.

The downwind cut wall is also a concern. It causes stagnation in the flow as it is shifted over the top, and wind speed is consequently low in the downwind ditch. This effect is known to cause deposition of snow upwind of buildings and other steep structures. A close example is the upwind drift for solid snow fences, that can extend as long as 12 times the fence height (Tabler, 1988). To account for the reduced flow speed underneath the downwind cut, alternative A4 was introduced. It causes air to be more easily drained away from the road area and increases the speed of the flow, probably reducing drift accumulation downwind of the road.

Alternative A5 presents a gentle slope cut that results in two-dimensional flow. The drift behaviour here can be predicted by the methods introduced in Figure 2 and Figure 3. Seen on Figure 14, the wind speed above the road is relatively high through a 100 m long area at the middle of the cut. Even so, the two-dimensional equilibrium snowdrift is expected to grow over the road and cause problems along the whole section, especially near the cut ends where the storage capacity for drifted snow is very low. A gentle slope solution for this case that would guaranty a drift-free road claims a ditch width of up to 29 m according to Figure 2. This implies more than 36000 m^3 additional rock excavation, which in terms of the information in Table 1 means earthwork volumes of 168 % compared to alternative A0. Due to the high

excavation costs for rock, this is hardly a real option and a steep cut is therefore more realistic.

Now, looking at the 30° incident, three alternatives were presented (Figure 15). This incident angle generally presents less snow drifting hazard, although it is known that the cut entrance and exit are vulnerable. The introduction of alternative A1 here is very likely to reduce the problems, both providing better visibility at the cut exit and move the sedimentation at both ends away from the road. However, the role of the downwind cut edge should be kept in mind. Widening the ditch as in A1 does not help against possible problems caused by the downwind cut edge. Low wind speed is registered in the downwind ditch, as a result of the stagnation effect discussed earlier. A gentle slope instead of a steep cut on the downwind side might eliminate this problem.

For the two-dimensional flow situation appearing in A5, very little snow problems are expected. Anyhow, both ends of the cut might still introduce some risk since the cut edge is very close to the road and drifts reach the road sooner. Under this angle, the active slope angle of the cut in the direction of the wind is 1:10 instead of 1:5 for the nearly perpendicular case (95°). The possible drift formations starting at the cut edge are bound to reach equilibrium stage before reaching the road. Visibility is supposed to be no worse than it would be on a fill section.

6.2 Conclusion and future works

Wind flow in steep road cuts was analysed with respect to the snow drifting conditions and new design principles were developed. The results improve the understanding of snow drifting behaviour in road cuts. It has been demonstrated that the wind flow around the road can be controlled to some extent to reduce the snow problems. Expanding the ditch width at the cut ends as suggested by alternatives A1 through A4 is a promising option, not only for the snow control but also will it provide a pleasant visual appearance in the landscape. It can be assumed that this approach will benefit both simple sidehill cuts and double cuts. For double cuts, a steep upwind cut combined with a gently sloping downwind cut as in A4 is probably better than a steep cut on both sides.

Snow control is more difficult if more than one wind direction are involved. A measure that serves one wind direction might not do any good for another direction. Therefore, the design might have to compromise between different wind directions. Any alternative measures to reduce the snow problems should be seen in light of the additional construction cost and the benefits for road accessibility, safety and maintenance costs. The earthwork volumes given in Table 1 show that expanded ditch width at the cut ends adds little to the overall costs.

As the methods applied in this study rely on interpretation of wind flow simulations, the validity of the current results and conclusions needs a further confirmation. Due to the complex flow geometry involved and the sparse physical basis for existing numerical methods on the simulation of turbulent multi-phase flows, further numerical work is not likely to provide answers. Even though scaled

model experiments out in nature or a wind tunnel investigation might be helpful, only a full scale implementation of the proposed alternatives can reveal their potential.

ACKNOWLEDGEMENTS

REFERENCES

Beljaars, A.C.M., Walmsley, J.L. and Taylor, P.A., 1987. A mixed spectral finite-difference model for neutrally stratified boundary-layer flow over roughness change and topography. Boundary-Layer Meteorology 38: 273-303.

Blevins, R.D., 1992. Applied fluid dynamics handbook. Krieger Publ. Co., Malabar.

Budd, W.F., Dingle, W.R.J. and Radok, U., 1966. The Byrd Snowdrift Project: Outline and basic results. Studies in Antarctic Meteorology, Antarctic Research Series 9: 71-134.

Davies, T.D., Palutikof, J.D., Guo, X., Berkofsky, L. and Halliday, J., 1995. Development and testing of a two-dimensional downslope model. Boundary-Layer Meteorology 73: 279-297.

Gatski, T.B., Hussaini, M.Y., Lumley, J.L. and ,(Editors), 1996. Simulation and Modeling of Turbulent Flows. Oxford University Press, New York.

Gauer, P., 1999. Blowing and drifting snow in alpine terrain: A physically-based numerical model and related field measurements. Mitteilungen des Eidgenössischen Institutes für Schnee- und Lawinenforschung. Eidgenössisches Institut für Schnee- und Lawinenforschung, Davos.

Gauer, P., 2001. Numerical modeling of blowing and drifting snow in Alpine terrain. Journal of Glaciology 47: 97-110.

Kobayashi, D., 1972. Contributions from the Institude of Low Temperature Science. Hokkaido University, Sapporo.

Lang, R.M. and Blaisdell, G.L., 1999. Passive snow removal at the Pegasus Runway, McMurdo, Antarctica. Cold Regions Science and Technology 29: 75-88.

Liston, G.E. and Sturm, M., 1998. A snow-transport model for complex terrain. Journal of Glaciology 44: 498-516.

Norem, H., 1975. Designing highways situated in areas of drifting snow. Draft translation 503. CRREL, Hanover, New Hampshire.

Norem, H., 1994. Snow Engineering for Roads. Handbook no. 174. Norwegian Public Road Administration, Road Research Laboratory, Oslo.

Pomeroy, J.W. and Gray, D.M., 1990. Saltation of Snow. Water Resources Research 26: 1583-1594.

Raithby, G.D. and Stubley, G.D., 1987. The Askervein Hill Project: A finite control volume prediction of three-dimensional flows over the hill. Boundary-Layer Meteorology 39: 247-267.

Schmidt, R.A., 1986. Transport rate of drifting snow and the mean wind speed profile. Boundary-Layer Meteorology 34: 213-241.

Stull, R.B., 1988. An Introduction to Boundary Layer Meteorology. Kluwer Academic Publishers, Dordrecht.

Sundsbø, P.A., 1997. Numerical modelling and simulation of snow drift. Thesis. Norwegian University of Science and Technology, Narvik.

Tabler, R.D., 1988. Snow Fence Handbook. Tabler & Associates, Laramie, Wyoming.

Tabler, R.D., 1994. Design Guidelines for the Control of Blowing and Drifting Snow. SHRP-H-381. National Research Council, Washington, DC.

Taylor, P.A. and Teunissen, H.W., 1987. The Askervein Hill Project: Overview and background data. Boundary-Layer Meteorology 39: 15-39.

Tennekes, H. and Lumley, J.L., 1972. A first course in turbulence. MIT Press, Cambridge.

Thiis, T.K., 2000. Experimental validations of numerical simulations of snowdrifts around buildings and in terrain. Thesis. Norwegian University of Science and Technology, Trondheim.

Thordarson, S. and Norem, H., 2000. Simulation of two-dimensional wind flow and snow drifting application for roads: Part I & II. In: Hjorth-Hansen, E., Holand, I., Løset, S. & Norem, H.(Editors), Snow Engineering. Recent Advances and Developments. Proceedings of the fourth International Conference on Snow Engineering, Trondheim, Norway, 2000. A.A. Balkema, Rotterdam, pp. 437-452.

Uematsu, T., Kaneda, Y., Takeuchi, K., Nakata, T. and Yukumi, M., 1989. Numerical simulation of snowdrift development. Annals of Glaciology 13: 265-268.

White, F.M., 1988. Fluid Mechanics. McGraw-Hill Book Company, New York.

Wood, N., 1995. The onset of separation in neutral, turbulent flow over hills. Boundary-Layer Meteorology 76: 137-164.

Paper V:
Design criteria for roads in snow-drifting areas

Design criteria for roads in snow-drifting areas

Skuli Thordarson and Harald Norem

Norwegian University of Science and Technology,
Department of Road and Railway Engineering,
7491 Trondheim, Norway
TEL: +47 7359 4710/FAX: +47 7359 7020
E-mail: thordars@stud.ntnu.no

ABSTRACT: During strong winds, drifting snow causes problems on roads in many harsh winter climate countries. Increased snow-removal costs, reduced access and safety problems are typical results of excessive snowdrift sedimentation and bad visibility along many roads in the exposed regions. This paper introduces some of the results from a research program including numerical experiments and field surveys. The research was done to enhance knowledge on drifting snow behaviour on roads and to develop design criteria for better road and highway construction in mountainous areas and other areas where frequent snowfall and strong winds occur. The study is mainly based on CFD (Computational Fluid Dynamics) and field measurements. Simulations of wind flow were compared to snow cover surveys from roads in Iceland and Norway and the results have been used to develop recommendations for engineers. An important goal for this study has been to use CFD to develop geometric relationships that can be applied in road planning. The results presented herein include guidelines to evaluate the efficiency of natural snow deposition zones and their equilibrium snowdrift capacity. Furthermore, an example of three-dimensional flow under a steep road cut is presented. A theoretical study on the performance of different guard rail profiles in drifting snow is also present. We conclude that CFD is a suitable tool for developing recommendations for road engineering in snow-drifting areas.

1. INTRODUCTION

1.1 Background

Winter problems on roads can be severe in some harsh winter climate regions. Among the most important problems are slippery road surface due to ice and snow, excessive snow amount on the road due to snow fall and drifting snow and reduced visibility during snow storm. An EU-financed study [1] concludes that as much as half the annual road maintenance budget in Northern Scandinavia is dedicated to winter

maintenance. Cost of snow removal alone can be as much as 80 % of the winter maintenance budget according to the same study.

Concerning problems caused by drifting snow, the severity of these is strongly dependent on the road design and the location of the road with respect to terrain features and climatic factors. Therefore, better roads in snow drifting areas will result in savings in road maintenance costs, higher safety level and better accessibility for the traffic.

1.2 Numerical wind flow simulations

By using CFD (Computational Fluid Dynamics), the wind flow over the terrain adjacent to the road can by calculated. Through known relations between the wind speed distribution and the behaviour of snow drifting, such calculations give the opportunity to evaluate the quality of alternative design solutions. Problems of different geometric scales can be simulated, and hence both the path of the road through a difficult snow drifting site and road cross section can be investigated. More advanced use of CFD implements simulation of the snow drifting together with the wind flow, so called two-phase flow modeling. Some experiments with two-phase numerical simulation of snow drifting and sedimentation have been done by several investigators. However, most snow drifting models have limited use in engineering applications due to questionable accuracy, but great improvements have been achieved in the recent years. Plain wind flow simulations are more realistic and allow for qualitative comparison of snow drifting conditions without raising questions on the validity of the calculated drift formations. For this reason, the current study is based on wind flow calculations supported by in-situ field observations on roads.

1.3 Objective

In 1998, a Ph.D. study program was started at the Norwegian University of Science and Technology. The goal for the program is to enhance knowledge on, and develop engineering guidelines for road design in snow-drifting areas. The current paper summarizes some topics and results of the project, which final report is scheduled for defence in 2002.

Previous studies that have been reviewed in the project is the work of Norem [2,3] and Tabler [4]. Norem did model experiments with sand in water to simulate snow drifting on roads and has also presented detailed field observations. The guidelines of Tabler are mainly based on statistical analysis of field measurements. The current study is based on many common problems treated by these authors. The advantage of the current study is the ability to numerically analyse the wind flow around roads and confirm fluid-dynamically assumptions from previous studies, as well as to investigate new topics that previously have remained unexplored. In this study, a commercially available engineering flow solver is used, Flow3D (Flow Science, NM USA). The system is very suitable for this purposes because different geometric forms can easily be integrated into the model.

2. METHODS

2.1 Wind flow simulations

Outline of the simulation process is as follows:

1. Integration of terrain and road geometry into the model.

2. Choice of suitable wind profile and boundary conditions.

3. Simulate until a steady state solution is achieved.

4. Analysis of wind velocity distribution and streamline pattern.

For relative comparison of design alternatives, geometric details can be changed and the four steps repeated. Regarding the last step, it should be explained briefly here how wind velocity and streamlines can be helpful to interpret drifting snow behaviour. Experiments and theory have shown that the snow transport capacity of the wind (saturated flow) is related to the wind speed by a third power relationship:

$$Q \approx C(U - U_{th})^3 \qquad (1)$$

where Q is the snow drifting rate in kg per meter width across the flow, U is the local wind speed measured at reference height and U_{th} is the threshold wind speed necessary to initiate snow transport. The constants C and U_{th} are dependent on the snow cover conditions such as cohesion and surface structure. Assuming that the wind is fully saturated with snow particles at a given location, any decrease in the wind speed downstream from that location should lead to snowdrift build up on the ground, as the snow transport capacity of the wind decreases by the third power of the wind speed reduction. The more the wind speed drops along a given path along the flow, the faster the sedimentation or drift build up occurs. As the sedimentation gradually builds up a drift formation on the ground and consequently raises the ground surface, the wind speed increases again and the sedimentation slows down. When the equilibrium snowdrift surface is reached, the wind speed is practically as high as in the upstream area above the initial sedimentation zone. Should the wind not be saturated with snow in the area before the wind speed reduction, sedimentation need not necessarily occur, since the wind still may have excess capacity to transport the snow particles further downstream. This concept is confirmed in section 3.2.

In a three-dimensional flow situation, the picture is usually not as simple. Sedimentation can then happen at relatively high wind speeds, because the snow concentration in the air can differ greatly from place to place when three-dimensional flow is present. Under these conditions, streamlines can be very helpful to understand the flow. Streamlines represent the path of fluid particles through the flow, and make it possible to graphically sketch the flow behaviour.

2.2 Field data

When designing a road through a snow drifting area, some minimum data has to be available. Besides topographic data, some weather information is necessary. The most important is knowledge on which wind directions bring the largest quantities of drifting snow. These are the directions associated with the highest wind speeds and precipitation. It is important to note that these need not be the same as the prevailing or most frequent wind directions in the area.

In an open landscape, data from meteorological observation stations near the actual area can be used. On the other hand, if the road is located in mountainous and steep surroundings, some local investigations might be appropriate because of how strongly the landscape can modify and redirect the wind flow. The total average winter precipitation or snow depth on the ground is also important. The design should be chosen with respect to the expected snow amount on the site.

For the purposes of the current project, detailed weather information was acquired at two actual road sites during the winters of 1999 and 2000. Automatic weather stations were installed at road no. 1 at Bolstadarhlidarbrekka in Northern-Iceland and at road Fv-232 through Kaperdalen valley on the island of Senja in Northern-Norway. At the latter site, detailed observations on visibility along the road during snow-storms were also done. The results from the visibility observations are presented in the project final report.

3. RESULTS

3.1 General Issues

The demands to a road in a snow-drifting area have previously been summarized by Norem [2,3]. The most important of these are to avoid snow deposits on the road, to ensure little snow transport across the road for better visibility and to facilitate for the maintenance of the chosen design. In practice, the road design often has to be a compromise between construction costs, safety, accessibility and maintenance costs.

When an existing road section is to be rebuilt or modified because of snow drifting problems, or when a new road is planned, some principal questions have to be answered. For this first step of the planning process the road should be divided into suitable sections of uniform terrain characteristics and the expected flow conditions. For each section it is important to find out whether the flow will behave two- or three-dimensionally when the prevailing snow drifting wind direction is present. An example of a two-dimensional situation is treated in section 3.2. Under such conditions, the chosen cross section for the road may function properly along the whole road section if changes in topography and the direction of the road with respect to the wind are moderate.

An example of a three-dimensional flow is presented in section 3.3. When the wind flow behaves three-dimensionally, the snow problems can sometimes be found at unexpected places.

Another important question is whether the road is located in a high wind speed area where snow is eroded from the ground or if it lies in a snow sedimentation area. It is to prefer that as long sections as possible lie in an erosion zone, as long as the wind speed itself is not hazardous to the traffic. Under such conditions, a road cross section that ensures a self-cleaning road surface can be chosen. However, road sections where the drifting snow is blown over the road without the sedimentation of snow on the road can present visibility problems if the upwind fetch of available snow cover is long. Snow fences have often proved helpful for better visibility in such situations.

If the road on the other hand must be placed in a natural snow sedimentation area, a sufficient storage capacity for sedimented snow should be offered. The snow storage capacity should be large enough to prevent that the equilibrium snowdrift surface reaches the road.

3.2 Two-dimensional drift equilibrium

In mountainous or hilly terrain, some sections of a road will inevitable lie in leeward facing slopes. Consequently, the road may be located in a natural snow deposition zone, which may lead to excessive snow amounts on the road. In such places, the possible amount of drifting snow and the equilibrium shape of the drift on the ground has to be known and accounted for in the road design to avoid problems. When very large quantities of drifting snow are expected, or when providing high enough storage capacity for sedimented snow is not feasible, the road should either be placed down-stream of the equilibrium snowdrift pattern or up-stream of the deposition zone.

To better understand the snow drifting conditions on down-slopes, we simulated the wind flow along several terrain profiles [5]. Our results indicate that the horizontal wind speed gradient close to the surface, dU/dx, gives information on the rate of drift build-up and the stage of drift development towards equilibrium. A schematic presentations of our findings is displayed in Figure 1. The calculated wind speed is used together with the equation in section 2.1 to write the curve of relative transport capacity along the surface, Q_{rel}.

Upwind (to the left) of location X_d, the wind speed and hence the transport capacity is usually constant if the terrain slope is constant (Figure 1). It can be stated that the value of Q_{rel} at X_d represents the actual snow transport rate, since the fall in Q_{rel} downwind from that point results in sedimentation. It means in other words that the wind is fully saturated with drifting snow and can sustain no drop in speed without depositing snow on the ground. Therefore, it is convenient to normalize Q_{rel} to that value and set the transport capacity to 100 % at X_d.

Before any sedimentation has happened, the original ground surface, S_g, gives the Q_{rel} curve marked Q_g. During an intermediate stage of snowdrift build up, snow surface S_i, the snow transport capacity and the snow drifting rate fall according to curve Q_i. In theory, a drift surface has reached it's maximum or equilibrium stage, S_e, when the wind speed or snow drifting rate no longer falls along it's surface. Hence, the equilibrium curve Q_e is constant at the same value as at location X_d.
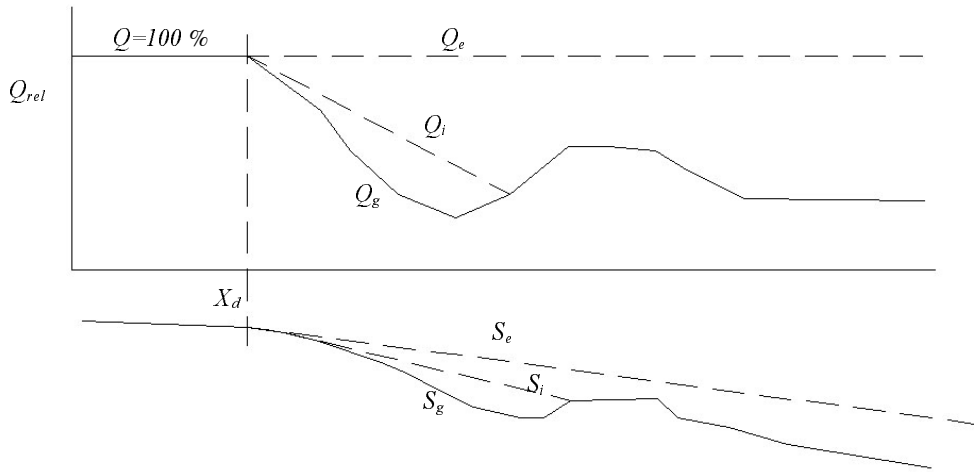
Figure 1 Snowdrift development, wind from left to right. The upper figure shows the calculated relative transport capacity and the lower one is an example of a typical terrain profile on a leeward slope together with drift surfaces. Symbols are explained in the text.
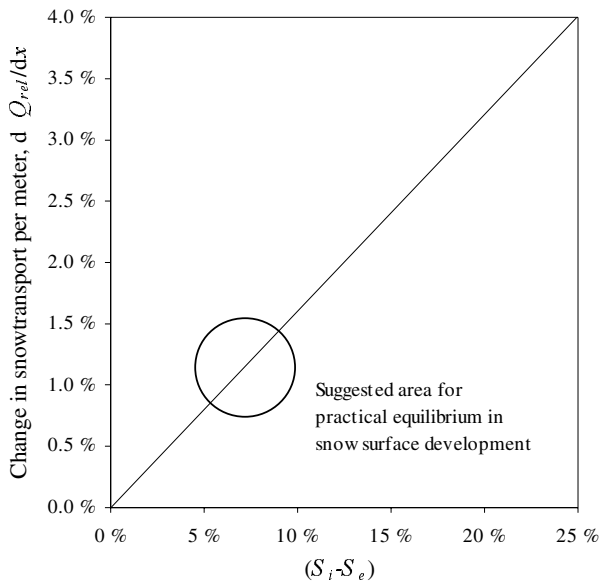

Figure 2 The linear relationship between drop in snow transport rate, Q_{rel}, and the deviation of the intermediate drift surface, S_i, from the theoretical equilibrium surface, S_e

156

When we write the drift slopes S_i and S_e as the tangens of the slope angle ($\mathrm{d}z/\mathrm{d}x \times 100$ %) and the slope of the Q_{rel} curve as percentage drop per meter ($\mathrm{d}Q_{rel}/\mathrm{d}x \times 100$ %), our results indicate a linear relationship between the slope of Q_i and (S_i - S_e). This is illustrated in Figure 2.

The diagram in Figure 2 indicates that as the intermediate drift surface slope S_i develops towards S_e, the drop in snow transport rate decreases towards zero. Steep Q_i indicates high loss of snow transport along the surface, hence the sedimentation of snow on the ground occurs fast at this stage. As the slope of Q_i gets smaller, the rate at which snow deposits becomes lower. Therefore, in many practical situations, the snow surface will not have reached the theoretical maximum, S_e, by the end of the winter. This will of course depend on the drifting snow amounts and the storage capacity of the deposition area.

According to our field measurements and simulations, a practical equilibrium level for $\mathrm{d}Q_{rel}/\mathrm{d}x$ might be between 1 % and 1.5 % per meter downwind from the drift starting point at X_d (Figure 2). This is equivalent to (S_i - S_e) of about 5 % to 10 %. Before applying the principle presented here, the theoretical equilibrium slope, S_e, has to be estimated. In many situations, S_e, will be a direct extension of the terrain slope upwind from location X_d, but must nevertheless be evaluated with respect to the landscape both upwind and downwind from the road.

3.3 Three-dimensional flow in road cuts

Steep terrain or rock cuts along the road will usually result in strong lateral flow deflection or even separated flow. The resulting flow must be described three-dimensionally. Common snow problems on roads underneath steep cuts is high accumulation of snow particles in the air, resulting in poor visibility, and snow deposits on the road.

As an example of this, we present results from wind flow simulations of two different cut designs. Both present a 300 m long road cut through a simplified ridge that reaches the maximum height of 7 m halfway along the road. The example reflects an actual situation found at a the site for a new road align that is planned on road no. 1 at river Thjorsa in South-Iceland. The two alternatives are shown in Figure 3. Plots of relative wind speed distribution at ground level and streamlines for the two examples are presented in Figure 4. The incident angle of the wind is chosen as 95° or almost perpendicular to the road.
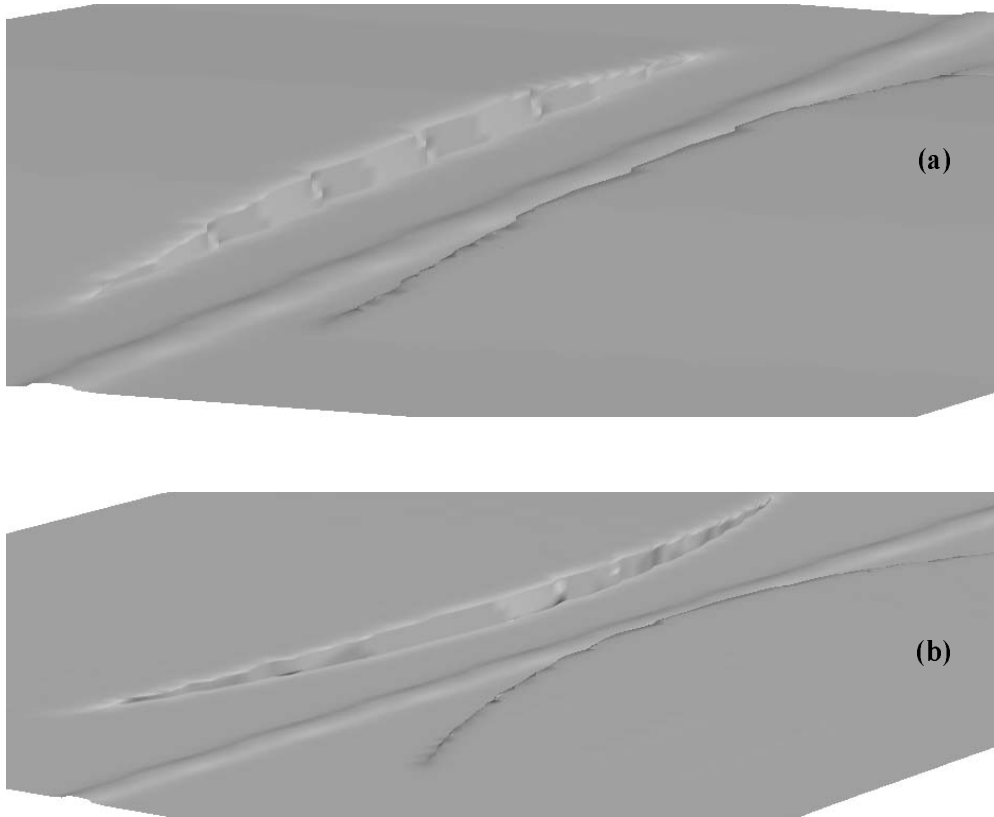
Figure 3 The two design alternatives of road cuts through a terrain ridge treated in the report. Alternative (a) is a conventional steep cut along a straight line, (b) is a steep cut along a path that forms and arc in the horizontal plane and therefore the ditch widens out in both ends.
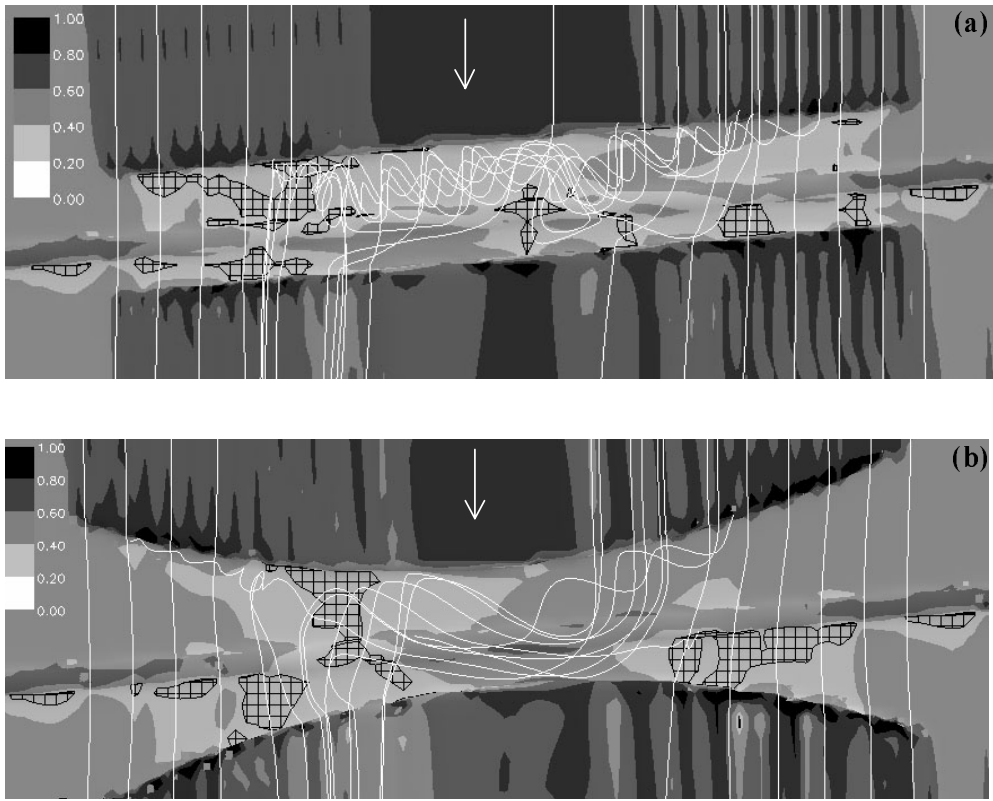
Figure 4 Plots of relative wind speed distribution and streamlines. Wind direction is indicated by the arrow. The areas marked with black squares indicate the lowest relative velocity, 10 % of the reference value. The streamlines are crossing the road at 1.5 m above the road, the eye level of the drivers.

The streamlines in Figure 4 show how the flow is deflected in a vortex underneath the steep wall and travels along the road. The main difference between alternatives (a) and (b) is the higher velocity over the road in (b) and less circulation of air over the road. Simulations for the case where the incident angle of the wind is 30° to the road show even more difference in the expected snow problems in favor of alternative (b).

3.4 Guard rails

Guard rails on the road shoulder are well known to cause snow drifting problems. The use of guard rails is avoided in many regions and special guard rails that cause less problems have even been used.

The ability of a specified guard rail type to collect snow on the road and cause visibility problems can be evaluated by the air resistance or drag force that the rail exerts on the flow. The drag force that a body exerts on the flow is written as;

$$F_D = \frac{1}{2} \rho\, U^2 A\, C_D \qquad (2)$$

where F_D is the drag force, ρ is the density of the air, U is the flow speed, A is the projected frontal area of the body and C_D is the drag coefficient associated with the body shape.

High drag profile type generates more turbulence in the flow and also reduces the wind speed more than a low drag profile type, and will consequently cause larger snow problems on the road. In addition to providing low drag, a suitable guard rail profile for use in snow-drifting areas also has to be durable against the forces from creeping snow-banks and forces from the snow removal equipment.

A theoretical comparison of some chosen guard rail profiles is presented in Table 1. The reference guard rail profile has a circular cross section. The oval shapes in the table are dimensioned such that the mechanical strength of the profiles in the horizontal direction is the same as for the circular profile (the moment of inertia about the vertical axis, I_z, divided by half the profile width).

The comparison shows that the air resistance and hence the snow collecting ability of the guard rail can be reduced dramatically by choosing an oval shape in stead of a circular one, without decreasing the profile strength against horizontal impact from cars. A conventional W-shape guard rail of 300 mm height would give relative drag force of approximately 300 % compared to the shapes in Table 1.

Numerical wind flow simulations have been done in the current study to analyse the effect of different guard rail shapes on the wind flow over the road. The results are well suitable as a basis for comparing profile shapes, but for more realistic comparison, some full scale outdoor experiments are necessary.

Table 1: Example of guard rail shapes. The calculated profile strength is based on solid cross sections, for example wood beams.

Profile shape	Aspect ratio b/h	C_D	Profile strength $\dfrac{I_z}{\frac{1}{2}b}$ (mm³) /10⁵	Profile width b (mm)	Profile height h (mm)	Relative F_D $C_D \dfrac{h}{200}$
Circle	1.0	1.0	7.85	200	200	100 %
Oval	1.5	0.75	7.84	229	153	57 %
Oval	2.0	0.55	7.85	252	126	35 %

4. CONCLUSIONS AND FURTHER WORKS

The paper has introduced the use of Computational Fluid Dynamics for snow drifting studies on roads. We find numerical wind flow simulations a useful method to learn new things about the subject of snow drifting on roads and develop guidelines for engineers.

The practical results presented in the text deal with drifting snow depositions on leeward slopes, three-dimensional flow in steep road cuts and the evaluation of guard rail profiles. For snow sedimentation on leeward slopes, we introduce the concept of theoretical equilibrium snowdrift surface as a reference value for evaluating the most likely practical snow surface to use when choosing cross section for the road and the adjacent terrain. The example on steep road cuts indicates that there is an advantage of widening the ditch at the ends of the cut to pass the drifting snow through with less generation of turbulence and reduction of the potential sedimentation areas. At last some theoretical considerations on the air resistance of guard rail profiles is presented. An oval shape profile with aspect ratio (width/height) equal to 2 is a promising profile for further testing.

More detailed results from the topics treated in this report and results from other experiments on snow drifting in road engineering are presented in the final report that is scheduled in 2002. Among the other topics treated there are studies on the effect of road embankment slope and height and the effect of lateral slope of the road surface (superelevation).

ACKNOWLEDGEMENTS

REFERENCES

[1] Roadex, 2000. Subproject B, *Winter Maintenance*. EU Northern periphery program.

[2] Norem, H. 1975. *Designing highways situated in areas of drifting snow*. Draft translation 503. Hanover, New Hampshire: CRREL.

[3] Norem, H. 1994. *Snow Engineering for Roads*. Handbook no. 174. Oslo: Norwegian Public Road Administration, Road Research Laboratory.

[4] Tabler, R.D. 1994. *Design Guidelines for the Control of Blowing and Drifting Snow*. SHRP-H-381. Washington, DC: National Research Council.

[5] Thordarson, S. & Norem, H. 2000. Simulation of two-dimensional wind flow and snow drifting applications for roads, Part I & II. In Hjorth-Hansen et al. (ed.), *Snow Engineering: Recent Advances and Development*. Proceedings of the 4th International Conference on Snow Engineering. A.A Balkema, Rotterdam.

Paper VI:
Wind tunnel experiments and numerical
simulations of snow drifting around an
avalanche protecting dam

Wind tunnel experiments and numerical simulation of snow drifting around an avalanche protecting dam

Skuli Thordarson

Norwegian University of Science and Technology,
Department of Road and Railway Engineering,
7491 Trondheim, Norway.
TEL: +47 7359 4710 / FAX: +47 7359 7020.
E-mail: thordars@stud.ntnu.no

ABSTRACT: To learn about wind flow and snow drifting around avalanche dams, experiments were done in the Joules Verne Climatic Wind Tunnel. The paper reports the results from numerical wind flow simulations that were done to support the findings from the wind tunnel. Satisfying the model similitude criteria for the wind tunnel configuration was difficult due to the inevitable small geometric scale of the model, while on the contrary the snow drifting conditions in the facilities were full scale. By comparing numerical wind flow results of full scale and model scale dams with the snow pattern observed in the wind tunnel, it was possible to conclude that albeit poor model similitude, the snowdrifts on the windward side of the wind tunnel model are likely to indicate the full scale natural situation.

Key words: Avalanche dam, model similitude, numerical simulation, snow drifting, wind tunnel.

1. INTRODUCTION

1.1 Background

For protecting inhabited areas and other infrastructure against snow avalanches, large collecting or deflecting dams have been built in some countries. Wind flow and snow drifting around such dams has not been investigated in detail before, and better knowledge about this subject is of interest for three main reasons: (1) Avalanche dams may not be as effective for protection if the planned geometry is altered due to wind-transported snow depositing close to the dam. Snowdrifts collected against the mountain facing side of the dam will decrease its effective height and thereby increase the risk of avalanches passing over the dam. (2) Dams are more effective to stop or deflect avalanches the further down in the avalanche path they are located, and are therefore generally located close to the protected area, often a road or a village. Drifts collected on the leeward side of the dam can therefore slide down as minor avalanches

into the protected area. (3) Since these dams are usually large and present severe modification to the local wind flow, they may cause deposition of snowdrifts in the protected area and other wind induced problems.

The current study is a supplementary work to a wind tunnel investigation that was carried out in the Joules Verne Climatic Wind Tunnel in Nantes. The current author was a participant in the wind tunnel experiments, which were described in detail by Haraldsdottir et al. [11]. In the cold wind tunnel, which provides full scale snow drifting with artificial snow particles, the snow drifting around a model avalanche dam was investigated. Different wind directions and dam curvature were tested. Independent of scaling criteria for full scale validity of the wind tunnel results, the study gave a qualitative comparison of the tested alternatives. The problems with fulfilling the different scaling criteria for small scale testing are well known, and therefore such qualitative comparison of alternatives within the given model system are an alternative that can be helpful in engineering applications. Another example of this approach is the experiments done by Gurer [10], where different snow fences were tested in a cold wind tunnel. Also, Baker and Dutch [2] compared porous and solid snow fences using sand in a wind tunnel, a study where similitude to snow drifting was not included.

1.2 Objective

The objective of the current study is to investigate the scaling criteria for the wind tunnel work reported by Haraldsdottir et al. [11] and to evaluate the validity of the results for full scale avalanche dams. The work was divided into two main steps: (1) By reviewing previous work by others, the most important similitude parameters for the wind tunnel tests were identified and their deviation from the prototype was estimated. (2) Numerical simulations of the wind flow around avalanche dams were done for the wind tunnel model (height 0.2 m) and the prototype (height 20 m) respectively, adopting the appropriate value for the model parameters found in the first step.

Figure 1 presents a sketch of the model dam used by Haraldsdottir et al. They treated four different wind directions and several dam curvatures. The current study however, only includes a straight dam perpendicular to the wind and a straight dam aligned 30° to the wind direction. On the leeward side of the dam, the wind tunnel tests resulted in drift formations that are different from and relatively smaller than expected, but the upwind drifts appeared more convincing. The current study revealed that the flow pattern on the windward side of a straight dam is similar for both model and prototype regardless of the wind incident angle. For the leeward side an important difference was found between a perpendicular dam and an oblique one: For a perpendicular dam, the simulated wind flow pattern leeward of the dam differs considerably between model and prototype. On the other hand, for the 30° aligned dam, the simulated flow pattern was identical for the scale model and the prototype, both on the windward and on the leeward side of the dam.

Due to the large length of the prototype avalanche dam to be tested (300 m), the model scale for the wind tunnel tests was bound to be small, even in the relatively
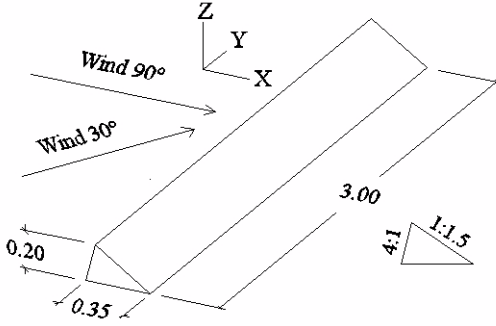
Figure 1 The model geometry from the wind tunnel. Dimensions given in meters. Arrows indicate the two wind directions treated in the report.

large facility used. To include the whole dam structure in the wind tunnel, a geometric scale of 1:100 was necessary. With full scale snow drifting in the wind tunnel, similitude parameters are consequently severely distorted between the model and prototype. It should be emphasised that the goal of the current study is thus not to seek recommended scales for geometry and flow velocities in wind tunnel testing, but to retroactively evaluate the experiments reported by Haraldsdottir et al. [11]. Albeit poor matching of similitude parameters in the wind tunnel tests, I conclude that the current results support the validity of the windward drifts from the wind tunnel for full scale interpretation. For the leeward situation it is more difficult to come to an conclusion, especially since the leeward drifts modelled in the wind tunnel appeared very small and no prototype reference drifts are available.

2. MODEL SIMILITUDE

2.1 Flow description

The boundary layer flow in the lowest part of a stable atmosphere is commonly described by the logarithmic wind profile [24]:

$$u(z) \ = \ \frac{u_*}{\kappa} \ln\left(\frac{z}{z_0}\right) \tag{1}$$

where u is the wind speed at height z. The aerodynamic roughness height, z_0, is a measure of the surface roughness on the ground and gives the theoretical height at which the wind speed is zero. The shear stress in the flow at ground level is an important parameter considering drifting snow. The friction velocity in eq. (1), u_*, is a measure of the shear stress, τ_0, caused by the surface wind on the ground:

$$u_* \ = \ \sqrt{\frac{\tau_0}{\rho_0}} \tag{2}$$

Here, ρ_0 is the density of air and τ_0 designates the sum of turbulent and molecular shear stresses on the ground. If the roughness height, z_0, and wind speed at a given

height, $u(z)$, is known, the friction velocity, u_*, can be calculated by eq. (1). Per definition, eq. (1) should only be valid along a flat ground. When the ground is not flat, the vertical velocity profile will depart from eq. (1) and the friction velocity need not necessarily be linearly related to the wind speed at a given height. Over a rolling or more complex terrain, $u(z)$ will thus only give a rough estimate of the friction velocity. The closer to the ground $u(z)$ is known, the more accurate will the prediction of u_* be.

Many investigators have presented formulas describing the quantity of snow transport in terms of the friction velocity or wind speed at a reference height. Amongst these are Kobayashi [14], Pomeroy and Gray [21] and Schmidt [22]. The snow drifting capacity of the wind is generally found to have approximately third power relationship with the wind speed or the friction velocity. The empirical transport formulas often have the form:

$$Q = a(u_* - u_{*\text{th}})^3 \qquad (3)$$

where the constant a is found by regression analysis on experimental data and $u_{*\text{th}}$ represents a threshold friction velocity for drifting snow. The friction velocity is u_* (m/s) and Q (kg/s m) is the snowdrift rate per unit width.

Although numerical modelling of snow drifting is not the subject of the current study, some of the previous work on that subject should be mentioned here. Numerical snow drifting methods are generally either based on two-fluid models or particle tracking models. Models have e.g. been developed by Decker [7], Uematsu et al. [30], Liston and Sturm [15] and Gauer [9]. Due to fast increasing computer resources and better models the numerical modelling of snow drifting for engineering applications is becoming a real option.

In their two-dimensional simulations of wind flow over a downslope hill, Thordarson and Norem [29] showed that the spatial variations in wind velocity or u_* give a good estimation on sedimentation areas and the relative build-up rates of snowdrifts. They showed how the horizontal wind speed gradient, du/dx, can be transformed to a horizontal snow transport gradient, dQ/dx. A negative value of this gradient results in snowdrift sedimentation, given that the wind is fully saturated with snow particles. A high negative value will cause high rate of snowdrift build-up on the ground. When the conditions on the other hand must be described three-dimensionally, the saturation of drifting snow in the air varies substantially and sedimentation of drifts will occur at different wind speeds in the same flow. An example of this phenomena is secondary vortices generated by flow separation around the observed geometry. Vortices that travel non-parallel to the mean flow tend to gain high concentration of snow particles which will be sedimented at relatively high wind speeds as the vortex bursts or the snow concentration exceeds the transport capacity of the vortex.

By dimensional analysis, a set of dimensionless parameters that describe the character of the flow can be derived. These parameters are also used to ensure similitude of a given model system compared to the prototype or the full scale natural

conditions. A wind tunnel system can be configured to satisfy the different parameters according to which features of the flow are important. However, matching all the relevant parameters at the same time is usually impossible, especially in multi phase flows such as snow drifting. Modelling work will thus most often be a compromise where similitude of the most important parameters for the given situation should be ensured and the less important parameters allowed to be distorted.

2.2 General flow similitude

The wind tunnel tests on snow drifting around an avalanche dam have two main similitude criteria to deal with. The first is the similitude of the air flow itself over the dam structure. The challenge here is to recreate the flow pattern and spatial wind speed distribution around the structure as it would appear in full scale nature. The second criteria is regarding the snow particle behaviour.

First treating the pure airflow, the wind flow over an avalanche dam will be considered as a flow over complex terrain or a hill. Relevant parameters to check are the Froude number, Reynolds number and the relative roughness. These parameters will be defined and discussed in the following text.

The Froude number measures the ratio of inertia and gravitational forces in a flow. In atmospheric flow over obstacles, such as a hill or a ridge, the internal Froude number gives a measure of the importance of stratification in the air. Given a thermally induced density profile in the vertical direction, $\rho(z)$, a characteristic frequency, N, for oscillations of vertically displaced air parcels in the flow is defined as follows [6]:

$$N^2 = -\frac{g}{\rho_0}\frac{d\rho}{dz} \tag{4}$$

where ρ_0 is a reference density and g is gravitational acceleration. When $d\rho/dz < 0$ the fluid is stably stratified and the equation has an oscillating solution with frequency N. Now the Froude number for the flow over an obstacle with a length scale, L, can be written:

$$Fr = \frac{U}{NL} \tag{5}$$

Stratification effects are important in the flow if Fr in eq. (5) is lower than or equal one. In the absence of stratification the Froude number is unbounded ($\rightarrow \infty$) and not a relevant parameter for the flow. Hence, in a homogeneous fluid without free surface the Froude number can be dismissed, since the gravity induced body force on a fluid element is balanced by the buoyancy resulting from the gravity induced pressure gradient in the fluid [5]. The flow in the wake of the obstacle will thus depend on the geometry and the upstream velocity profile [16]. For multi phase flows however, such as snow drifting, the buoyant forces between the different phases ensure the relevance of the Froude number, although in another form than presented by eq. (5).

The ratio of inertia and viscous forces in the flow is measured by the Reynolds number

$$Re = \frac{UL}{\nu} \tag{6}$$

where U and L are velocity and length scales respectively and ν is the kinematic viscosity of the fluid. Re is the most central parameter in all flow modelling, especially in low speed wind tunnel testing [3]. In most flow modelling, Re is considered a minimum requirement, but it should be noted that flows can behave similar over a wide range of Re. Separated and recirculating flows are strongly dependent on the Reynolds number and the turbulence intensity in the upwind profile, a situation that is true for the perpendicular configuration of the current tests of an avalanche dam.

The relative roughness, that is the surface roughness on the upwind fetch compared to the size of a particular obstacle on the ground, indicates the strength of the flow response due to the obstacle. The relative boundary layer thickness (height of the boundary layer compared to the obstacle size) serves the same purpose. For the flow over a 2D surface-mounted cylinder, which has similarities with the 2D simulations and the perpendicular incident angle for the 3D case of the current study, Solberg [23] states that Re is essential, together with the non-dimensional boundary layer thickness, δ/D, where δ is the boundary layer thickness and D is the cylinder diameter. The boundary layer thickness, δ, is often defined as the height, z, up to where $u(z)$ reaches 99 % of the strength of the free stream or geostrophic wind, U_g. The definition can be written as $u(\delta) = 0.99\ U_g$.

Another related parameter, used by Wood [31] when describing the flow over hills, is a non-dimensional length scale, λ/z_0, where λ is a horizontal length scale of the hill. When inverted, z_0/λ, this parameter can represent the non-dimensional roughness. The non-dimensional boundary layer thickness and the non-dimensional roughness are related as follows: For a given wind speed at the top of the boundary layer, $u(\delta) = 0.99\ U_g$, exploration of eq. (1) reveals that the height, $z = \delta$, is linear with the roughness parameter, z_0, because for a constant speed, $u(\delta)$, the term $\ln(\delta/z_0)$ from eq. (1) must be constant. In other words, it has been shown that changes in the surface roughness, z_0, will be reflected in the same proportional changes in boundary layer thickness, δ. The two parameters, δ/D and z_0/λ, can thus substitute each other.

To work with the relative boundary layer thickness, a relative roughness is presented here, where H is the height of the avalanche dam:

$$z_{0(rel)} = \frac{z_0}{H} \tag{7}$$

Increased non-dimensional boundary layer thickness (or roughness) tends to decrease slightly the recirculation length in the wake of the obstacle according to Castro and Fackrell (1978) and others, as referred by Solberg [23]. Increased non-dimensional

roughness is also known to induce flow separation higher up and at lower critical slopes on the leeward side of hills [31].

2.3 Snow drifting similitude

Physical modelling of snow drifting has been done by many investigators and many model systems have been tried. To mention some different model systems; Tabler [26] used scaled outdoor models (scale 1:30) with natural snow drifting and Anno and Konishi [1] used activated clay particles as a substitute for snow in a wind tunnel. The activated clay particles gave good results thanks to their coagulative properties. Iversen [12] used walnut shell granulate and glass beads of different densities in a wind tunnel and Norem [18] used sand suspended in water. Common with all physical modelling of snow drifting is the challenge to satisfy the scaling criteria in order to obtain good results. Authors have partly focused on the same similitude parameters and in part their experiences differ on the importance of each parameter. Iversen [12] compiled an overview of the parameters favored by several investigators, and Naaim-Bouvet [17] has reviewed the parameters used by Kind, Iversen, Anno and Tabler.

The following section reviews only the most central parameters that are relevant to snow drifting in order to establish a basis for the evaluation of the results from the wind tunnel [11]. It excludes discussion on the development or build-up rate of drifts and the dependency of roughness parameter, z_0, with the concentration of drifting snow in the air. In fact, the layer of saltating particles acts as an increased physical roughness on the ground with respect to the flow outside the saltation layer [20]. In the wind tunnel test section, the model was placed such that only 20 m of upwind fetch with snow on the ground was present to feed the wind with snow particles. This fetch is short compared to natural conditions and would hardly suffice to alter the wind profile outside the saltation layer to a remarkable extent.

The most important forces describing the behaviour snow particles in free flight are drag, gravitational and inertia forces [13]. Thus the investigation of the relationship between these forces is of interest when deducing similitude parameters for snow drifting. Considering a spherical solid particle suspended in a fluid at rest, balancing the particle weight and drag force in the vertical direction yields a Froude number on the form

$$Fr = \frac{W_p^{\ 2}}{g\,D}\,\frac{\rho_0}{\rho_p - \rho_0} \tag{8}$$

where W_p is the terminal fall velocity of the particle, D is the diameter and ρ_0 and ρ_p are the densities of the fluid and particle. Here, the drag coefficient is assumed to be the same for both model and prototype. For correct scaling of paths for suspended particles, a kinematic similarity is demanded, and thus the ratio of horizontal to vertical velocity must be matched, U/W_p. This allows for the substitution of U for W_p in eq. (8). The parameter has been called a densimetric Froude number and was considered by Norem [18] when using sand and water to simulate the drifting snow

on roads. The ratio of drag to inertia force from the particle equation of motion yields another form of this parameter,

$$Fr = \frac{U^2}{gL} \frac{\rho_p}{\rho_p - \rho_0} \tag{9}$$

where L represents a length scale in the model or prototype. If both the model and prototype fluid is air, the ratio $[\rho_p/(\rho_p - \rho_0)]$ is practically equal to one and the parameter is consequently reduced to $U^2/(gL)$. If this parameter is compared to

Owen's proposed relationship for mean saltation heights[20], $h \sim u_*^2/(2g)$, it is reasonable to argue that the length scale L in eq. (9) actually can be related to the mean height of saltating particles. In that sense, the parameter presented in eq. (9) is important to ensure that the model and prototype have the same saltation trajectories relative to geometric scale. Kind [13] also introduces Froude scaling to ensure the scaling of saltation heights.

Iversen [12] states that the use of Fr in snow drifting studies is irrelevant unless scaled with density ratios and had a good correlation using an expression originating from Bagnold:

$$Fr = \frac{U^2}{gL} \frac{\rho_0}{\rho_p} \tag{10}$$

where U is the free stream velocity and L is a reference length scale in the model. The density scaling in eq. (10) is different from that in eq. (9) and thus the two parameters can not be fulfilled simultaneously for all given systems of particles and transporting fluid. Furthermore, if both eq. (8) and eq. (10) are to be followed, the particle diameter has to be reduced to the same scale as other geometric dimensions in the model. The resulting scale model particles would in many cases be so small that electric forces would probably become dominant. It is generally accepted that scaled modelling can be done without complete geometric similitude of the particles.

For the purposes of reduced scale modelling under full scale wind and snow drifting conditions as in the present study, the above arguments suggest that the velocity scale should follow the square-root of the geometric scale as stated by eq. (9), an argument that also was followed by Tabler [26] in his outdoor modelling experiment.

Another important parameter for snow drifting according to Iversen [12] is the ratio of the friction velocity, u_*, see eq. (3), and the threshold friction velocity, $u_{*\text{th}}$:

$$\frac{u_*}{u_{*\text{th}}} \tag{11}$$

For values of this parameter slightly above one, snow transport is mainly as surface creep and saltation. Higher values indicate that the amount of transported snow is increased and that larger portion of the snow transport is by suspended particles.

3. METHODS

3.1 Wind tunnel experiments

The Joule Verne Climatic Wind Tunnel has a 25 m long experimental chamber, the width is 10 m and the height is 7 m. The effective working cross section for uniform snow drifting is about 3 m. Snow is produced by sprinkling water from snow guns at the entrance of the test section, forming a thin snow cover on the floor before each experiment. The humidity of the air in the tunnel is low and for the actual experiments, the temperature was set as low as -15° to ensure dry snow properties. The snow particles produced by the snow guns are spherical and have a diameter distribution between 0.1 mm to 0.5 mm. The density of the snow cover prior to snow relocation by drifting varies from 320 kg/m^3 to 460 kg/m^3. The Jules Verne Climatic Wind Tunnel was described by Gandemer et al. [8].

The model used by Haraldsdottir et al. [11] for the wind tunnel tests (Figure 1), a 3 m long triangular profile of height $H = 0.2$ m with side slopes of respectively 4:1 and 1:1.5, was located 17 m downwind from the inlet nozzle. The model could be rotated for a chosen wind direction and this report treats the results for the perpendicular case, experiment WT90, and for a wind direction oriented 30° from the dam longitudinal axis, experiment WT30. With the steeper side (4:1) of the model dam facing the wind in both experiments, this setup represents snow drifting from the mountain and towards the dam in full scale natural interpretation. Snow depths in front of the model dam were measured by sliding a paper sheet through the drift and tracing the snow surface with a pen. The drift shapes drawn on the paper sheets were then digitized. Snow pattern was also photographed from the tunnel roof.

Both experiments referred to in this report were run with wind speed of 15 m/s for 3.5 minutes. The threshold wind speed for initiating saltation was around 6 m/s. In advance of each experiment, the snow guns produced artificial snow for 20 minutes, to obtain a few centimetre thick snow cover on the floor. A detailed description of all the wind tunnel experiments is found in Haraldsdottir et al. [11].

3.2 Numerical simulations

3.2.1 General

The flow solver used is Flow3D (Flow Science, Los Alamos, NM USA). This code has been used for atmospheric flows and snow drifting studies before by Sundsboe [25], Thiis [28] and Thordarson and Norem [29]. The code solves the Reynolds-averaged Navier-Stokes equations on a finite difference scheme. Turbulence closure of the set of equations is achieved by a standard $k - \varepsilon$ model.

In order to compare wind flow over a full scale dam and the scale model from the wind tunnel, simulations were done for a 20 m high dam and for a 0.20 m dam. To investigate the configuration with wind perpendicular to the dam, both two- and three-dimensional simulations were done. For the 30° incident wind, only three dimensional simulation is relevant.

3.2.2 Model scale 1:100 inlet velocity

For the simulations in model scale 1:100, representing the flow in the wind tunnel, the inlet boundary wind profile was determined by numerically simulating the wind flow through the wind tunnel, Figure 2. At the tunnel floor just inside the nozzle a 10 cm high flap was set up to artificially thicken the boundary layer by feeding it with turbulence. Note that the true situation in the wind tunnel is three-dimensional because the experimental chamber is wider than the inlet nozzle, but here the two dimensional situation representing the centre plane is simulated. The resulting vertical wind speed profile at distance 17 m from the inlet is shown on Figure 3.

According to this simulation, the wind flow in the tunnel is divided into four regimes, labelled in Figure 2 and 3: (1) from the floor and up to 0.5 m height there is a turbulent boundary layer, (2) from 0.5 m and up to 1.8 m height an inviscid uniform velocity inertia dominated layer exists and (3) in the interval from 1.8 m to approximately 3.7 m a turbulent shear layer originating from the nozzle upper wall is present. The top layer (3) interacts with the reverse separation bubble remaining under the tunnel ceiling (4). By regression analysis of the bottom layer (1), a best fit logarithmic profile, eq. (1), with roughness height $z_0 = 0.0002$ m and friction velocity $u_* = 0.642$ m/s was found.
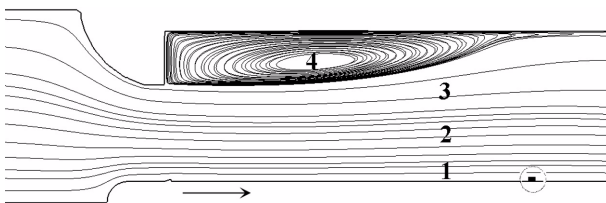

Figure 2 Streamline plot of simulated wind flow in the wind tunnel. Numbers refer to different flow regimes referred in the text. Model location marked with a dotted circle.

3.2.3 Natural scale inlet velocity

A chosen velocity scale for the full scale nature (or prototype) simulations has to interpret a situation that would be expected to cause snow drifting around the dam. However, the velocity has to be examined with respect to the scaling criteria studied in previous section. Using the wind speed at the top of the model dam ($z = 0.20$ m) as a reference velocity, the velocity profile deduced before ($z_0 = 0.0002$ m and $u_* = 0.642$ m/s) yields $U_{ref} = u(0.20) = 11.1$ m/s. This value is close to what was observed in front of the model dam when the nozzle velocity in the tunnel was set to 15 m/s.
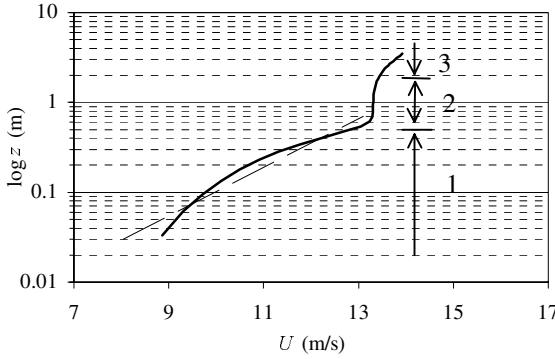
Figure 3 Simulated mean wind field in the wind tunnel with nozzle speed of 15 m/s. This vertical profile is taken at the dam location. The numbers indicate the different flow regimes referred to in the text. Best fit curve for the flow regime next to the floor is plotted as a segmented line.

The Reynolds criterion is fulfilled when $U_M L_M = U_N L_N$ from eq. (6), where the subscripts refer to parameters from the wind tunnel model, M, and nature, N, respectively. For $U_M = 11.1$ m/s and $L_N = 100 L_M$ a velocity scale $U_N = 0.1$ m/s for the full scale case is demanded. Of course, this velocity falls way out of the actual range for snow drifting. Since the model and nature snow drifting conditions are the same, the velocity scale for the full scale nature, U_N, is bound to be of the order 10 m/s. This fact claims a Reynolds number that is two orders of magnitude higher for the nature than for the model, $Re_N = 1.7 \times 10^7$ whereas $Re_M = 1.7 \times 10^5$. The difference is expected to be significant for the flow structure in the perpendicular case, where the flow is recirculating and strong velocity gradients occur. However, the impact on the oblique wind direction is more uncertain, as the flow will no longer separate on the edges of the dam but more or less be deflected.

Matching the Froude numbers directly, $U_N = U_M \sqrt{L_N / L_M}$ from eq. (9), would ensure that the particle paths are correctly scaled with the geometry. This gives a velocity scale U_N of order 100 m/s. Even in an extreme hypothetical situation, a wind speed that high would not adjust the saltation height, but throw the snow particles into suspension with the air. It is evident that the saltation paths will by no means be scaled correctly between the wind tunnel model and full scale nature.

Apparently, the best thing to do in the situation is to choose a velocity scale and boundary layer structure that are in the range for actual snow drifting conditions and preserve the relative roughness of the flow between the model and nature. That can be done by having the same value of $z_{0(rel)}$ in eq. (7) in both scales. The wind tunnel roughness is already determined as $z_0 = 0.0002$ m. Hence, eq. (7) suggests a roughness height $z_0 = 0.02$ m for the nature. This roughness height is close to what is observed over an open countryside with sparse vegetation [4]. Now, keeping the friction velocity the same for both model and nature, $u_* = 0.642$ m/s, the reference velocity at top of the dam is the same for both systems, $U_{ref} = u(H) = 11.1$ m/s according to eq. (1). The resulting distortion of the Reynolds and Froude numbers becomes; $Fr_M = 100 \, Fr_N$ and $Re_M = Re_N / 100$.

3.2.4 Two-dimensional simulations

The main purpose of the two-dimensional (2D) numerical simulations is to obtain a comparison with previous numerical work as well as to compare to the perpendicular case of the three-dimensional simulations. The simulation domain is $10\,H$ high and $40\,H$ long and the dam structure is placed at distance $10\,H$ from the inlet boundary. The letter H defines the dam height. This configuration is the same as used by Solberg [23] when simulating the two-dimensional flow over a circular cylinder at a plane wall. The flow over an avalanche dam has many similarities to flow over a circular cylinder at a plane wall, that is of fundamental interest to fluid mechanics and is thus studied by numerous authors.

Two simulations were done, one for the model from the wind tunnel, $NUM_{2D}90_M$, and one for a dam in full scale nature, $NUM_{2D}90_N$. The calculation mesh has horizontal and vertical spacing of $H/20$ around the dam structure and is otherwise variable in both directions, giving a total of 8700 mesh cells. Inlet wind conditions are determined by eq. (1) with $z_0 = 0.0002$ m for the scaled model simulation and $z_0 = 0.02$ m for the natural scale simulation. The same friction velocity is applied in both cases, $u_* = 0.642$. The top boundary has a constant pressure, outflow boundary is continuative (all derivatives in the flow direction set to zero) and the bottom is set with a no-slip condition.

3.2.5 Three-dimensional simulations

Three-dimensional wind field simulations (3D) were done for both the perpendicular dam, $NUM_{3D}90_M$ and $NUM_{3D}90_N$, and for the oblique incident angle, $NUM_{3D}30_M$ and $NUM_{3D}30_N$. Boundary conditions are the same as before. Summary of details for these simulations and the 2D simulations described above is in Table 1.

Table 1: Details on numerical wind field simulation setup

Simulation	Domain dimensions (H) [a]			Mesh spacing (H) [b]			Total number of mesh cells
	Length [c]	Width	Height	*dx*	*dy*	*dz*	
$NUM_{2D}90_{M,\,N}$	40	-	10	1/20	-	1/20	8700
$NUM_{3D}90_{M,\,N}$	35	35	8	1/10	1/2	1/20	434 000
$NUM_3\text{-}30_{M,\,N}$	50	30	8	3/4	1/2	1/10	103 500

a. Dimensions in terms of H, dam height.
b. Values given for closest spacing around the model. Spacing is otherwise variable.
c. Dam is located at $10\,H$ downstream from the inlet boundary.

4. RESULTS

4.1 Wind tunnel results

From the wind tunnel study reported by Haraldsdottir et al. [11], only the results relevant for the purposes of the current study are presented here. Photographs of the snow pattern from the wind tunnel tests are presented in Figures 4 and 5. Measured snow depths at 10 cm distance (0.5 H) upwind from the dam are plotted in Figure 6 and snow depths in selected profiles upwind from the model dam are presented in Figure 7.

4.1.1 Perpendicular dam, WT90

It is evident from the snow depths in front of the perpendicular dam, which theoretically should be symmetric about the center normal, that the snow drifting in the wind tunnel is not uniform across the floor. This depart from symmetry is also clear in the drift formations around the dam ends in Figure 4, where the wind scoop around the left corner is larger than around the right corner. A tight schedule for the wind tunnel experiments did not allow for repeated control tests on this matter.

The measured snow profiles in Figure 7 indicate that the snow depth in front of the dam starts to increase at distance 4 H upwind. At 2 H, the height of the snow surface increases rapidly towards the dam.
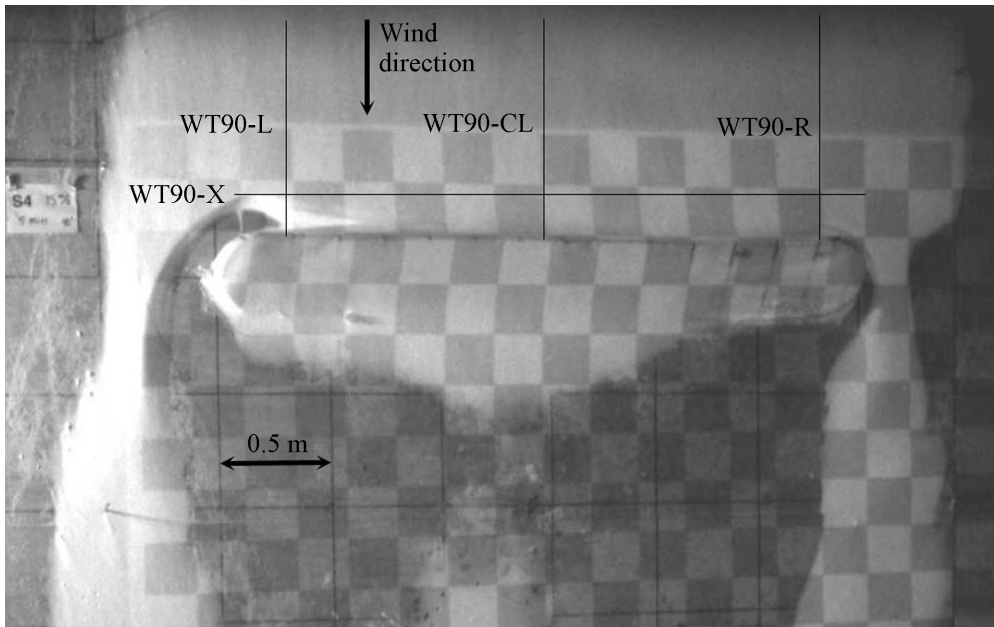

Figure 4 Snowdrift pattern around the perpendicular dam in the wind tunnel, experiment WT90. Location of snow profiles plotted in Figures 6 and 7 is shown. Accumulated snow appearing white, the tunnel floor is dark. Checkered shades are projected on the model.
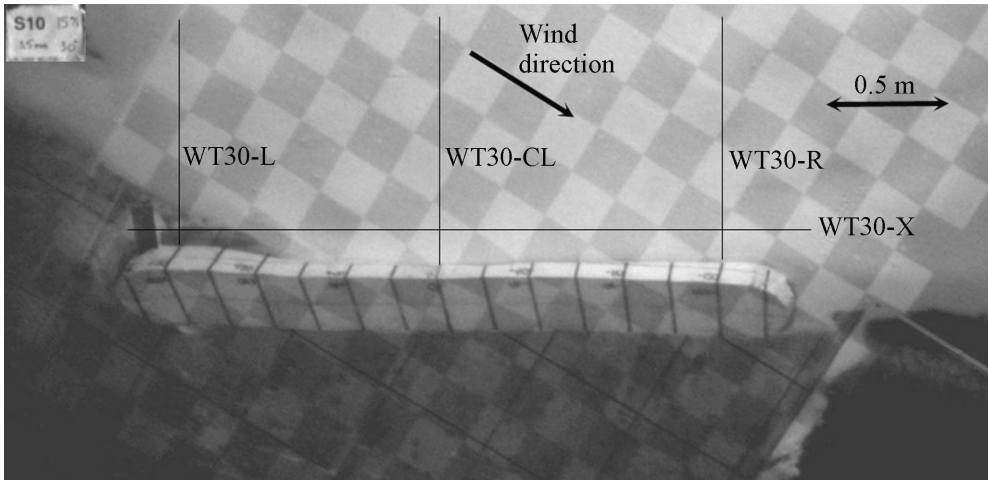
Figure 5 Snowdrift pattern around the 30° aligned dam in the wind tunnel, experiment WT30. Location of snow profiles plotted in Figures 6 and 7 is shown. Accumulated snow appearing white, the tunnel floor is dark. Checkered shades are projected on the model.

4.1.2 Oblique dam, WT30

Figure 5 is a photograph of the snowdrift pattern from the wind tunnel when the wind direction was aligned 30° from the dam longitudinal axis. Figure 6 shows that the snow depth increases gradually along the dam in the direction of the wind, from left to right. The snow profiles in Figure 7 show that the drifts start to grow higher at distance 2 H upwind from the dam.
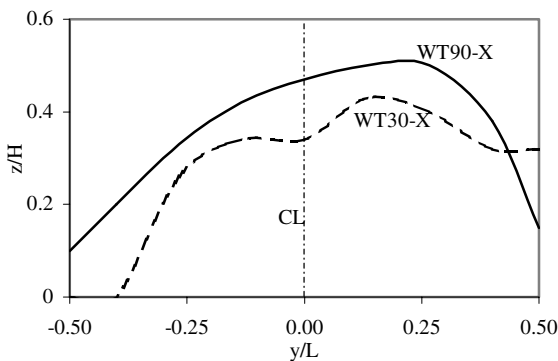

Figure 6 Measured snow profiles parallel to the dam at upwind distance 0.5 H (0.1 m). The location of the profiles is marked in Figures 4 and 5.
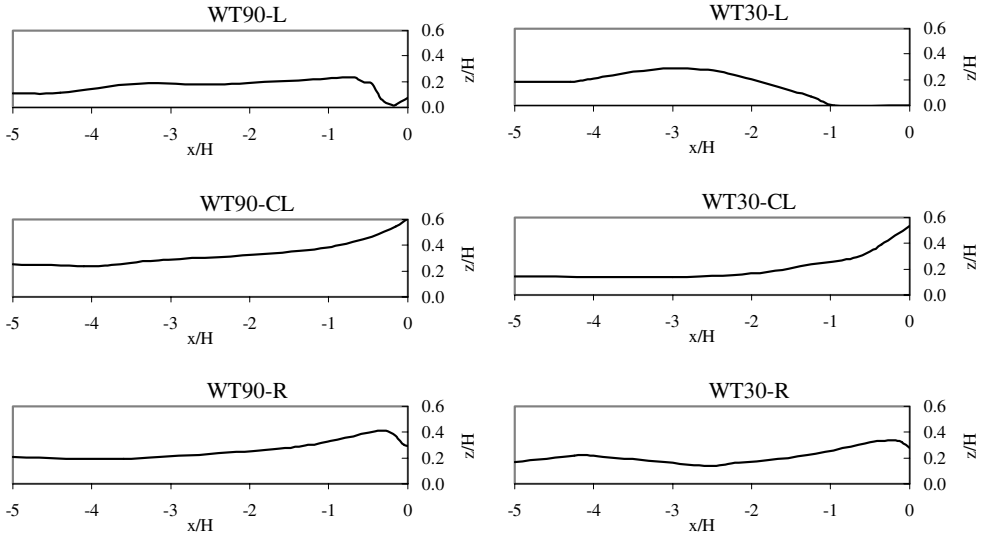
Figure 7 Measured snow profiles shown in Figures 4 and 5.

4.2 Numerical wind flow simulation results

4.2.1 Two-dimensional perpendicular dam

The two-dimensional simulation on the scaled model with dam height $H = 0.2$ m, $NUM_{2D}90_M$, lies in the same Reynolds number area as the simulations of Solberg [23]. As a control on the quality of the current simulations, these are compared to Solberg's results in Figure 8. The separated flow causes a large recirculating bubble
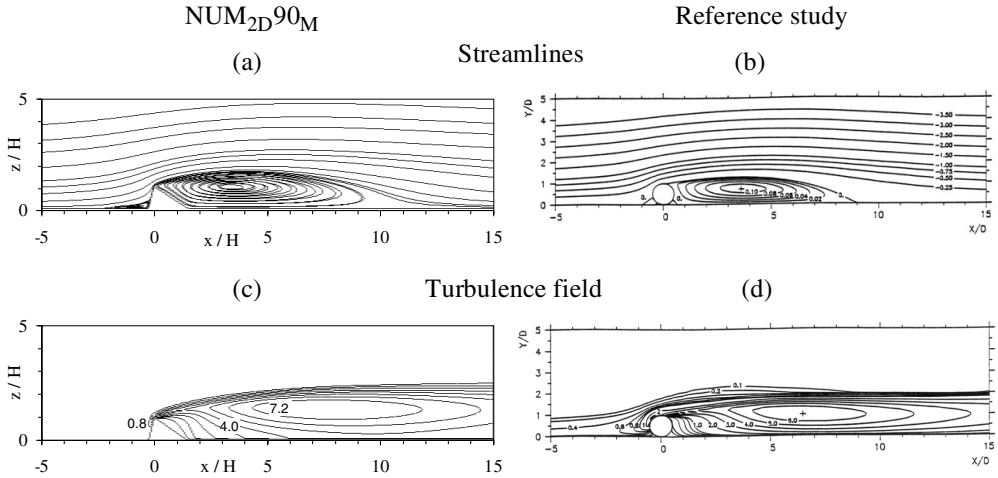

Figure 8 Comparison of the current 2D simulation of the wind tunnel model, $NUM_{2D}90_M$, and the simulation by Solberg [23] of the flow over a surface mounted cylinder. Mean flow streamlines in (a) and (b). Turbulence field $(k/U_{ref}^2) \cdot 10^2$, where k is turbulent kinetic energy in (c) and (d). The Reynolds number is of the order 10^5 in both cases.

on the leeward side, with high turbulent fluctuations. The recirculating area is both higher and longer for the model dam than for the cylinder, possibly as a result of the less streamlined geometry of the dam. However, the turbulence field is very similar and confirms that the current simulations are representative for the flow situation studied here.

Compared to the full scale simulation which has a hundred times higher Reynolds number (Figure 9), the mean wind speed in the wake of the scaled model is as low as 10 % of the reference wind speed, $U_{ref} = u(H)$, but exceeds 110 % U_{ref} close to the ground in the full scale simulation. The turbulence field is also weaker in

Mean wind speed

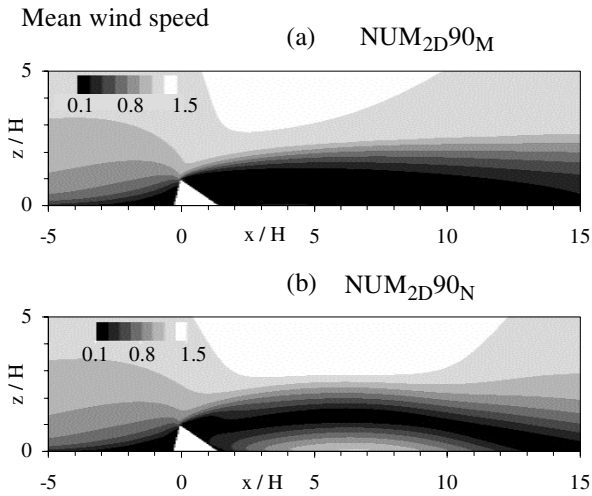(a)   NUM$_{2D}$90$_M$

(b)   NUM$_{2D}$90$_N$

Figure 9 Relative wind speed distribution from the two-dimensional simulations. In (a), wind tunnel model, $Re = 1.7 \times 10^5$, and in (b), full natural scale, $Re = 1.7 \times 10^7$.

NUM$_{2D}$90$_N$

(a) Streamlines
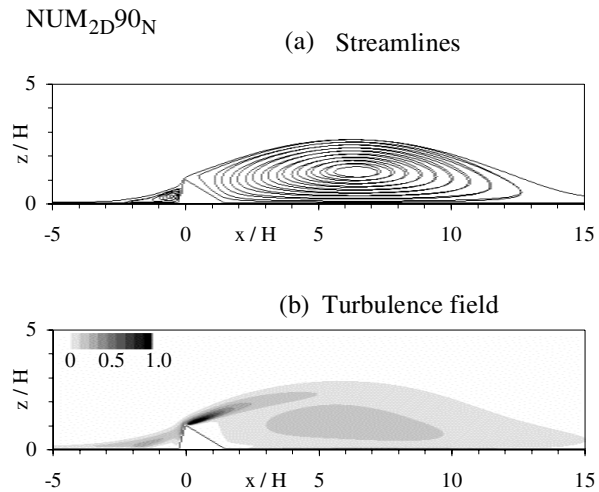

(b) Turbulence field

Figure 10 Results from the natural scale simulation, streamlines in (a) and turbulence field in (b). Note that the turbulence field is an order of magnitude weaker than for the model scale, show in Figure 8 (c).
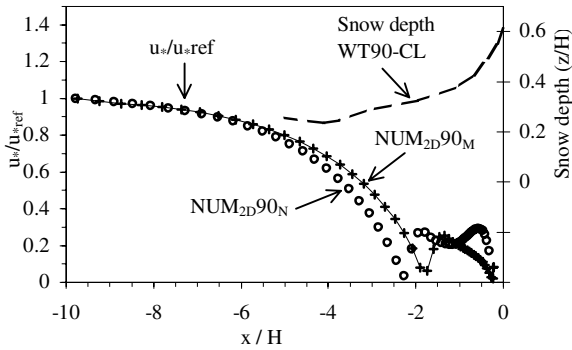
Figure 11 Perpendicular dam. Relative friction velocity distribution along the ground upwind from the dam. Snow depth in front of the wind tunnel model is also plotted against the right-hand axis.

$NUM_{2D}90_N$, as well as the streamline pattern is different (Figure 8 (a) and (c) and Figure 10). The leeward recirculation area is both longer and higher for the natural scale, $NUM_{2D}90_N$.

This great difference in the flow between the two scales is due to viscous effects and evidently a result of the different Reynolds number. However, looking at the flow upwind from the dam in Figure 9, it can be seen that the wind speed pattern is similar for both simulations. To show this similarity, the friction velocity development at the ground is plotted in Figure 11. Upwind recirculation stretches as far as $2\,H$ from the dam in both cases and is coincident with the sharp increase in drift thickness at the wind tunnel model, also plotted on Figure 11.

4.2.2 Three-dimensional perpendicular dam

The model dam tested in the wind tunnel has length to height ratio $L/H = 15$. According to snow fence data [27], the end edges of a snow fence create flow conditions that cause the lee drift to reach a shorter distance as far as $12\,H$ from the edge and towards the center normal of the snow fence. This means that a snow fence has to be at least $24\,H$ long to be fully effective. By this argument it should be reasonable to assume that the flow behind an object of length $15\,H$ is governed by the end effect from the edges, and hence should no part of the wake have a two-dimensional character.

This is also the case in the results from the three-dimensional simulations of the perpendicular dam. Figures 12 and 13 show the relative wind speed distribution at ground level for the two scales tested, together with the streamline pattern. As for the 2D simulations, the flow behaves different behind the dam in the two scales, but the upwind flow pattern looks more similar.

In the downwind wake of the scaled model, $NUM_{3D}90_M$ (Figure 12), the wind flow is governed by a vortex originating from the end edge, travelling almost parallel to the dam towards the center where it meets the vortex from the opposite edge. This vortex rotates in a nearly vertical plane. In $NUM_{3D}90_N$ on the other hand (Figure 13), the flow is governed by a motion in horizontal plane, and the streamlines are more irregular. It is evident that there is less renewal of air in the wake for the natural scale.
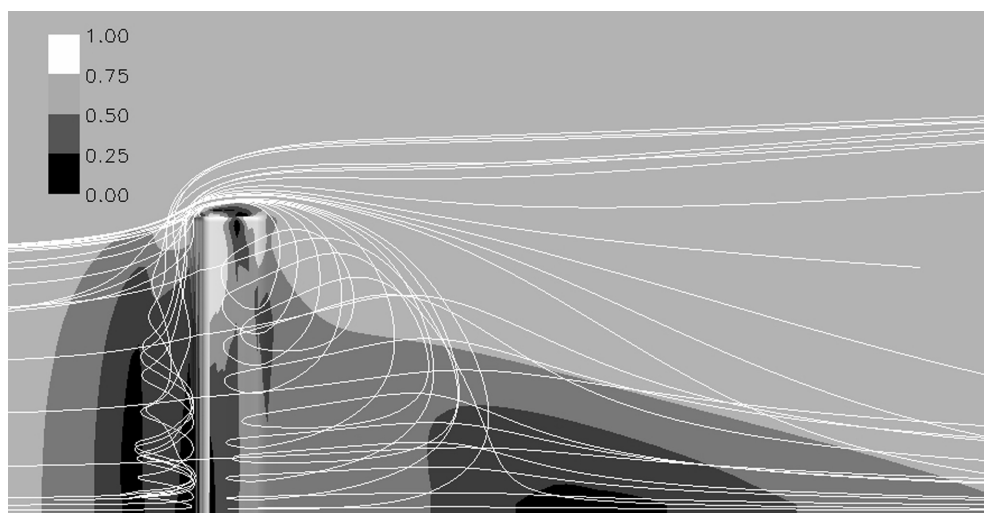
Figure 12 Results for experiment NUM$_{3D}$90$_M$, wind tunnel model dam in scale 1:100. The lower edge of the figure is at the center normal of the dam, which acts as a symmetry plane in the simulation. Plane view of the relative wind speed distribution at ground level is shown by gray scales. Streamline pattern for the main features of the flow is plotted in white.
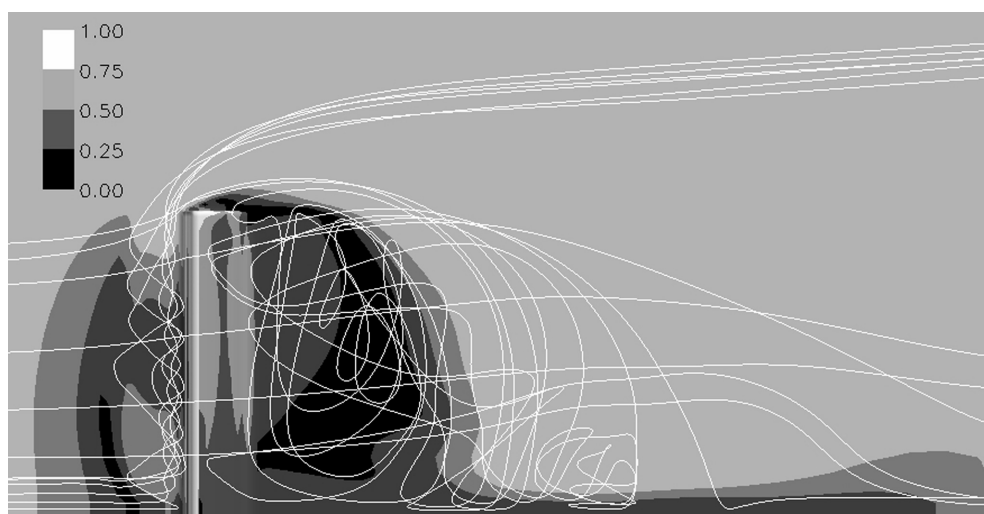

Figure 13 Results for experiment NUM$_{3D}$90$_N$, full scale avalanche dam. The lower edge of the figure is at the center normal of the dam, which acts as a symmetry plane in the simulation. Plane view of the relative wind speed distribution at ground level is shown by gray scales. Streamline pattern for the main features of the flow is also plotted.

The location of the area with lowest wind speed is different and the wind speed is generally lower in the wake for the natural scale simulation.

The upwind vortex has similar dimensions in both scales and is mainly fed by the air that hits the dam around the center. Also the relative wind speed distribution at ground level follows more or less the same pattern.

4.2.3 Three-dimensional 30° aligned dam

The simulations for the 30° aligned dam are according to the results less affected by the scaling (Figures 14 and 15), since the wind speed distribution and streamline pattern are almost identical. A profile of the relative friction velocity along a line parallel the wind through the dam center is plotted in Figure 16. It is somewhat
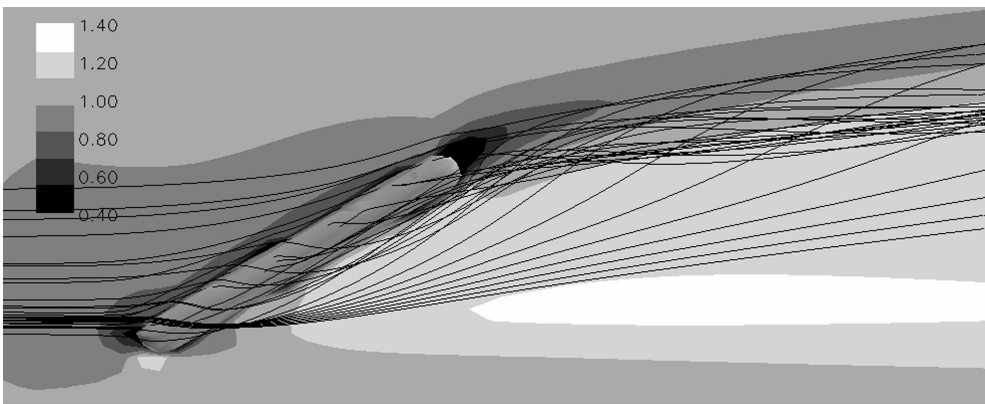

Figure 14 Simulation $NUM_{3D}30_M$, wind tunnel model dam in scale 1:100. Gray scales indicate relative wind speed distribution at ground level. Streamlines plotted in black.
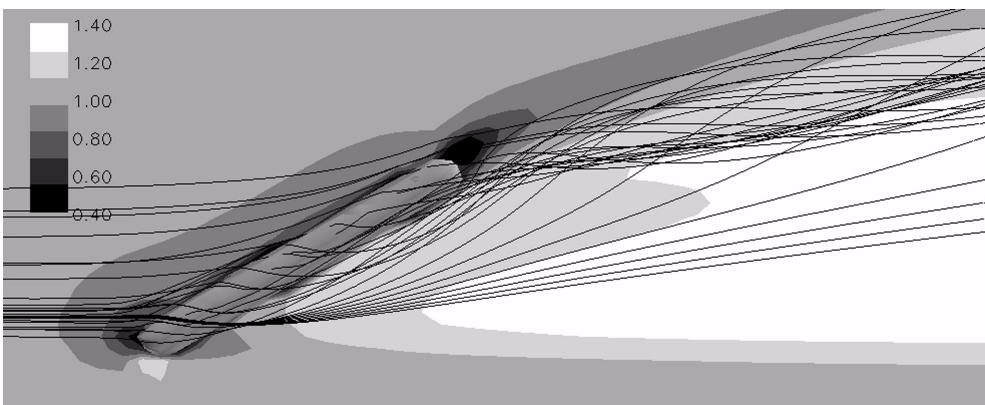

Figure 15 Simulation $NUM_{3D}30_N$, natural scale dam. Gray scales indicate relative wind speed distribution at the ground. Streamlines plotted in black.
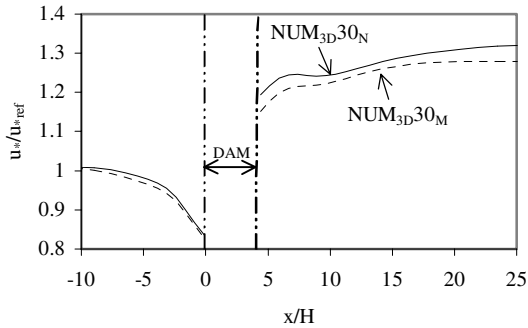
Figure 16 Oblique dam, 30°. Relative friction velocity development along a line parallel the wind through the dam center.

surprising that the speed of the flow in the wake is actually at least 20 % higher than the upwind condition, and this area of high wind speed reaches far downstream. Streamline analysis of the wake, showed that the air travelling close to the ground behind the dam originates from a level higher up from the ground upwind of the dam, and due to the velocity gradient in the vertical direction of the inlet wind, this air is moving much faster than the air at lower levels. The dam deflects the low level flow to the side, and thus forcing the air from higher levels down to the ground in the dam wake.

5. DISCUSSION

The objective of the numerical wind field simulations was to obtain better understanding of the wind tunnel results and to provide comparison of scales to predicted wind flow and snow drifting around a full scale avalanche dam. This section seeks answers to two important questions; (1) How does the calculated wind flow correspond to the drift pattern observed in the wind tunnel, and (2), can the wind tunnel results be used to predict snowdrifts around a natural scale dam? Unfortunately, field data on snowdrifts around full scale dams is not yet available, so the answer to the second question must remain on a hypothetical level with the aid of the full scale wind flow simulations.

5.1 Dam perpendicular to the wind direction

The two-dimensional simulations merely serve as a control function to compare to previous simulation work on a related problem. The results presented in Figures 8 through 10 are in good agreement with the reference study cited.

5.1.1 Upwind situation

Although it has been argued in the previous section that the flow over the parallel dam will not be described two-dimensionally, the three-dimensional simulations show that

the wind speed reduction at ground level upwind from the dam is more or less uniform along the dam. This fact is seen on Figures 12 and 13.

The curves from the 2D experiments in Figure 11 actually describe the same friction velocity reduction as seen in the 3D experiments for the parallel dam. They show that the friction velocity gradually starts to decrease as far as $10\,H$ upwind from the dam. At $4\,H$, the curves fall very rapidly from about 70 % the original u_*, down to zero at $2\,H$ where the upwind transverse vortex starts. Looking at the snow profiles measured after experiment WT90 in Figure 7, it can be seen that the snow depth in front of the dam starts to increase at $4\,H$. According to this argument it is reasonable to conclude that the wind flow upwind from a perpendicular dam is approximately two dimensional in a sufficient distance from the ends. At distance about $2\,H$ from the ends, this two-dimensionality is no longer present as the flow is deflected around the corner.

In spite of poor matching of Froude numbers as discussed in section 3.2.3, the similarities of the upwind conditions for both model scales and the matching snowdrifts from the wind tunnel are a very positive result. Although saltating particles in the wind tunnel jump as high as the model dam itself and are easily thrown over it, it is possible that the particles transported as surface creep have compensated for the poor scaling of saltation paths and taken the place of saltating particles in front of a full scale dam. Regardless of this, the results support the idea of interpreting the upwind drifts from WT90 as an indicator of full scale behaviour of natural drifts, at least concerning the critical distance of $4\,H$ as a start for snowdrift sedimentation.

No drift measurements around full scale dams have yet become available, but the idea of using the sharp fall of the friction velocity curve as an indicator of snowdrift sedimentation in full scale nature is supported by the results of Thordarson and Norem [29]. They showed that a sharp fall in the friction velocity curve is coincident with the initiation of snowdrift sedimentation in a 2D situation.

5.1.2 Downwind situation

The drift pattern on the leeward side of the perpendicular dam is more difficult to deal with. The wind tunnel results showed almost no sedimentation in the leeward slope of the dam. Concerning a full scale natural situation, snowdrifts are frequently found on the leeward slopes of terrain features. These will often be found as cornice formations and can include large amounts of snow. However, no data has been found on how or if cornices will form on dams that are as high as 20 m. The possible formation of cornice drifts on the leeward slopes of avalanche dams will most likely be a function of the ratio in eq. (11), the height scale and the stage of windward drift development. Cornice drifts will not decrease the avalanche protecting function of a dam if the wind direction is the same as the flow direction of an avalanche but for the opposite wind direction the steep slope intended to interact with avalanche forces might be smoothed out if the drift amounts are substantial.

Large drifts are observed downwind of the ends of the wind tunnel dam, Figure 4. These drifts are built up by air that originates from the upwind vortex at the dam foot and is deflected downwind as the vortex rounds the corner of the dam. The streamline

pattern for both the scale model and the prototype simulations (Figure 12 and 13) is very similar in this area. The main difference is how the upwind vortex in the scale model takes a sharper turn around the corner than the natural scale vortex does. It seems likely that the full scale drift pattern would follow the results from WT90 regarding the end drifts. The large area of low wind speed behind the natural scale dam, seen in Figure 13 is not in connection with the end vortex. This area will probably be fed with drifting snow that blows over the dam and collect drifts. How this drift development will be compared to the end drift discussed earlier is difficult to say. Snow particles not caught up in the possible cornice high up on the leeward slope are likely to migrate into this area and deposit. In general it can be concluded that the leeward area of the perpendicular wind tunnel dam does not reflect the natural scale conditions due to the different Reynolds numbers encountered in the two scales.

5.2 Dam aligned 30° to the wind direction

The flow around the oblique dam is totally different than around the perpendicular dam. The main difference is that recirculation areas do neither form upwind nor downwind from the oblique dam. That kind of flow is less sensitive to viscous effects and Reynolds number, hence it must be the main reason for that why simulation results for the two scales (Figure 14 and 15) look almost identical in every aspect. It can be concluded that the geometric scaling of 1:100 is acceptable here, at least regarding the plain wind flow in absence of snow drifting.

The flow is divided by the dam, the air is partly deflected along the windward side and partly passes over the dam to be deflected along the leeward side. These two main streams then mix downwind from the far end of the dam.

5.2.1 Upwind situation

The upwind stream keeps a relatively high velocity along the dam and the air speed is less retarded in the area in front of the dam, compared to the perpendicular dam. This is reflected by the drift pattern from the wind tunnel, where the snow depths start to increase at distance $2H$ upstream from the dam. The area in front of the upwind corner of the dam is snow free and the drift thickness is at maximum somewhere downwind of the dam center as seen in Figure 6. The reason for this is probably that the upwind stream gradually becomes saturated with snow as it passes along the dam and its transport capacity is not enough to carry the snow past the dam.

5.2.2 Downwind situation

No drifts are observed on the downwind side of the dam as seen in Figure 5. Regarding the full scale natural condition, one might expect that snow would collect on the leeward slopes of the dam and in the area at the dam foot where the leeward stream travels. Again, these drifts are not prone to impact the functionality of the avalanche dam. Even though the plain wind flow is similar for the two scales in question, it may be assumed that failing to satisfy Froude scaling here has great impact on the leeward drifts.

The friction velocity profile presented in Figure 16 confirms the similarity of the wind flow between the two scales. Control simulations that were done with a uniform constant velocity inlet profile showed that the area downstream of the dam had lower friction velocity than the upwind area, something which is opposite for the current simulations where the downwind area gets higher friction velocity. This indicates that the scaling of the inlet profile according to the relative roughness principle introduced in eq. (7) is successful. Increased air speed at ground level in the downstream area is a result of the vertical velocity gradient of the inlet wind profile and streamline analysis shows that the low level flow is deflected aside and upper level flow is forced down to the ground in the far leeward area. This phenomena may have negative impact for the utilization of the area downwind from the dam all year around, creating at least 20 % higher wind speeds than otherwise would be observed.

The nature of the drift formations around the oblique dam have similarities to those observed around solid deflector fences [19]. The drift stretching from the downwind end can be very large and has to be encountered for in the planning of avalanche dams.

5.3 Concluding summary

Even though the wind tunnel experiments do not follow scaling criteria for snow drifting, it has been argued that the snowdrift patterns at the windward side of both the perpendicular and the oblique dam configurations are likely to be valid in full scale nature. It has been confirmed that wind speed analysis can predict snowdrift pattern to a certain extent where the flow conditions can be approximated as two-dimensional. The following list summarizes the most important conclusions of this study:

Conclusions for experimental similitude:

1. The leeward snowdrift behaviour appears not to be modelled correctly when geometric model scale of 1:100 is applied in full scale snow drifting conditions.

2. Controversially, the windward drifts appear to be correctly modelled.

3. The wind flow pattern leeward of a dam is sensitive to Reynolds number when the dam is perpendicular to the wind, but not when it is aligned 30° to the wind.

Practical conclusions for snow drifting around avalanche dams:

4. Disregarding the transverse upwind vortex at the dam foot, the wind speed reduction over the area in front of the dam is nearly uniform along the dam and may be regarded as two-dimensional.

5. The windward drift sedimentation initiates where the friction velocity falls rapidly, 4 H upwind from the perpendicular dam and 2 H from the 30° aligned dam.

6. In a large area downwind of a 30° aligned dam, the wind speed is about 20 % higher than in the absence of a dam.

6. ACKNOWLEDGEMENTS

REFERENCES

[1]   Anno, Y. and Konishi, T.: 1981, Modelling the effects of a snowdrift-preventing forest and a snow fence by means of activated clay particles, *Cold Regions Science and Technology* **5**, 43-58.

[2]   Baker, C.J. and Dutch, W.G.: 1995, An investigation into the potential use of solid snow barriers on the Snake Pass, Derbyshire, *Proceedings of The Institution of Civil Engineers* **95**, 151-160.

[3]   Barlow, J.B., Pope, A. and Rae, W.H.: 1999, *Low-speed wind tunnel testing*, Wiley, New York.

[4]   Barltrop, N.D.P. and Adams, A.J.: 1991, *Dynamics of fixed marine structures*, Butterworth-Heinemann, Oxford..

[5]   Blevins, R.D.: 1992, *Applied fluid dynamics handbook*, Krieger Publ. Co., Malabar.

[6]   Cushman-Roisin, B.: 1994, *Introduction to Geophysical Fluid Dynamics*, Prentice Hall, New Jersey.

[7]   Decker, R.: 1990, Continuum mixture theory with an application to turbulent snow, air flows and sedimentation, *Journal of Wind Engineering and Industrial Aerodynamics* **36**, 877-887.

[8]   Gandemer, J., Palier, P. and Boisson-Kouznetzoff, S.: 1997, Snow simulation within the closed space of the Jules Verne Climatic Wind Tunnel. In: Izumi, M., Nakamura, T. & Sack, R.(ed.), *Snow Engineering: Recent Advances. Proceedings of the third international conference on Snow Engineering, Sendai, Japan, 1996*, pp. 347-352, A.A. Balkema, Rotterdam.

[9] Gauer, P.: 1999, Blowing and drifting snow in alpine terrain: A physically-based numerical model and related field measurements. *Mitteilungen des Eidgenössischen Institutes für Schnee- und Lawinenforschung*, Eidgenössisches Institut für Schnee- und Lawinenforschung, Davos.

[10] Gurer, I., Sato, T., Kosugi, K., Kamata, Y. and Sato, A.: 2002, Comparison of the models of different types of snow fences in a cold wind tunnel. *Proceedings of the XIth PIARC International Winter Road Congress,* 28-31 January 2002, Sapporo, Japan.

[11] Haraldsdottir, S.H., Thordarson, S., Olafsson, H. and Norem, H.: 2002, Drifting snow around an Avalanche dam in a wind-tunnel, *Materiali Glyaciologicheskikh Issledovanii (Data of Glaciological Studies)* **93**

[12] Iversen, J.D.: 1980, Drifting-snow similitude transport-rate and roughness modeling, *Journal of Glaciology* **26**, 393-403.

[13] Kind, R.J.: 1976, A critical examination of the requirements for model simulation of wind-induced erosion/deposition phenomena such as snow drifting, *Atmospheric Environment* **10**, 219-227.

[14] Kobayashi, D.: 1972, *Contributions from the Institude of Low Temperature Science*, Hokkaido University, Sapporo.

[15] Liston, G.E. and Sturm, M.: 1998, A snow-transport model for complex terrain, *Journal of Glaciology* **44**, 498-516.

[16] Lugt, H.J.: 1983, *Vortex Flow in Nature and Technology*, John Wiley & Sons, New York.

[17] Naaim-Bouvet, F.: 1995, Comparison of requirements for modeling snowdrift in the case of outdoor and wind tunnel experiments, *Surveys in Geophysics* **16**, 711-727.

[18] Norem, H.: 1975, *Designing highways situated in areas of drifting snow. Draft translation 503*, CRREL, Hanover, New Hampshire.

[19] Norem, H. and Andersen, J.G.: 1975, *Design and location of snow fences. Contribution no. 49*, Norwegian Road Research Laboratory, Oslo.

[20] Owen, P.R.: 1964, Saltation of uniform grains in air, *Journal of Fluid Mechanics* **20**, 225-242.

[21] Pomeroy, J.W. and Gray, D.M.: 1990, Saltation of Snow, *Water Resources Research* **26**, 1583-1594.

[22] Schmidt, R.A.: 1986, Transport rate of drifting snow and the mean wind speed profile, *Boundary-Layer Meteorology* **34**, 213-241.

[23] Solberg, T.: 1992, *A numerical study of laminar and turbulent separated flows over a circular cylinder at a plane wall. Thesis*, Norwegian Institute of Technology, Trondheim.

[24] Stull, R.B.: 1988, *An Introduction to Boundary Layer Meteorology*, Kluwer Academic Publishers, Dordrecht.

[25] Sundsboe, P.A.: 1997, *Numerical modelling and simulation of snow drift. Thesis*, Norwegian University of Science and Technology, Narvik.

[26] Tabler, R.D.: 1980, Self-similarity of wind profiles in blowing snow allows for outdoor modeling, *Journal of Glaciology* **26**, 421-434.

[27] Tabler, R.D.: 1988, *Snow Fence Handbook*, Tabler & Associates, Laramie, Wyoming.

[28] Thiis, T.K.: 2000, *Experimental validations of numerical simulations of snowdrifts around buildings and in terrain. Thesis*, Norwegian University of Science and Technology, Trondheim.

[29] Thordarson, S. and Norem, H.: 2000, Simulation of two-dimensional wind flow and snow drifting application for roads: Part I & II. In: Hjorth-Hansen, E., Holand, I., Løset, S. & Norem, H.(ed.), *Snow Engineering. Recent Advances and Developments. Proceedings of the fourth International Conference on Snow Engineering, Trondheim, Norway, 2000*, pp. 437-452, A.A. Balkema, Rotterdam.

[30] Uematsu, T., Nakata, T., Takeuchi, K., Arisawa, Y. and Kaneda, Y.: 1991, Three-dimensional numerical simulation of snowdrift, *Cold Regions Science and Technology* **20**, 65-73.

[31] Wood, N.: 1995, The onset of separation in neutral, turbulent flow over hills, *Boundary-Layer Meteorology* **76**, 137-164.

Reports from The Department of Road and Railway Engineering

Report no.	Author	Title	Year
1	Kummeneje, Ottar	Rutebilstasjoner	1949
2	Riise, T.B.	Terrengets innflytelse på vindens retning og hastighet – styrke	1950
3	Lærum og Ødegård	Grunnlag for vurdering av den økonomiske verdi av vegforbedringer	1957
4	Ødegård, Erik	Vegen som forretning	1959
5	Ording, Jørgen	Undersøkelser av asfaltdekker i Trondheim	1961
6	Riise og Heim	Undersøkelse av torvmatters innflytelse på faste dekker	1962
7	Gustavsen, Øyvind	En analyse av trafikkutviklingen ved overgang fra ferje- til bruforbindelse	1964
8	Sagen, Ragnvald	Traffic Simulation	1967
9	Riise, T.B.	Blandingsjordarters telefarlighet	1968
10	Kvåle, Kjell	Studiereise på veganlegg i Alpeland	1972
11	Norem, Harald	Utforming av veger i drivsnøområder	1974
12	Svennar, Odd	Nærtrafikk-baner	1975
13	Arnevik, Asbjørn	Overflatebehandling	1976
14	Noss, Per Magne	Poresug i jordarter	1978
15	Slyngstad, Tore	Filler i bituminøse vegdekker	1977
16	Melby, Karl	Repeterte belastninger på leire	1977
17	Tøndel, Ingvar	Sikring av veger mot snøskred	1977
18	Angen, Eigil	Fukttransport i jordarter	1978
19	Berger, Asle Ketil	Massedisponering. Beregning av kostnadsminimale transportmønstre for planering av fjell- og jordmasser ved bygging av veier	1978
20	Horvli, Ivar	Dynamisk prøving av leire for dimenjonering av veger	1979
21	Engstrøm, Jan Erik	Analyse av noen faktorer som påvirker anleggskostnader for veger	1979
22	Hovd, Asbjørn	En undersøkelse omkring trafikkulykker og avkjørsler	1979
23	Myre, Jostein	Utmatting av asfaltdekker	1988
24	Mork, Helge	Analyse av lastresponsar for vegkonstruksjonar	1990
25	Berntsen, Geir	Reduksjon av bæreevnen under teleløsningen	1993

Report no.	Author	Title	Year
26	Amundsen, Ingerlise	Vegutforming og landskapstilpassing, Visuelle forhold i norsk vegbygging fra 1930 til i dag	1995
27	Sund, Even K.	Life-Cycle Cost Analysis of Road Pavements	1996
28	Hoff, Inge	Material Properties of Unbound Granular, Materials for Pavement Structures	1999
29	Lerfald, Bjørn Ove	Study of Ageing and Degradation of Asphalt Pavements on Low Volume Roads	2000
30	Løhren, Alf Helge	Økt sidestabilitet i kurver med små radier	2001
31	Hjelle, Hallgeir	Geometrisk modellering av veger i 3D	2002
32	Skoglund, Kjell Arne	A Study of Some Factors in Mechanistic Railway Track Design	2002
33	Garba, Rabbira	Permanent Deformation Properties of Asphalt Concrete Mixtures	2002
34	Thordarson, Skuli	Wind Flow Studies for Drifting Snow on Roads	2002